STA-2 2-D Hydraulic Modeling
(Linked Cells Model)
Task 1.8 Final Report

Science and Engineering Support Service (SESS)
Contract No. C-15988-WO04-05

South Florida Water Management District

April 19, 2005

Prepared by:
Sutron Corporation
Hydrologic Services Division (HSD)
6903 Vista Parkway N, Suite 5
West Palm Beach, FL 33411
Tel: (561)-697-8151

Prepared for:
South Florida Water Management District
Attn: Tracey Piccone, Project Manager
B-2 Building, 3rd Floor
3301 Gun Club Road
West Palm Beach, FL 32406

Table of Contents

List of Figures

List of Tables

STA-2 2-D Cells 1-3 Linked Model Final Report

STA Hydraulic Modeling Contract C-15988-WO04-05 (SESS Contract)

1. Introduction

Stormwater Treatment Area 2 (STA-2) is a primary component of the Everglades Construction Project mandated by the 1994 Everglades Forever Act (section 373.4592, Florida Statutes). It is situated generally on and surrounding the former Brown's Farm Wildlife Management Area and is located immediately west of Water Conservation Area 2A. STA-2 provides a total effective treatment area of 6,430 acres to treat stormwater runoff originating from the Hillsboro Canal and Ocean Canal drainage basins upstream of the S-6 Pump Station. The location of STA-2 is shown in Figure 1.

Two-Dimensional (2-D) hydraulic models have already been developed for Cell 1 and Cell 3 of STA-2 under steady flow conditions using the FESWMS/Flo2DH Software Program by other parties (SFWMD 2001a). Under Subtasks 1.1 to 1.4 of this contract, the development of new 2-D single-cell hydraulic models for Cell 2 and updated 2-D models for Cell 1 and 3 were completed (Sutron Corp. 2004a). Current project work is the continued effort to build 2-D linked hydraulic models for Cells 1-3 of STA-2, with new topographic data, additional project features, and performing transient and steady flow hydraulic simulations for STA-2. Model Calibration and Verification efforts under transient conditions are also addressed.

The calibrated models under transient flow conditions are later used to analyze steady flow simulation scenarios of STA-2 for Low, Design and High Flow conditions for existing STA-2 configuration and future enhancements as specified in the project scope of work. The majority of present tasks are spelled out under Task 1 of the contract scope of work, precisely under Subtask 1.5: STA-2 Linked cells Existing Model and Subtask 1.6: STA-2 Linked cells Enhanced Model.

This final report (Subtask 1.8) summarizes major results obtained in the modeling work for Subtask 1.5 as well as Subtask 1.6 of this project for the whole STA-2 and comments from District staff have been incorporated based on the draft report (Subtask 1.7).

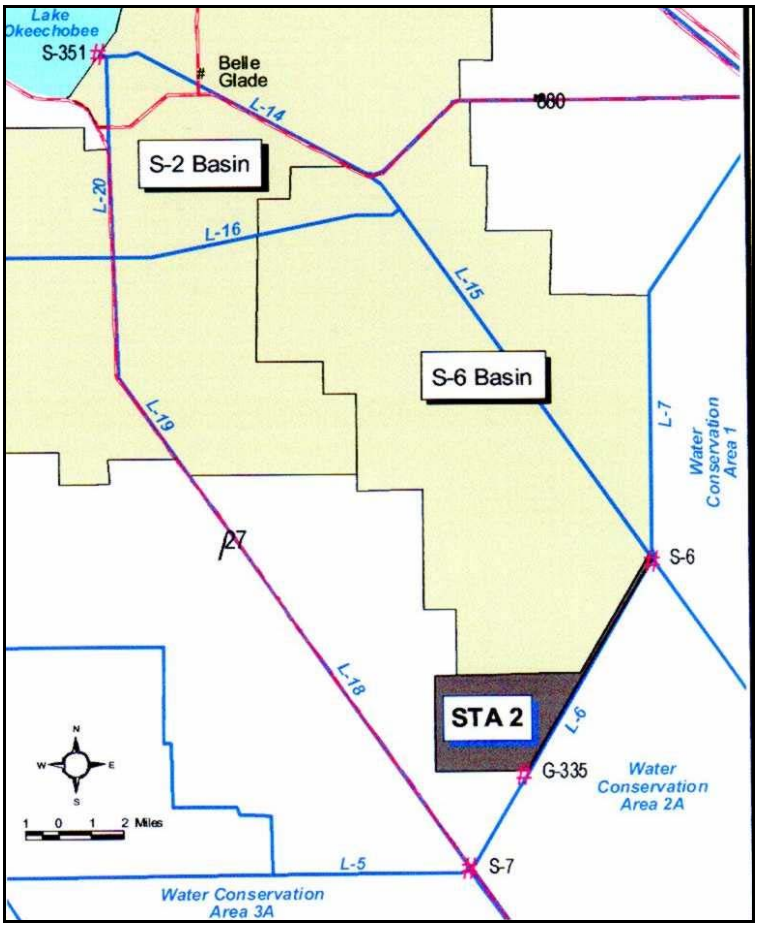

Figure 1: Location of STA-2

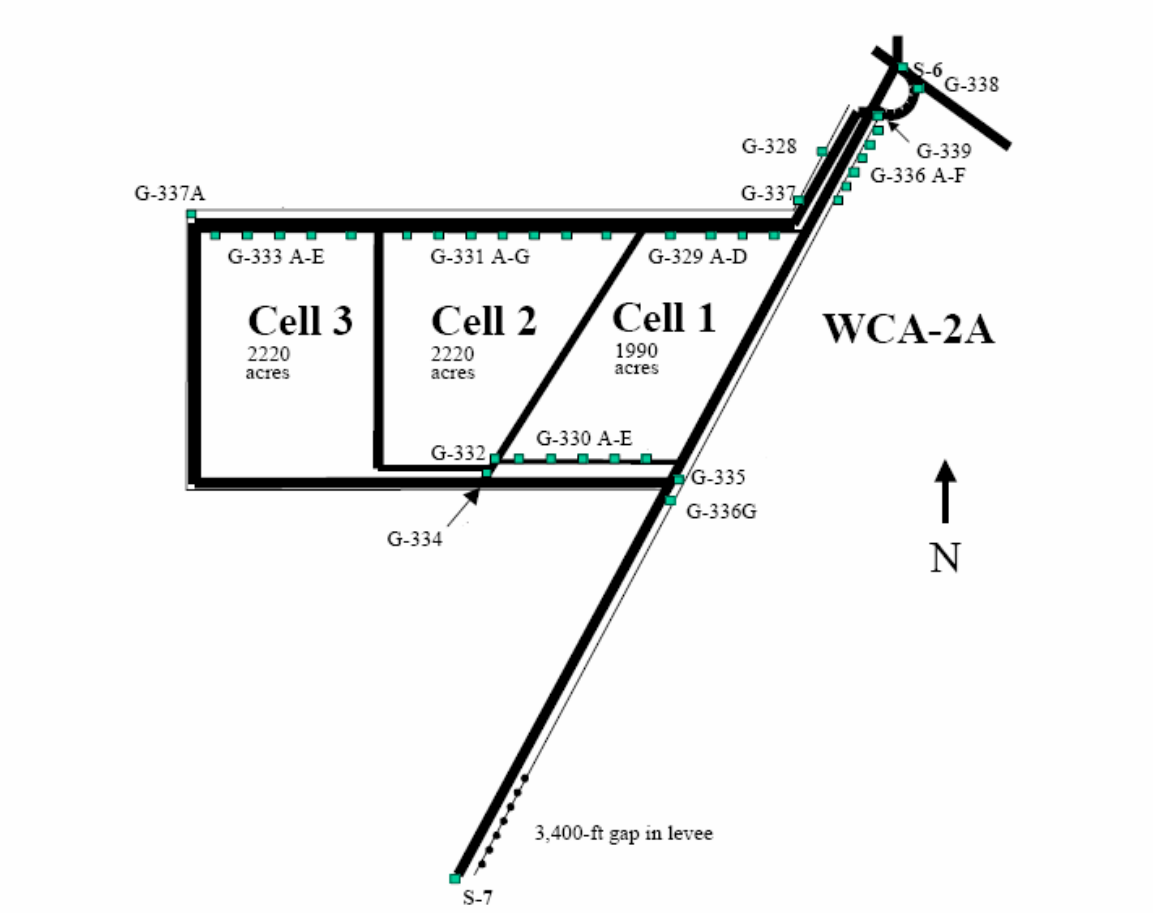

Figure 2: Schematic Map of STA-2 Layout (Existing Conditions)

2. Model Set-up

The FESWMS/FLO2DH computer program was selected by the District as the modeling tool for the current hydrodynamic modeling of STAs.

The computation engine FLO2DH is part of the Federal Highway Administration's Finite Element Surface-water Modeling System (FESWMS). It is a public domain model but the Graphic User Interface (GUI) through the Surface water Modeling System (SMS) is not free. FLO2DH simulates two-dimensional depth averaged hydrodynamic flows of surface water bodies using the finite element method. Additional information about the theoretical background of the model, its numerical method, its input and output data can be found in the User's Manual referenced in the report (Froehlich 2002).

Current STA-2 modeling work was completed with FLO2DH version 3.20 (updated on 10/29/2004) and SMS 8.1(built on June 2004).

2.1 Study Area: STA-2 System Hydraulics

The model domain of the cells 1-3 linked model includes the Supply/Inflow Canal, Cells 1-3, and the Discharge Canal (Figure 2).

Stormwater enters the system through pump stations S-6 and G-328. S-6 provides the primary source of stormwater flows to STA-2, with a total pumping capacity of 2,925 cfs. The agriculture pumping station G-328 provides drainage and irrigation for tributary farmlands and the total outflow (drainage to STA-2) capacity is 445 cfs. Water is conveyed through the Supply Canal and then the Inflow Canal. Flow through Cell 1 is controlled by inflow culverts G-329 A-D and outflow structures G-330 A-E. Inflow culverts G-331 A-G convey water into Cell 2 and gated spillway G-332 discharges treated flows from Cell 2. Cell 3 has gated culverts G-333 A-E as inflow control structures and outflow structure G-334 is located at the southeastern end of Cell 3, next to the Discharge Canal.

The Discharge Canal receives treated water from Cells 1-3 and the STA-2 outflow pump G-335 discharges flows from STA-2. Treated water eventually will be delivered into WCA 2A via interim divide structures G-336A-F and G-336 G.

During extreme storm events, diversion structures G-338 and G-339 can be open to facilitate flow diversion from STA-2 Supply Canal.

Seepage control is provided by the Seepage Collection Canal running along the Supply/Inflow Canal and the perimeter of treatment cells and ending near outflow pump station G-335. Seepage return pump stations G-337/G-337A discharge to the Supply Canal.

Since FLO2DH cannot simulate pumping stations, structure S-6/G-328 and G-335 are not represented as structures. They are treated as boundary conditions. The seepage collection canal is not part of the model domain since seepage losses cannot be explicitly simulated by FLO2DH. For short-term event-based flow simulations, seepage losses, rainfall (except for standard project storm) and evapotranspiration are considered negligible compared to structure inflow.

Inflow culverts G-329 A-D, G-331 A-G, G-333 A-E are simulated with FLO2DH's culvert option. Gated spillways G-332 and G-334 are simulated as weirs.

2.2 Topography and Vegetation

The land surface elevations were obtained from the 2003 STA-2 topographic survey provided by the District (Wantman, 2003). The resolution of the topographic survey is controlled by the 1,000 ft x 500 ft grid of survey points (Figure 3). The surveyed land surface elevations in marsh areas of STA-2 range from 7.26 ft NGVD to 14.16 ft NGVD (Figure 4). The highest surveyed point (14.16 ft NGVD) is located in Cell 1. It was observed that this isolated high elevation point caused some elements to dry out for most of model runs. After analysis of adjacent data points, this elevation did not appear realistic. It was therefore decided to adjust this isolated value to the elevation value of the neighboring surveyed points (approximately 12.50 ft NGVD).

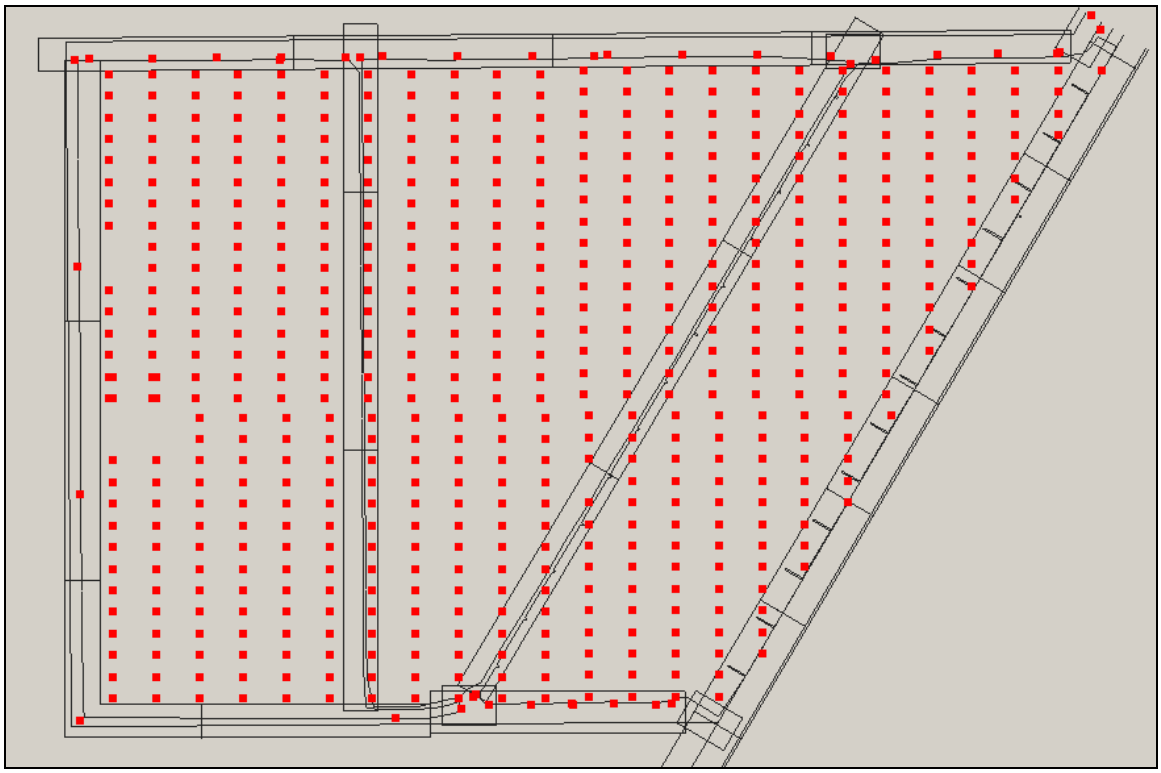

Figure 3: Topographic Survey Points

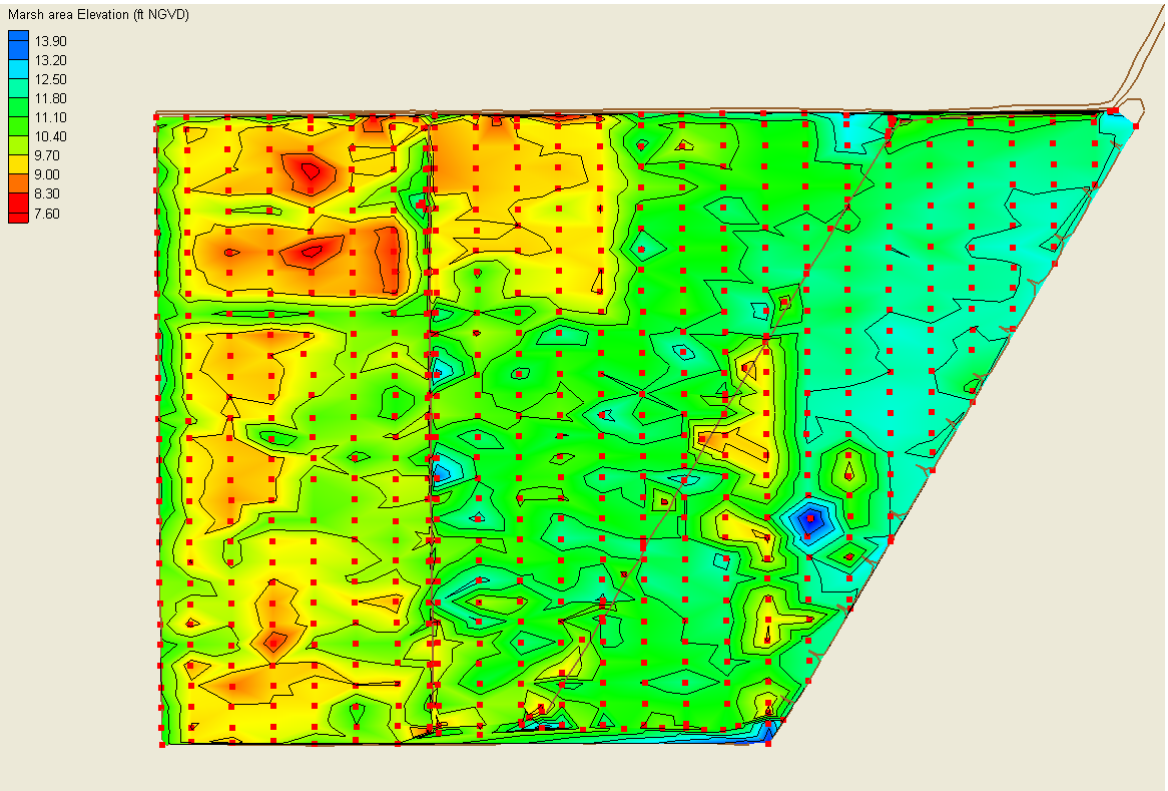

Figure 4: Contour Plot of Land Surface Elevations in the Marsh Areas

The Supply/Inflow Canal has a bottom elevation at -4.0 ft NGVD.

Major micro-topographic features in Cell 1 are the inflow distribution and outflow collection canals. The bottom elevation of the canals is about 7.0 ft NGVD. In the marsh area, the bottom elevation ranges from about 9.0 ft to 12.54 ft NGVD.

Cell 2 has a north to south borrow canal along its eastern boundary. The bottom elevation of the borrow canal ranges from about 1.0 ft at the north to -4.0 ft at the southern end. The borrow canal is plugged at intervals of about 200 ft. The distribution and outflow canals have a bottom elevation of about 7.2 ft and -4.0 ft NGVD, respectively. There is a remnant farm canal in the northwestern corner with a bottom elevation of about 4.0 ft NGVD. The range of bottom elevations is from -4.0 ft to 12.33 ft NGVD.

Cell 3 contains several transverse remnant farm canals and one longitudinal remnant farm canal situated parallel to the flow direction. The borrow canal at the eastern perimeter levee is regularly plugged and its bottom elevation ranges from 1.0 ft to -1.0 ft NGVD. The top-width of the borrow canal at the land surface level is about 25.0 to 75.0 ft. The ground surface elevation ranges from -4.0 ft to 11.95 ft NGVD.

Vegetative cover in STA-2 was from the STA-2 vegetation map (SFWMD 2003) shown in Figure 5. Cell 1 and Cell 2 are dominated by mature emergent cattails. The northwestern corner of Cell 2 is SAV (Submerged Aquatic Vegetation). Cell 3 was designed and started as SAV dominant and contains about 500 acres of the former Brown's Farm land area that is considered as emergent cattails. This information was used in assigning appropriate material types for STA-2 vegetations (Figure 6).

2.3 Finite Element Mesh

The model domain was divided into quadratic triangular elements by using the SMS mesh generation tools. Smaller elements were used to better represent local topographic features and possible local hydraulic gradient areas. Figure 7 is the finite element mesh used for simulation of STA-2 Existing Condition. It includes 3,405 triangular elements and 7,588 nodes. Grid refinement model runs were conducted to confirm that such a spatial scale of finite element mesh would still produce accurate model results while avoiding the longer run time associated with a much finer mesh.

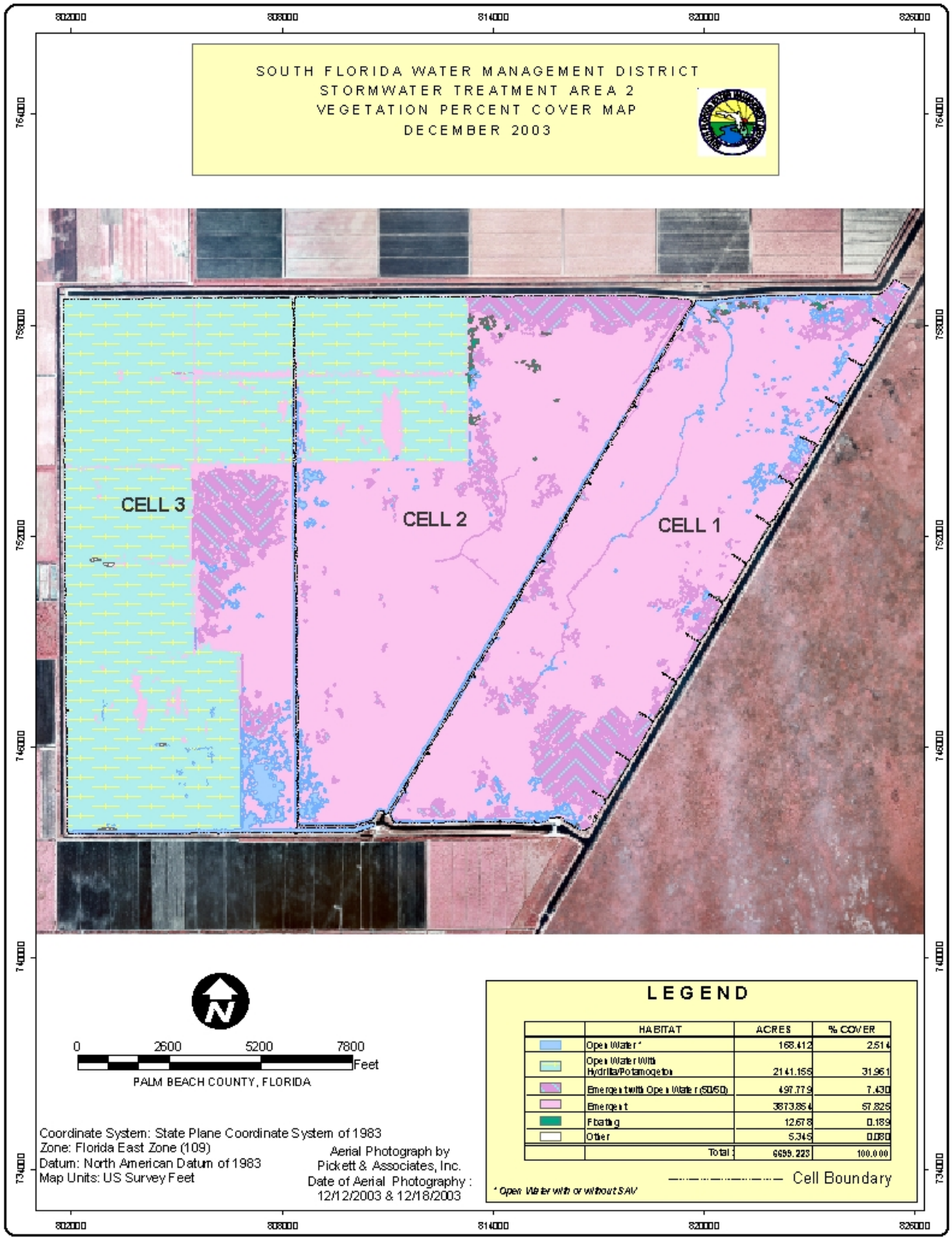

Figure 5: STA-2 Vegetation Map (SFWMD 2003)

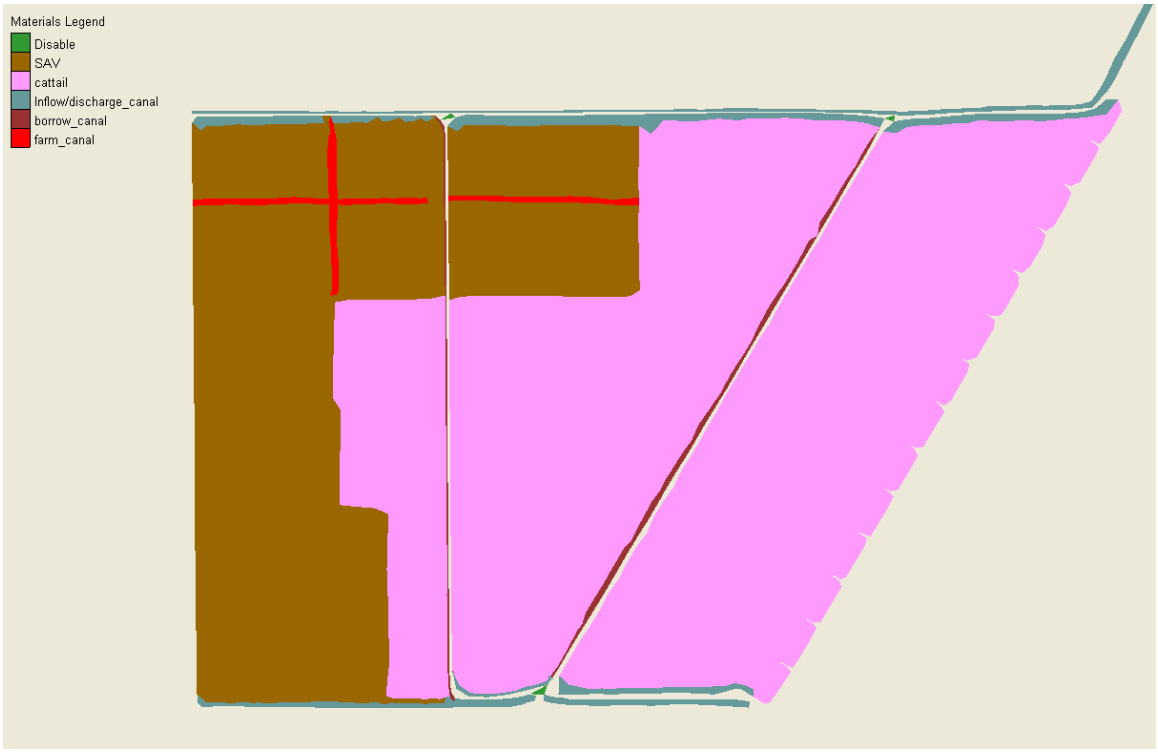

Figure 6: Material Types as Applied in the 2-D STA-2 Linked Cells Models

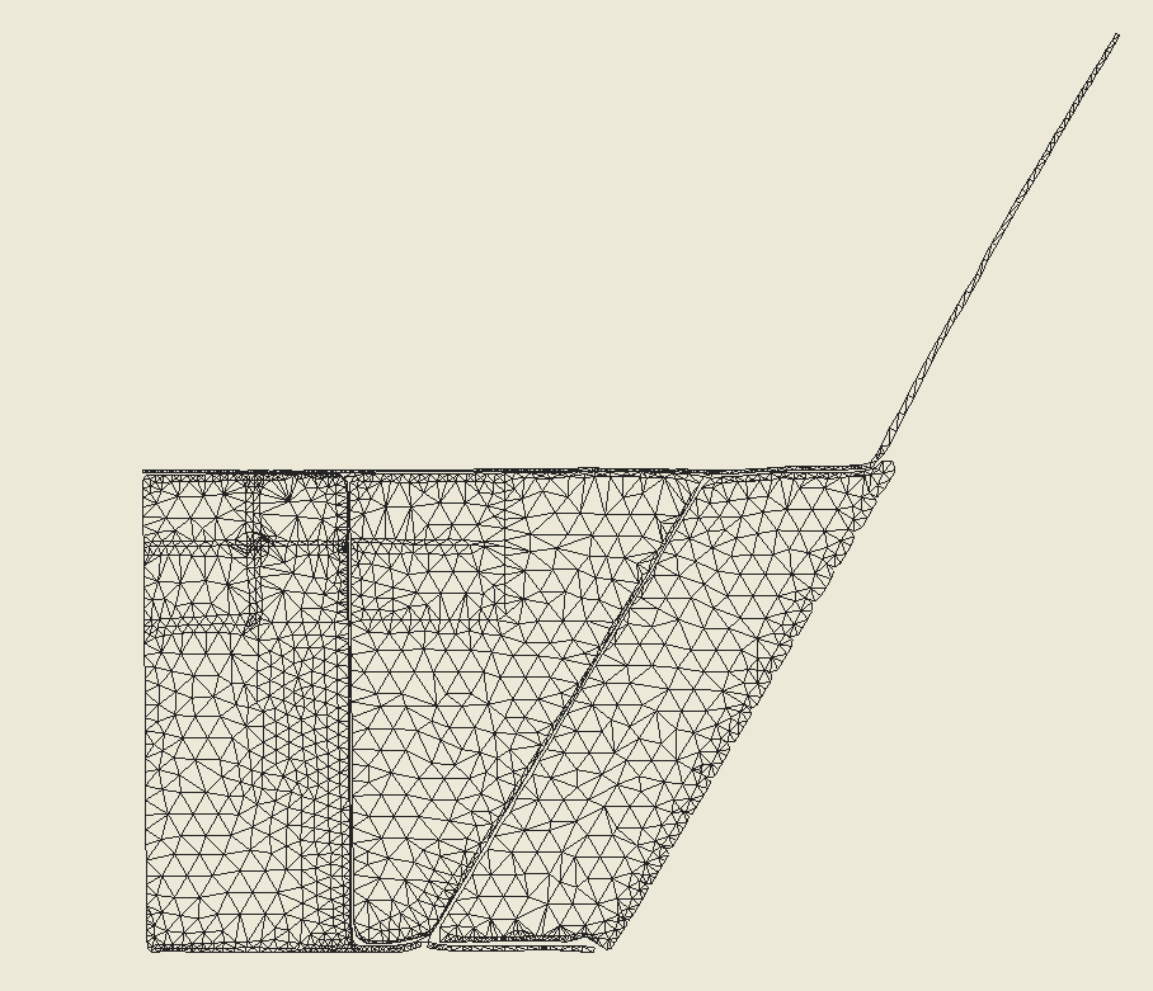

Figure 7: Finite Element Mesh for Existing Models

2.4 Control Structures

STA-2 control structures include pump stations, gated culverts, gated spillways and drop-inlet structures.

STA-2 pump stations include inflow pump stations S-6 and G-328, seepage return pump station G-337, and outflow pump station G-335. Pump stations cannot be explicitly simulated by FLO2DH. These pump stations are considered as specified stage/flow boundary or source/sink in model set-up.

Gated culverts G-329 A-D control inflow into Cell 1; gated culverts G-331 A-G control flow into Cell 2 and gated culverts G-333 A-E control flow into Cell 3.

Outflow from Cell 1 is controlled by culvert structures G-330 A-E with weir boxes installed upstream of the inlet.

Outflow from Cell 2 and Cell 3 is regulated by gated spillways G-332 and G-334, respectively.

Gate structures cannot be simulated by current version of FLO2DH 3.20 and all gated structures are assumed fully opened.

Some major geometry and parameters for STA-2 interior structures are listed in Table 1.

Table 1. Information on Interior Structures

Structure Name	G-329	G-330	G-331	G-332	G-333	G-334
Unit	A-E	A-D	A-G	2 gates	A-E	2 gates
Type	CMP	CMP/weir	CMP	spillway	CMP	Spillway
Entrance loss coefficient	0.5	0.5	0.5		0.5	
Manning's n	0.024	0.024	0.024		0.024	
Invert (ft)	8.9	5.6-7.2	8.5		8.6	
Crest (ft)		13.0		7.5		6.75
Flow line length (ft)	65	64	64		65	
Net length (ft)		20		32		32
Gate height (ft)	6.0		5.5	6.0	5.5	6.0
Diameter	72 inches	66 inches	66 inches		66 inches	

3. Model Calibration and Validation

Following (Refsgaard and Henriksen 2004), model calibration is the process of adjusting model parameters to reproduce historic stage/flow trend within predefined accuracy; model validation is the process of testing the predictive capability of a calibrated model for its intended purpose of application with independent data set that has not been used in model calibration. The term verification is reserved for the process of testing a model code (computer program) for the correctness and accuracy in its computation engine and governing equations.

Observed stage and flow data at inflow and outflow structures of treatment Cells 1 to 3 were used for model calibration and validation. There are no continuous stage-monitoring sites in the marsh area. A general calibration target of ± 0.25 ft is set for history matching.

The interior water depth data collected for water quality studies could not be used. As discussed in the previous STA-2 hydraulic modeling studies (Sutron Corp. 2004a and b),

they are not as reliable as continuous observed stage data at structure locations. These limited water depth data were also collected during relatively dry periods and water flow is static during most of the data collection time period.

By considering the limitation of FLO2DH in handling gate operations, the selected time period is 8/25/2004 to 9/15/2004 for model calibration and validation. Model calibration was run for a 240-hour time period (from 8/25/2004 to 9/4/2004). Model validation had to be cut down to five (5) consecutive days to avoid variable gate opening (9/5/2004 to 9/10/2004; 9/11/2004 to 9/15/2004). Without simulation of gate operations, it is very challenging to accurately reproduce historic flow and stage data.

All calibration target locations are headwater and tailwater levels of gated structures. The uncertainty and approximation in gates have an impact on model calibration and validation results. The representative gate opening values during 8/1/2004 to 10/1/2004 (Figures 8-12) demonstrated the difficulty in selecting time periods with constant gate openings for model calibration and validation.

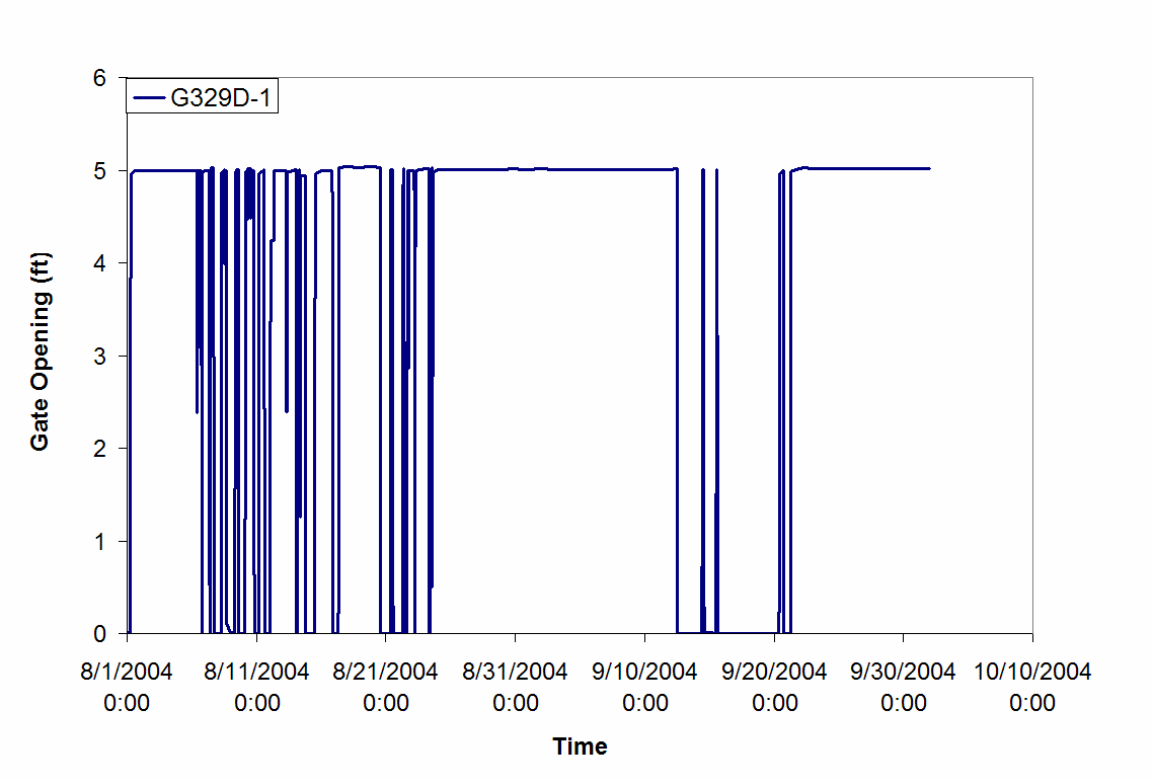

Figure 8: Gate Opening (G-329D)

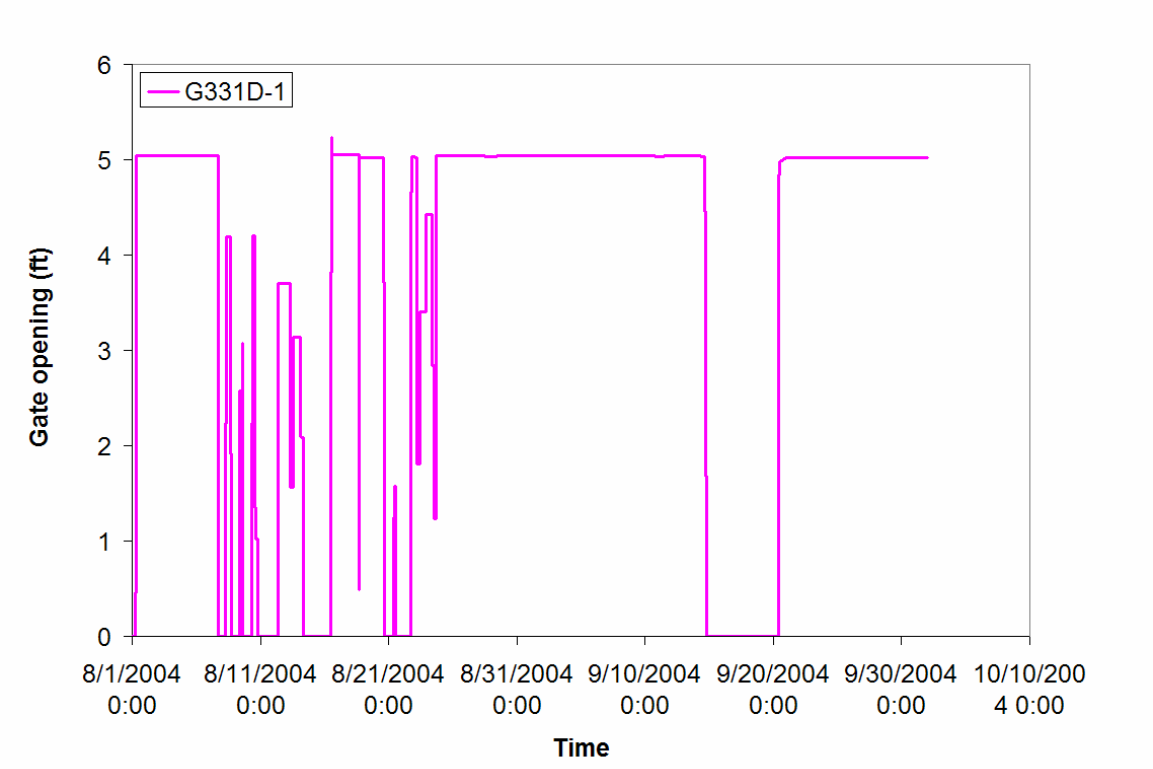

Figure 9: Gate Opening (G-331D)

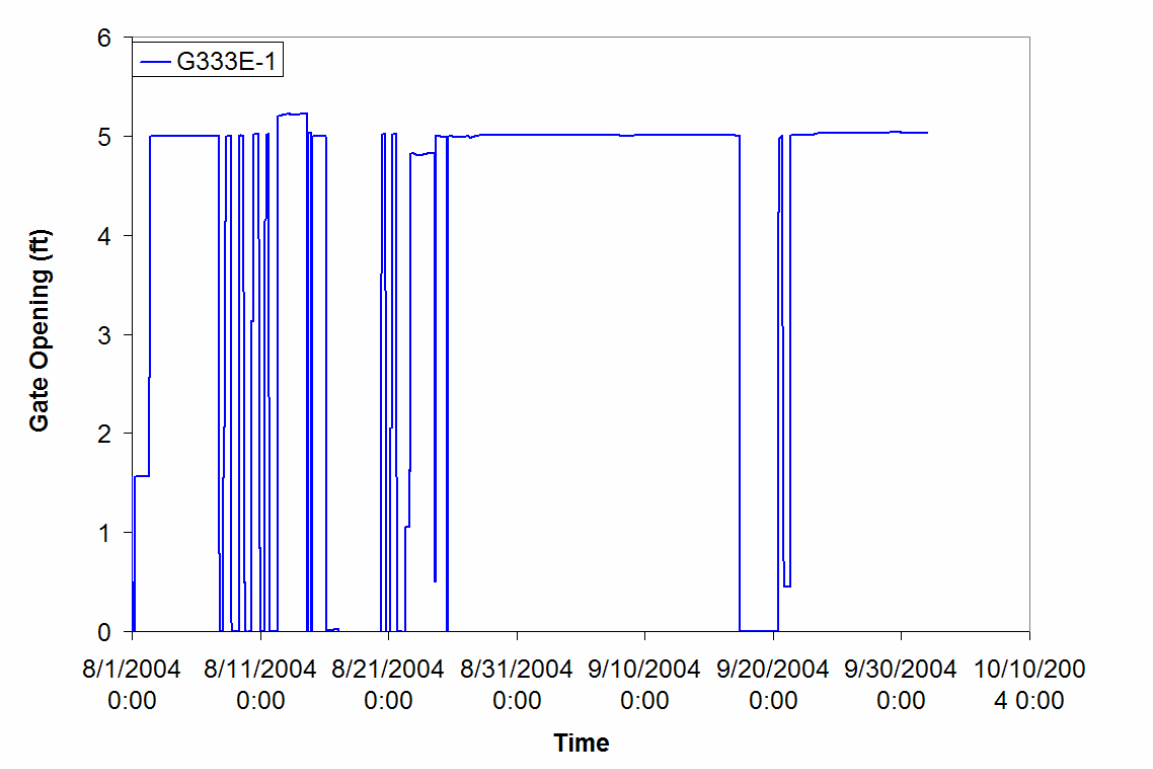

Figure 10: Gate Opening (G-333E)

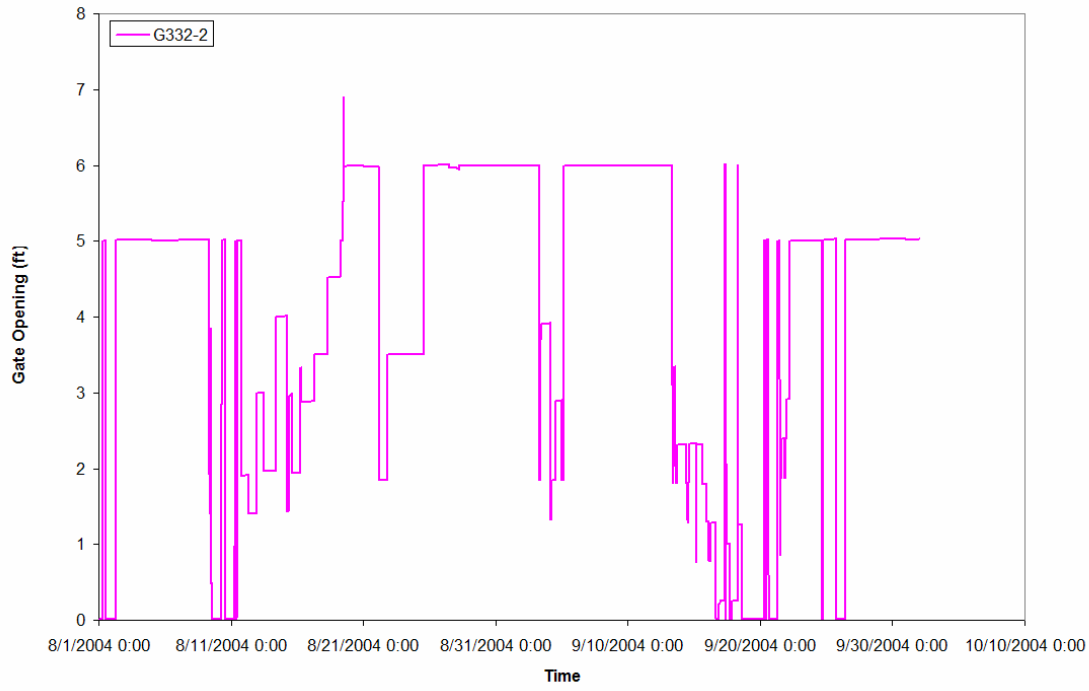

Figure 11: Gate Opening (G-332)

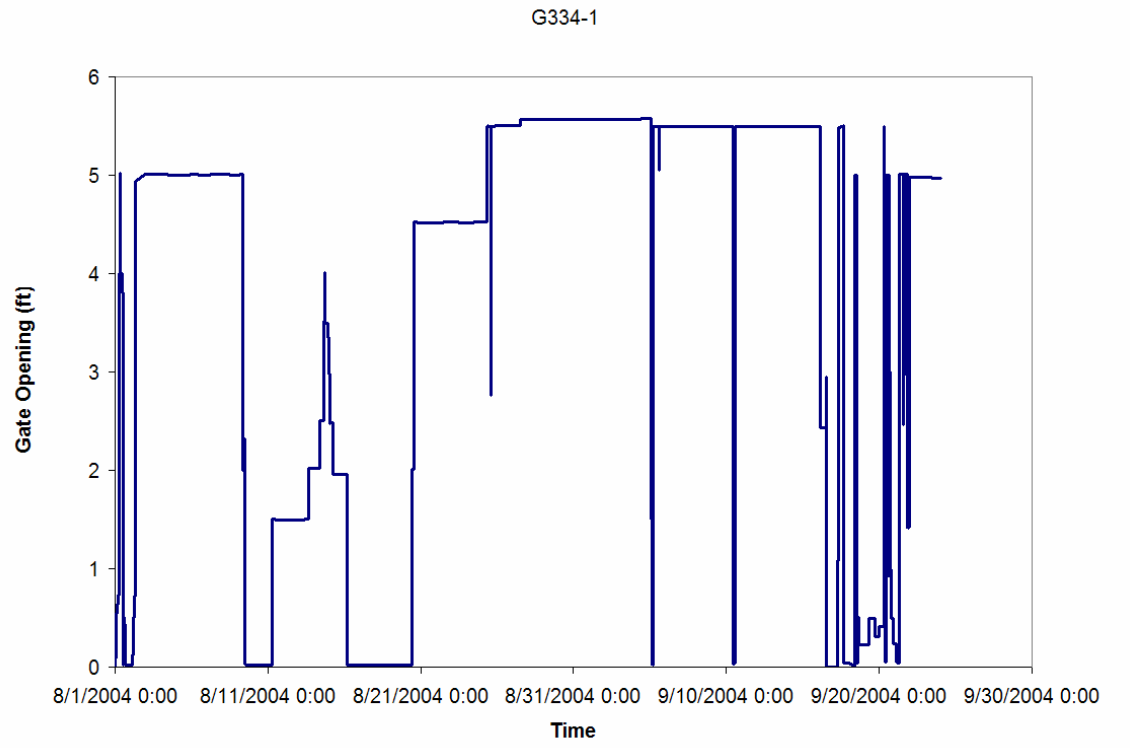

Figure 12: Gate Opening (G-334)

3.1 Model Calibration and Validation Strategy

The major concern in selecting historic data for model calibration and validation is the gate operations at interior inflow culverts. Because FLO2DH cannot handle partial gate openings, historic data with variable gate openings was avoided. Based upon a review of available STA-2 historic stage and flow data, the time period from 8/1/2004 to 10/1/2004 was selected as the primary time period for model calibration and validation. Eventually, the time period with constant gate opening: 8/25/2004 to 9/15/2004 was used.

Plots of gate opening location with inlet and outlet water depth time series during model calibration and validation phases are shown in Figures 13-18. Several combinations of flow conditions occurred and culvert flow computation was therefore complicated.

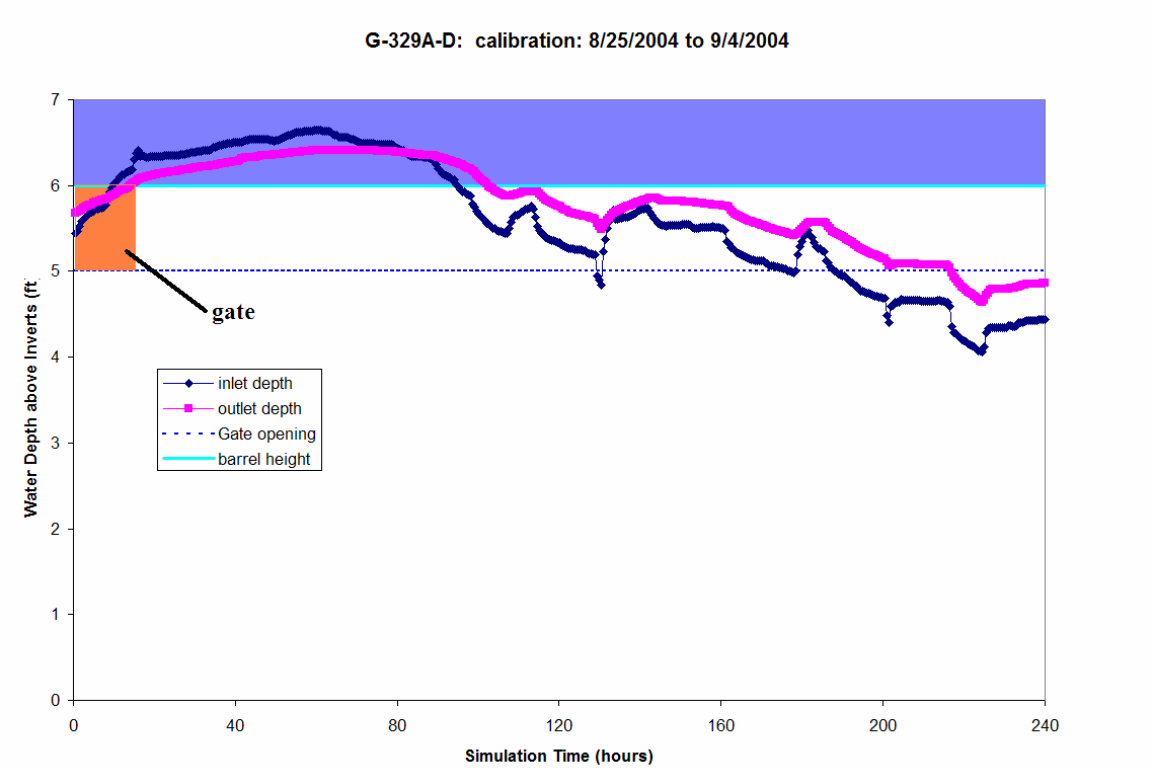

Figure 13: G-329 A-D Culvert Flow Condition during Model Calibration

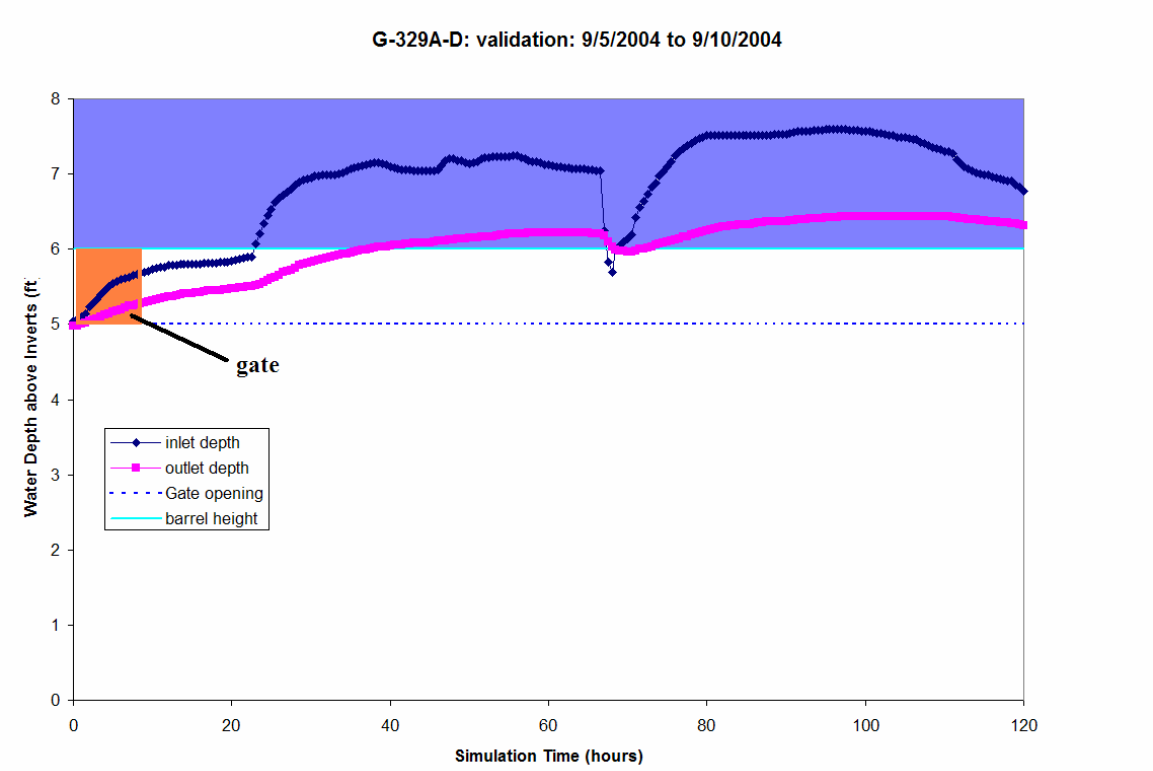

Figure 14: G-329 A-D Culvert Flow Condition during Model Validation

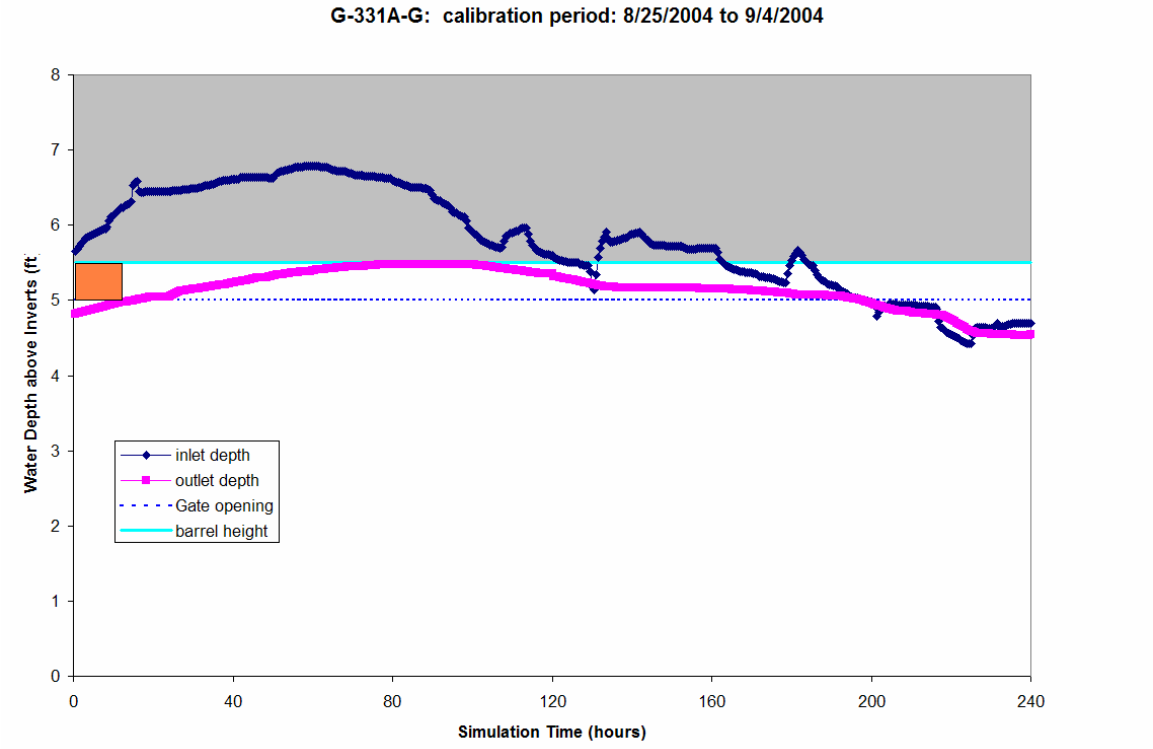

Figure 15: G-331 A-G Culvert Flow Condition (calibration: 8/25/2004 to 9/4/2004)

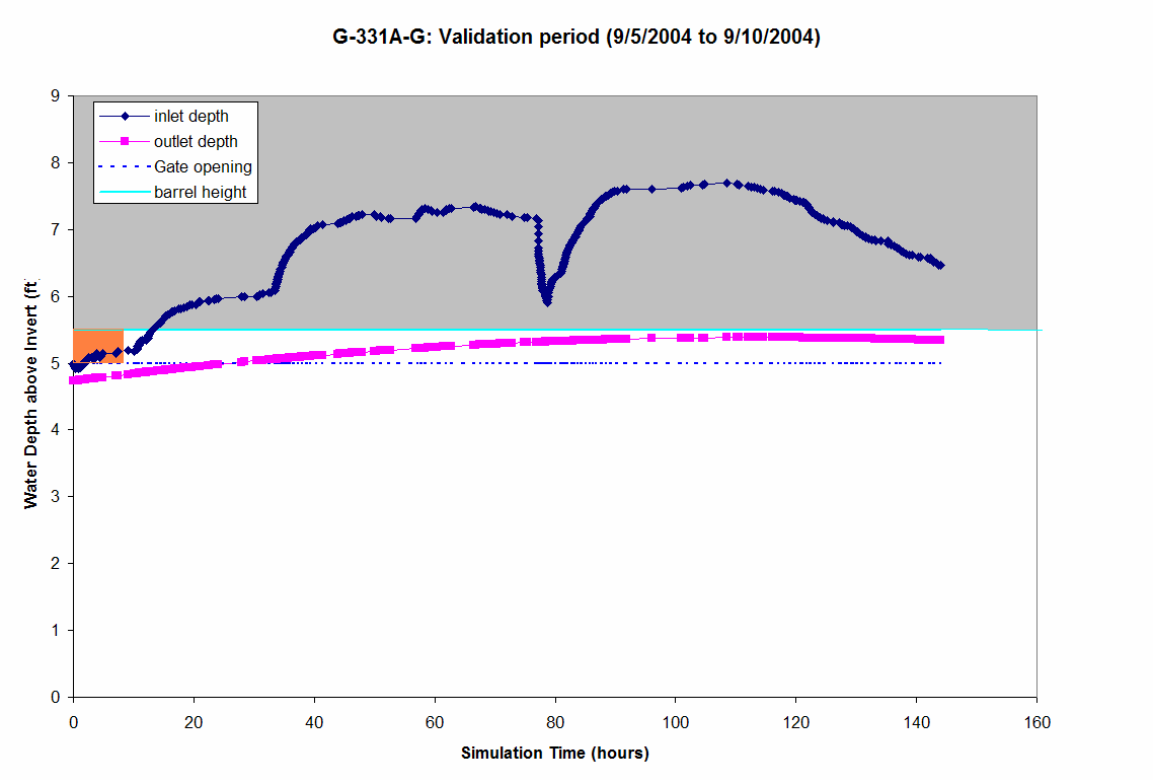

Figure 16: G-331 A-G Culvert Flow Condition (validation: 9/5/2004 to 9/10/2004)

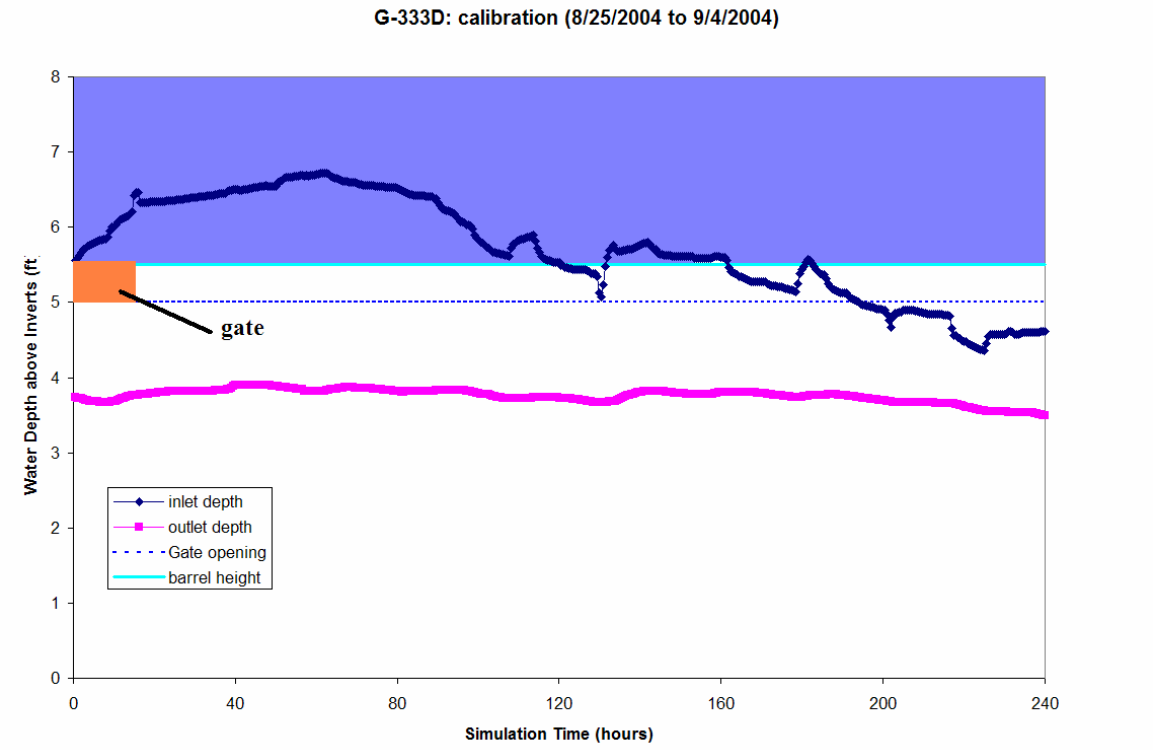

Figure 17: G-333D Culvert Flow Condition during Model Calibration

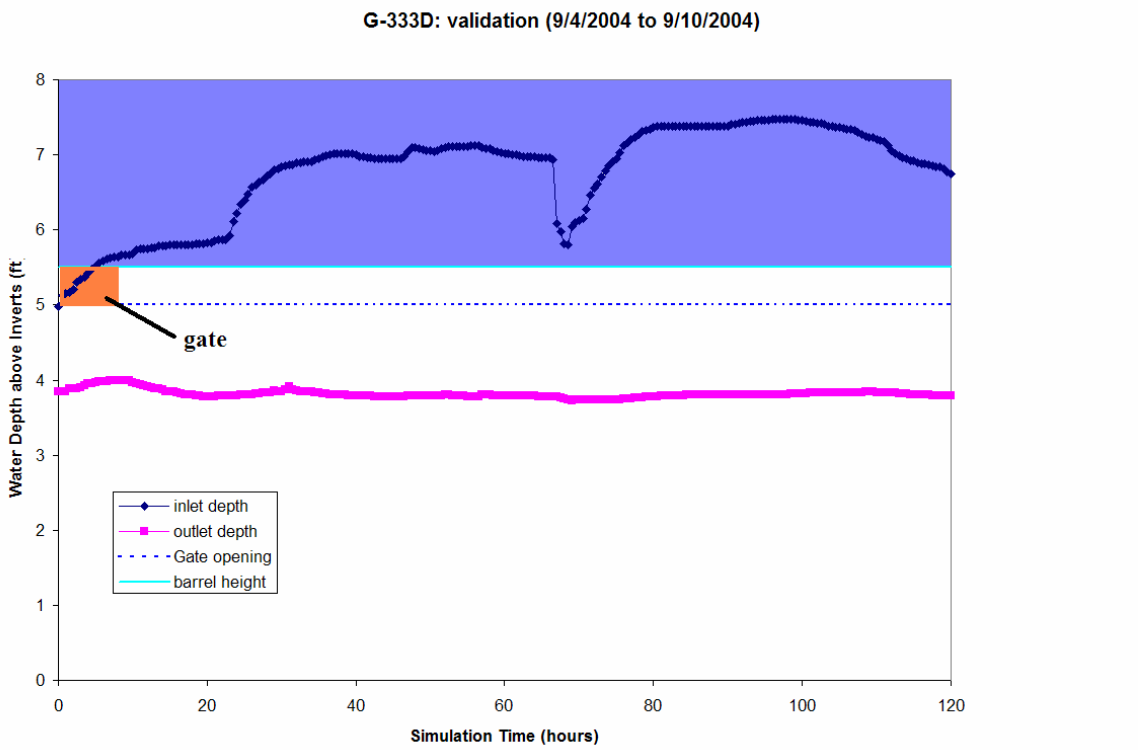

Figure 18: G-333D Culvert Flow Condition during Model Validation

Even within the selected time periods, the inflow culverts are not fully opened; a constant gate opening of 5.0 ft was maintained in contrast to a gate height of 5.5 ft for both G-331 A-G and G-333 A-E and 6.0 ft for G-329 A-D.

With this model set-up for model calibration and validation, there are ten valid observed stage locations that can be used as calibration/validation targets (Table 2).

Estimated flow data are available in the District's DBHYDRO database for all of these structures. These flow data are computed with flow rating equations calibrated with stream gauging data.

Table 2. Stage Recording Locations in STA-2 as Calibration Target

Stations	Description
G328_T	Tailwater elevation for the inflow structure G328 (Supply Canal stage, as boundary)
G329_H	Headwater elevation for the Interior culvert G329 (Inflow Canal stage)
G329_T	Tailwater elevation for the Interior culvert G329 (Cell 1 stage)
G330A_H G330D_H	Headwater elevation for G330A-D (Cell 1 stage)
G331B_T G331E_T	Tailwater elevation for the Interior culvert G331A-G (Cell 2 stage)
G332_H	Headwater elevation for the spillway G332 (Cell 2 stage, as Cell 2 boundary)
G333_T	Tailwater elevation for the Interior culvert G333A-E (Cell 3 stage)
G334_H	Headwater elevation for the outflow structure G334 (in Cell 3 , as boundary)
G332_T	Tailwater elevation for the outflow structure G332 (Discharge Canal stage)
G335_H	Water level at headwater of outflow pump station G335, as boundary
G331_H	Headwater elevation for the Interior culvert G331A-G (Inflow Canal stage)
G333_H	Headwater elevation for the Interior culvert G333A-E (Inflow Canal stage)

3.2 Approximation of Culvert Gate Opening

During model calibration and validation time periods, inflow culverts are not fully opened. The gate opening was maintained at 5.0 ft (actual operating condition).

The culvert flow rate computation in Flo2DH is:

$$Q_c = N_b C_c A_C \sqrt{2gH_C} \qquad \textbf{(1)}$$

N_b is the number of barrels; C_c is discharge coefficient; g is gravity; H_c is hydraulic head and A_c is full cross section area of culvert barrel.

There are two culvert flow conditions considered in FLO2DH. Under inlet control flow condition, flow at inlet is the controlling flow and is taken as orifice flow (submerged inlet) or weir flow (open channel flow); for outlet control flow, energy equation is applied to obtain the discharge coefficient (Figure 19).

The following formulas are excerpted from the FLO2DH 3.0 User's Manual (Froehlich 2002):

In the following formulas, Dc = interior height of culvert barrel; Q = barrel flow rate; So = culvert barrel slope; K', M, c', Y = coefficients that depend on culvert material, barrel cross section shape, and inlet characteristics; and m = 0.7 for mitered inlets, and -0.5 for all other inlets.

$$H_c = \begin{cases} z_s^h - z_{inv}; \textit{ for inlet control} \\ z_s^h - z_s^t; \textit{ for outlet control} \end{cases}$$

is culvert head, z_s^h = water-surface elevation at the upstream end of a culvert (that is, the headwater elevation), z_s^t = water-surface elevation at the downstream end of the culvert (that is, tailwater elevation); and z_{inv} = invert elevation at the culvert entrance. For inlet control flow,

$$C_c = Min\left\{ \sqrt{\frac{1 - \frac{D_c}{H_h}(Y + mS_o)}{2c'}}, \frac{1}{\sqrt{2}K'^{\frac{1}{M}}} \left(\frac{H_h}{D_c} \right)^{\frac{1}{M} - \frac{1}{2}} \right\}$$

where $H_h = z_s^h - z_{inv}$ is headwater depth. The first inlet control discharge coefficient is used when the culvert entrance is submerged and functions like an orifice; the second coefficient applies when the entrance is not submerged and acts as a weir. Discharge coefficients for outlet control flow are calculated as follows:

$$C_c = \frac{1}{\sqrt{1 + K_e + \frac{2gn_c^2 L_c}{\phi_n^2 R_c^{4/3}}}} \quad \text{Kf}$$

Under outlet control flow, the entrance loss coefficient (K_e) will have a direct impact on culvert flow rate.

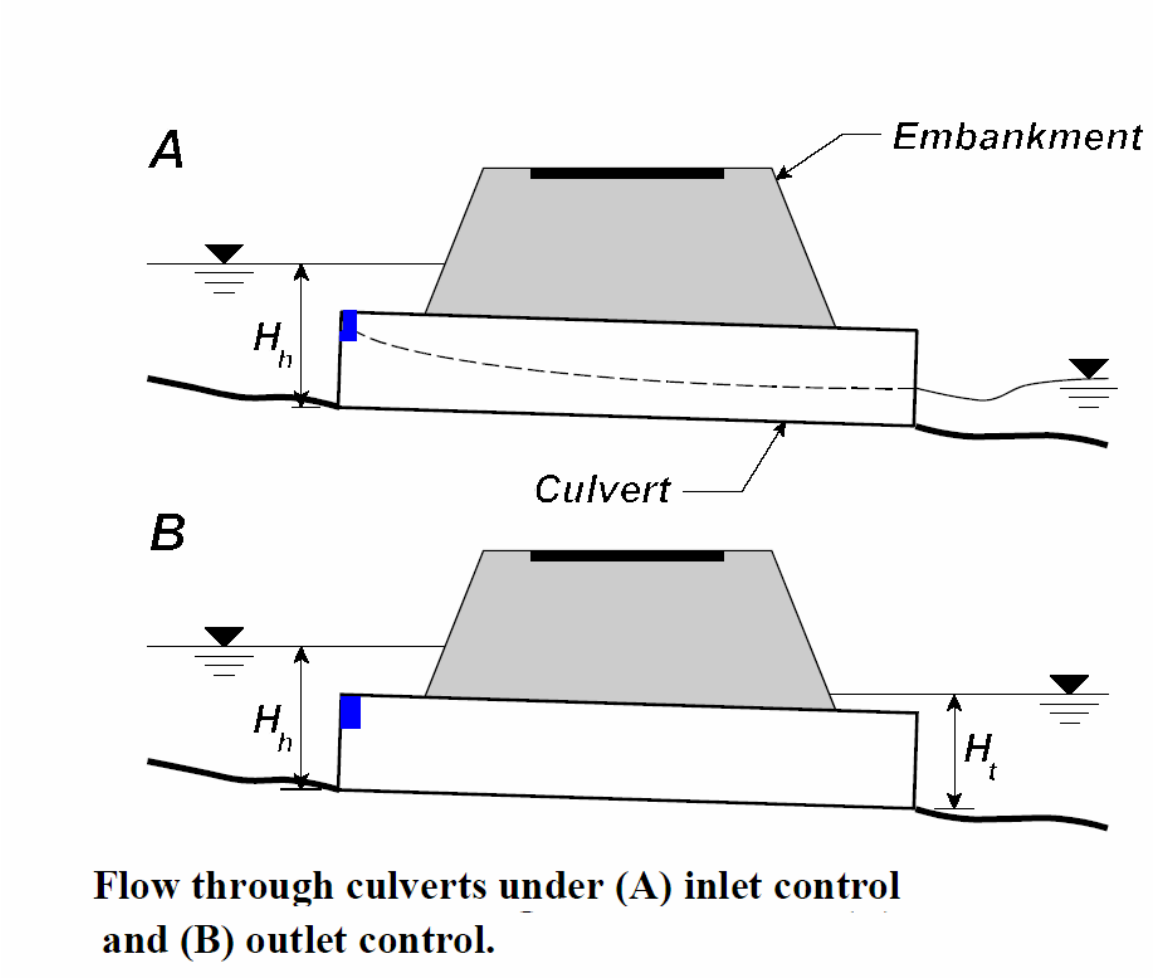

Figure 19: Culvert flow Conditions in FLO2DH (Gate is a slight modification from the original drawing)

Culvert flows during model calibration and validation time periods will be affected by partially opened gates. Since the FLO2DH culvert option assumes unregulated culverts, it is necessary to compensate for this limitation. Based on best professional judgment, it was decided to use the original culvert geometry but to try to approximate the gate effect on flow rate with the culvert discharge coefficient.

As for gated spillways, the only option is to simulate them as weirs. This is equivalent to free flow spillways.

3.3 Model calibration results

The G-328 tailwater level is the inflow boundary condition and G-335 headwater level is the outflow boundary condition for model calibration. The calibration model run was made with all interior culvert structures fully opened. Outflow structures G-332 and G-334 flow were not well represented by weir flow and it was decided to apply specified stages as boundary conditions at these two outflow locations.

Another issue which needed to be addressed was how to represent the partially opened gates at inflow culverts. The entrance loss coefficient value (K_e) was adjusted to accommodate the partial gate opening effects. Cell 2 is most sensitive to the effects of partial gate openings. For example, to compute the flow rate at culvert G-331A (outlet control in FLO2DH), a K_e value of 0.20 produced a better match to daily average flow in DBHYDRO and a K_e value of 0.5 underestimated the daily flow rate by about 8% (Figure 20). The simplified culvert flow computation in FLO2DH unexpectedly closely reproduced DBHYDRO culvert flows computed by the District's more complicated culvert routines in the FLOW Program. The District completed a new flow rating for G-329A-D, G-331A-G and G-333A-E by February, 2005. This new flow data was used in this flow comparison.

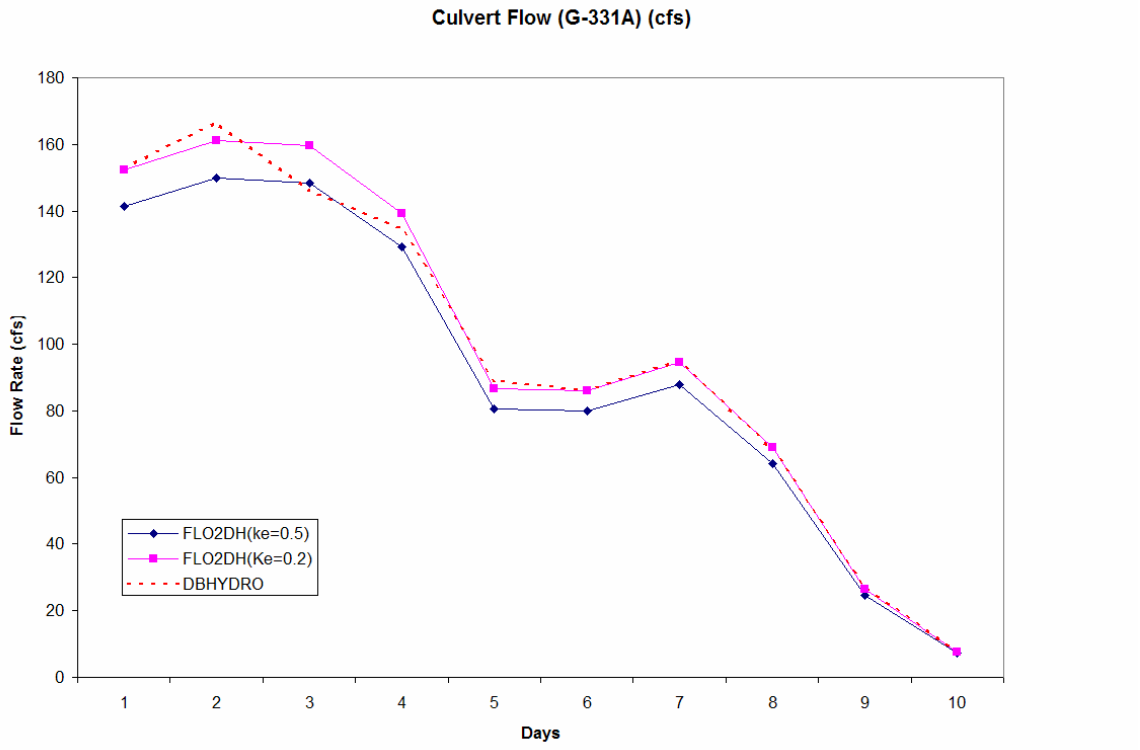

Figure 20: Comparison of Daily Average Culvert Flow (G-331A) (Flo2DH vs. DBHYDRO)

Overall model calibration shows good match between computed stage value and observed stage value at the target stations (Figures 21 to 33). Basic statistics including R-

square value, maximum absolute error and average absolute error are listed in Table 3. The model can capture the trend in stage values quite well, except for G-333_T (R^2=0.60). The maximum error was obtained after 24 hour from the beginning of the model runs to avoid initial condition impact.

Table 3. Statistics on Model Calibration

Stations	Maximum absolute error (ft)	Average absolute error (ft)	R-square
G328_T		As boundary	
G329_H	0.17	0.048	0.998
G329_T	0.10	0.024	0.998
G330A_H G330D_H	0.11 0.06	0.031 0.036	0.98 0.97
G331B_T G331E_T	0.18 0.06	0.098 0.022	0.82 0.98
G332_H		As boundary	
G333_T	0.17	0.089	0.60
G334_H		As boundary	
G332_T	0.19	0.075	0.99
G335_H		As boundary	
G331_H	0.19	0.092	0.99
G333_H	0.16	0.057	0.99

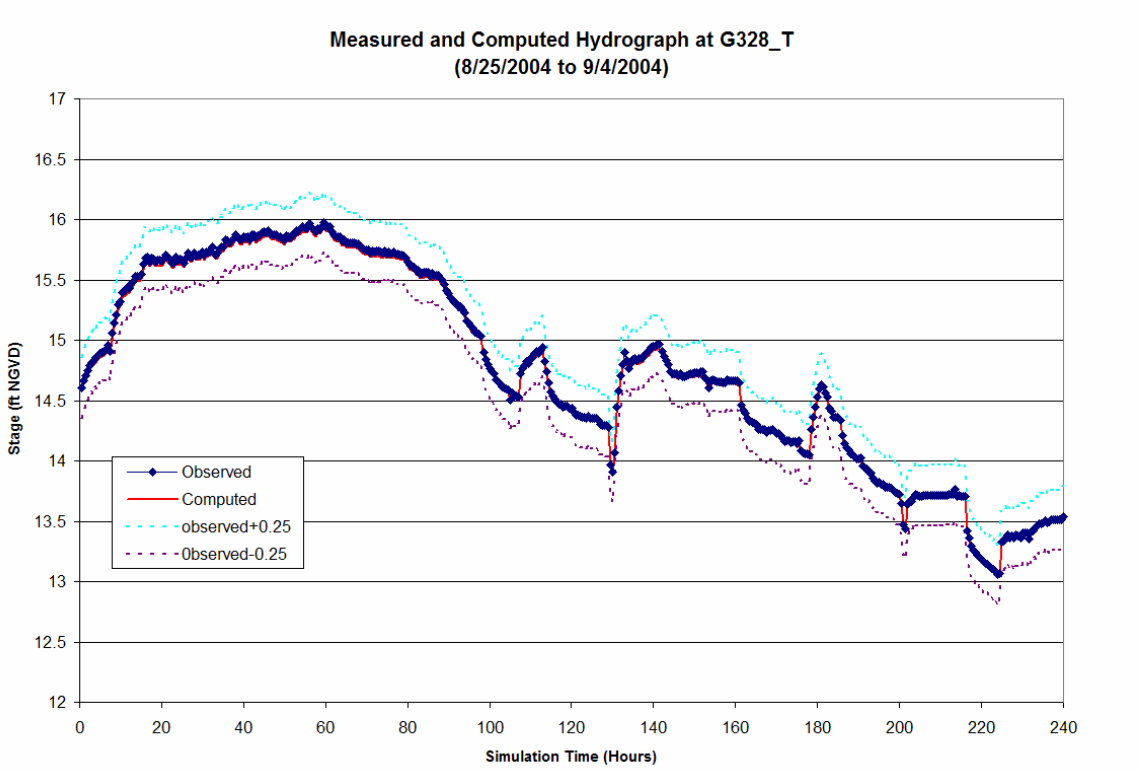

Figure 21: Computed and Measured Stage Hydrograph at G328_T (as boundary condition) (calibration: 8/25/2004 to 9/4/2004)

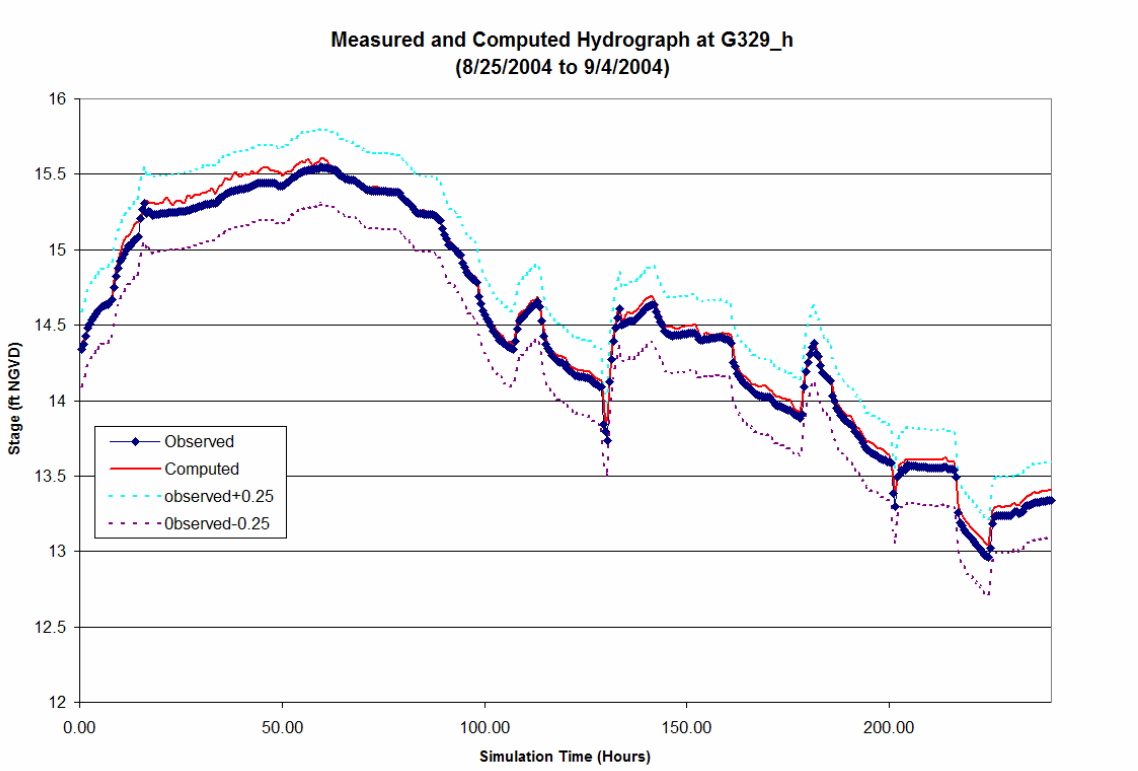

Figure 22 Computed and Measured Stage Hydrograph at G329_H (calibration: 8/25/2004 to 9/4/2004)

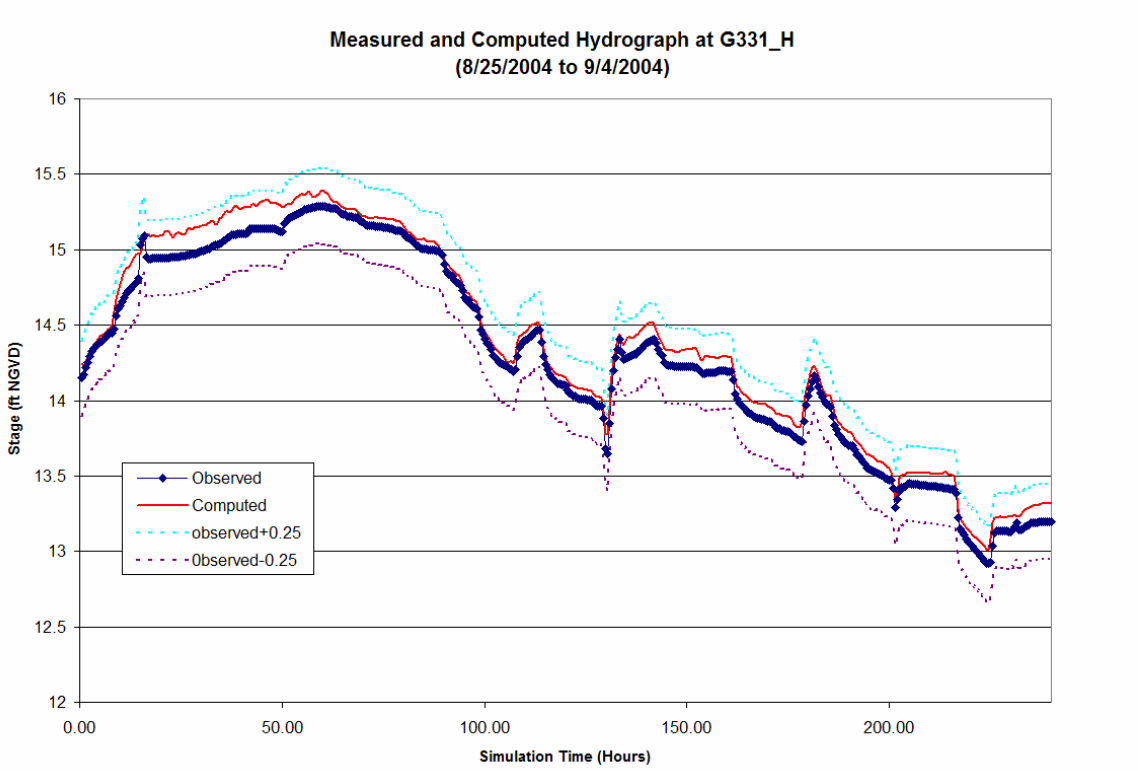

Figure 23 Computed and Measured Stage Hydrograph at G331_H (calibration: 8/25/2004 to 9/4/2004)

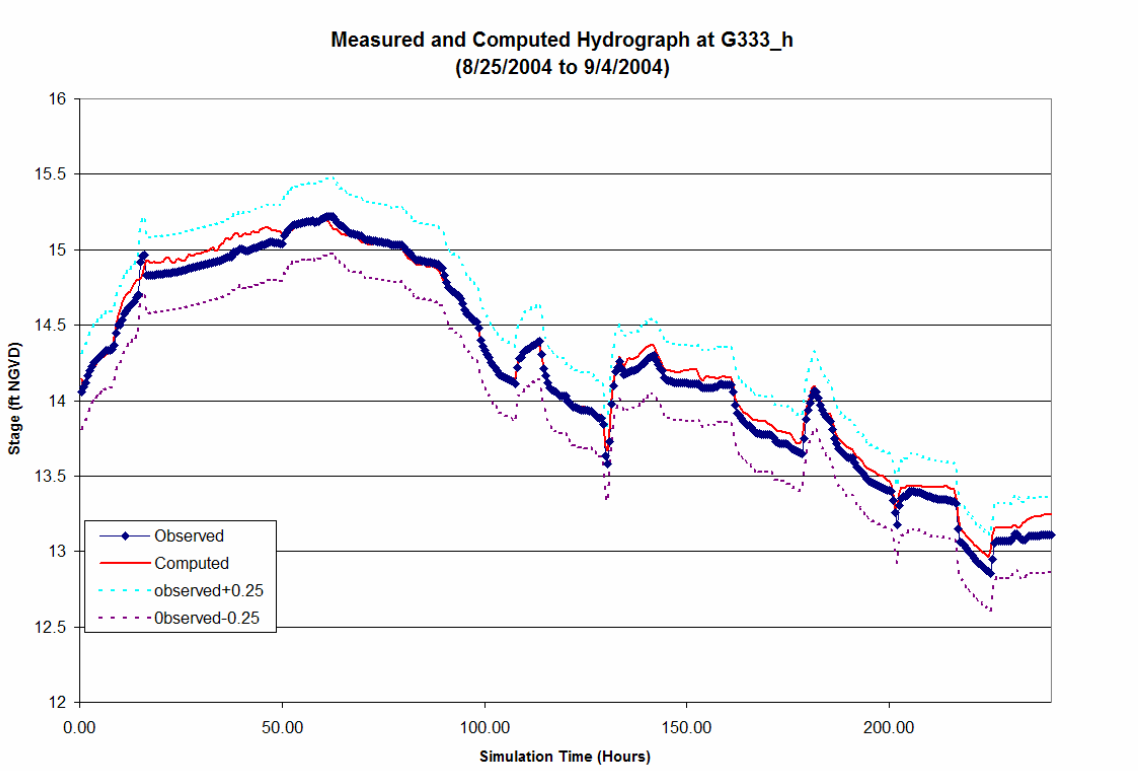

Figure 24 Computed and Measured Stage Hydrograph at G333_H (calibration: 8/25/2004 to 9/4/2004)

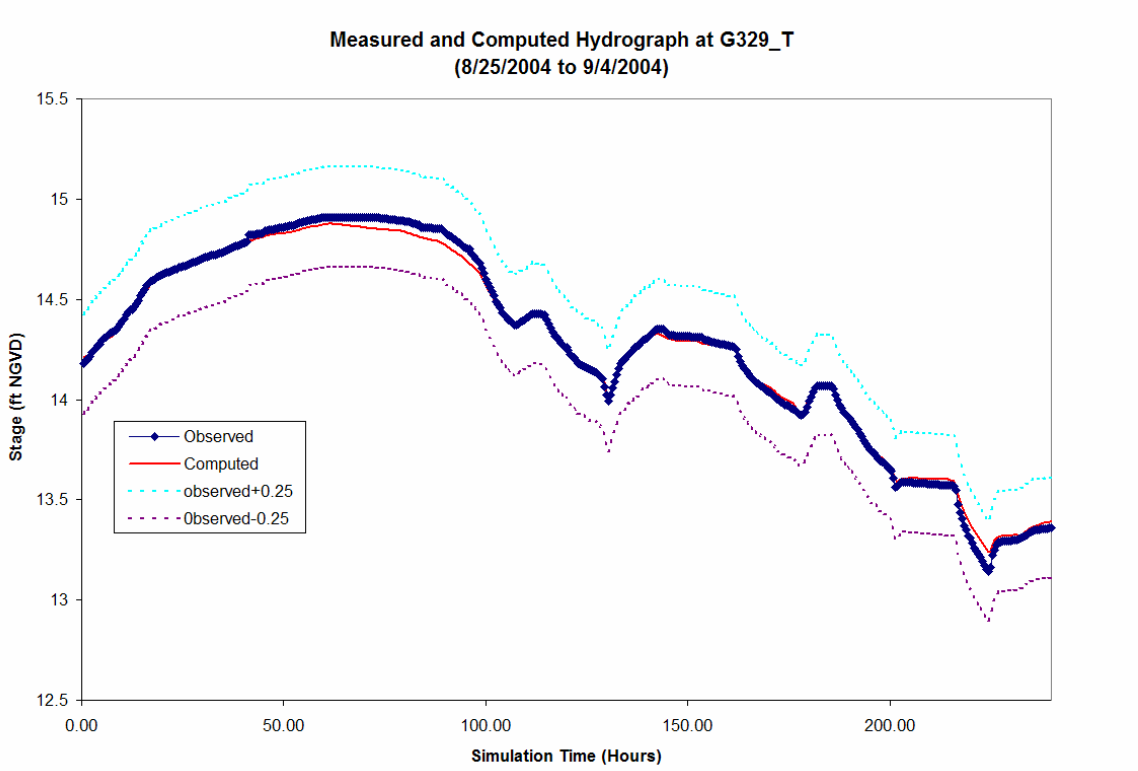

Figure 25 Computed and Measured Stage Hydrograph at G329_T (calibration: 8/25/2004 to 9/4/2004)

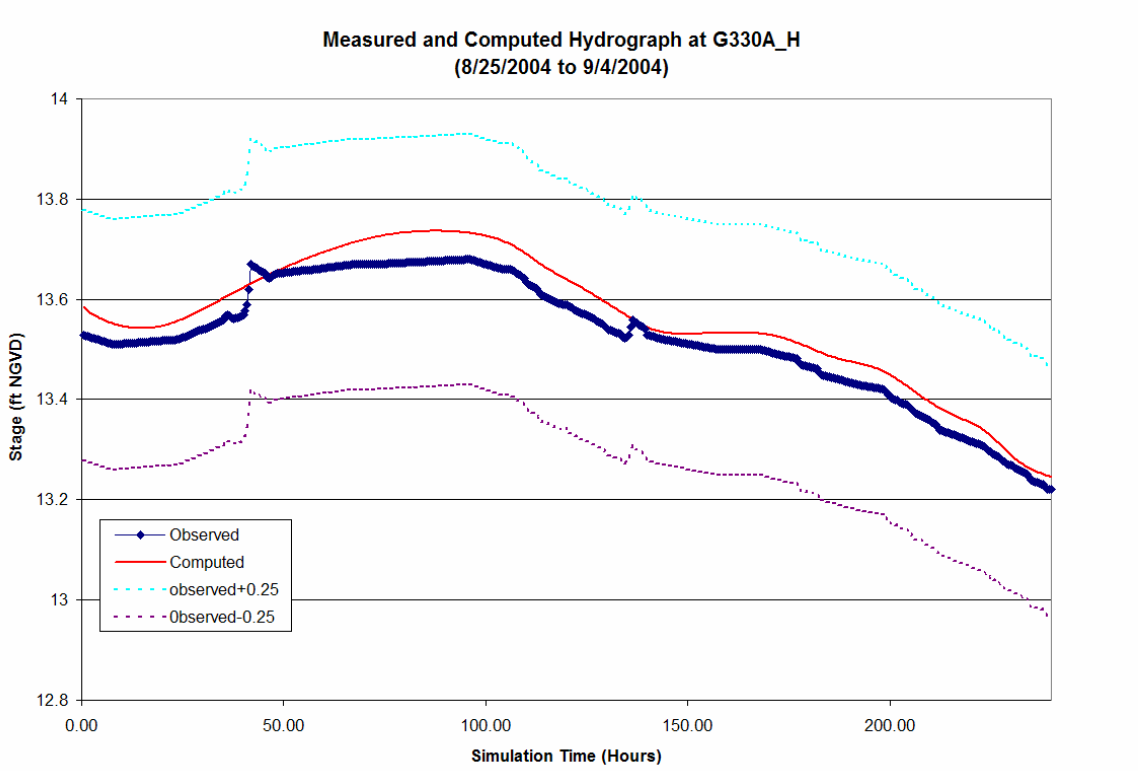

Figure 26 Computed and Measured Stage Hydrograph at G330A_H (calibration: 8/25/2004 to 9/4/2004)

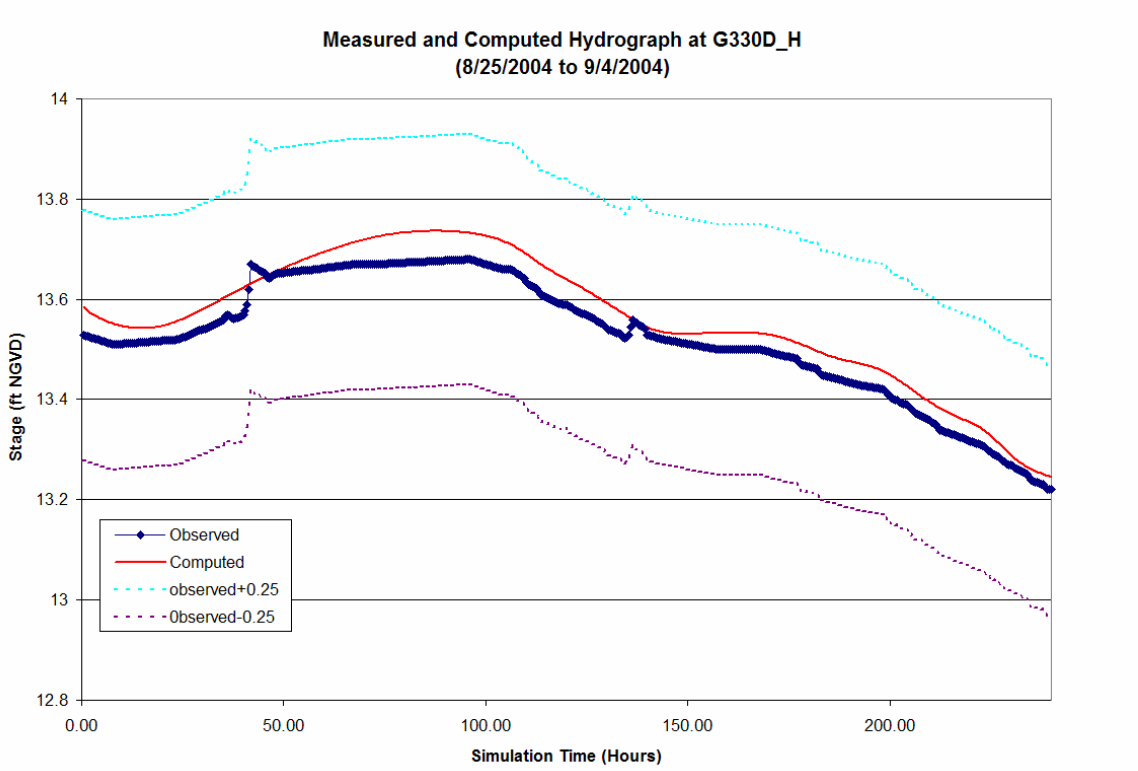

Figure 27 Computed and Measured Stage Hydrograph at G330D_H (calibration: 8/25/2004 to 9/4/2004)

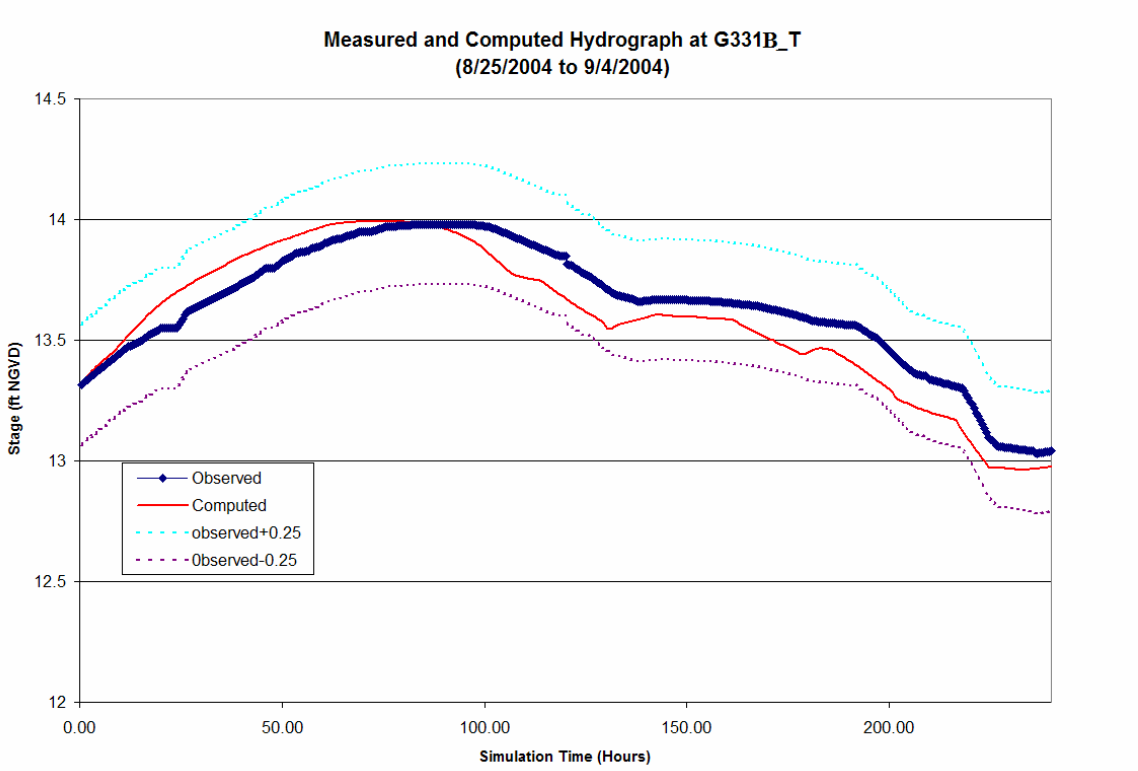

Figure 28 Computed and Measured Stage Hydrograph at G331B_T (calibration: 8/25/2004 to 9/4/2004)

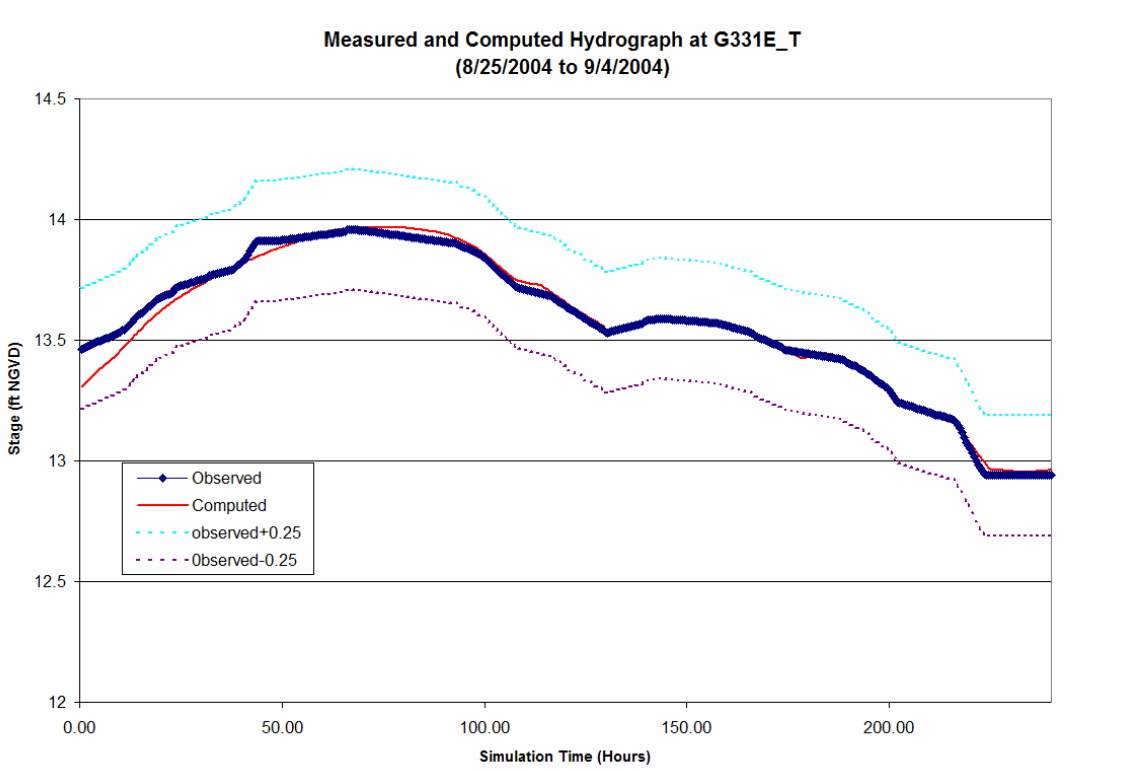

Figure 29 Computed and Measured Stage Hydrograph at G331E_T (calibration: 8/25/2004 to 9/4/2004)

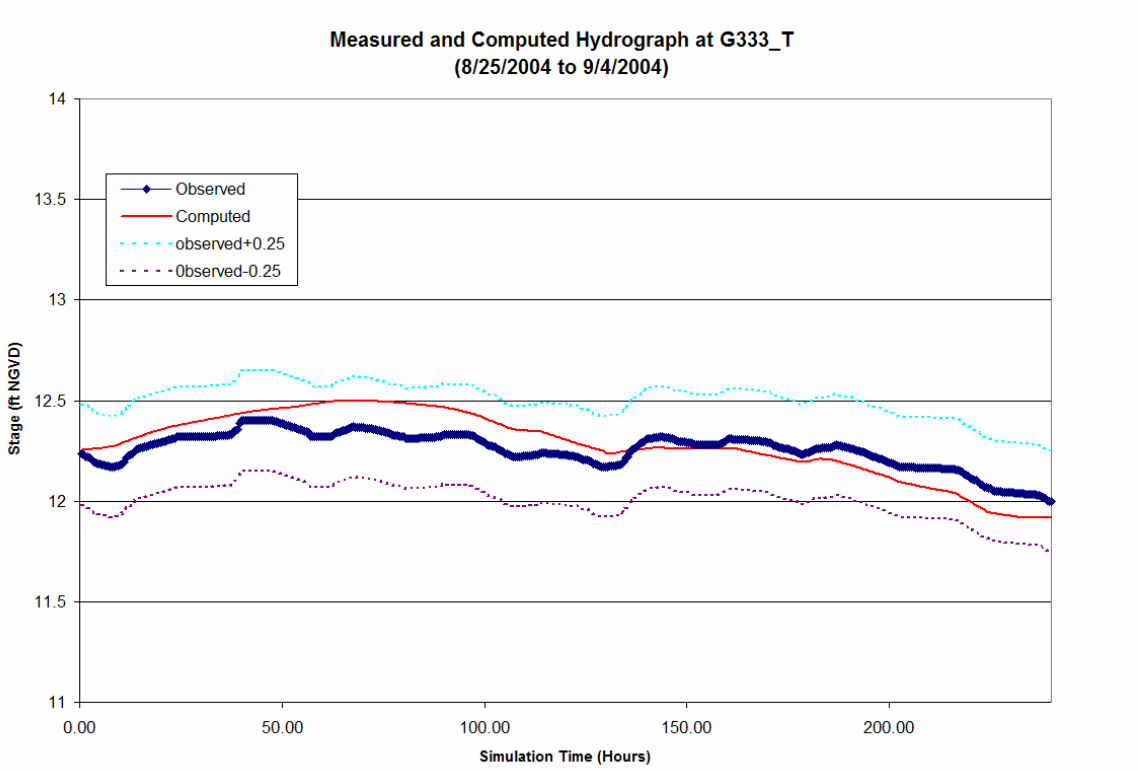

Figure 30 Figure 31 Computed and Measured Stage Hydrograph at G333_T (calibration: 8/25/2004 to 9/4/2004)

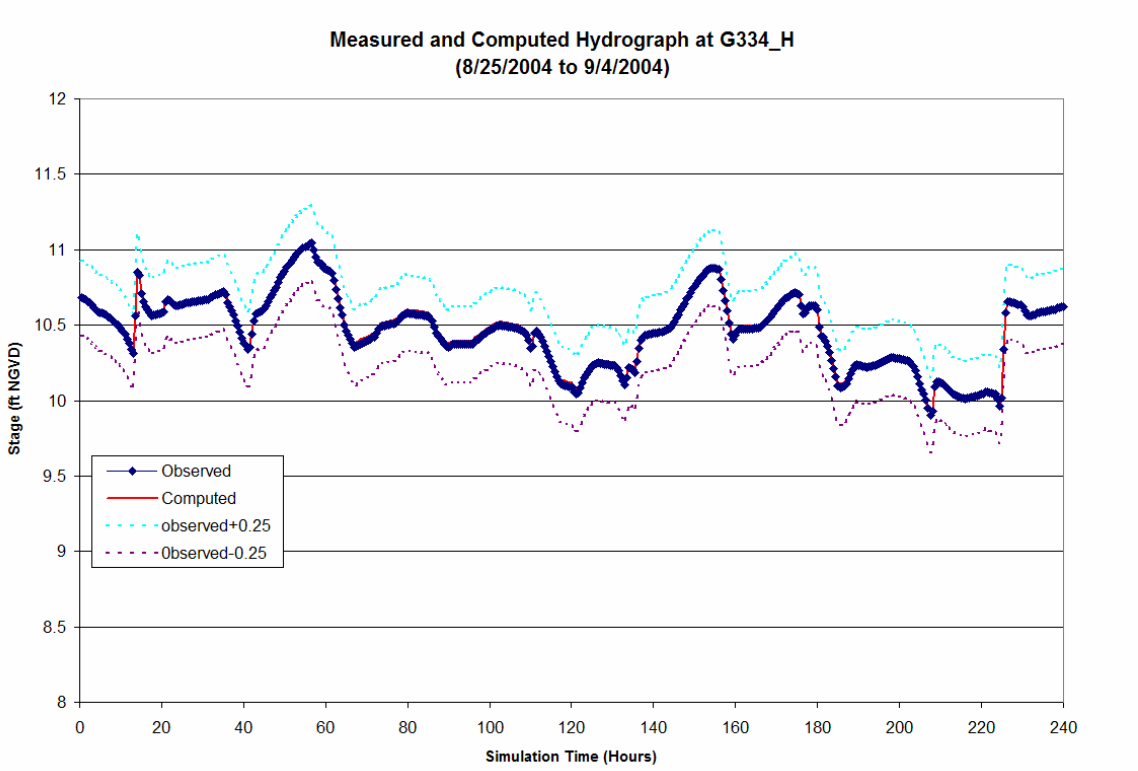

Figure 32 Figure 33 Computed and Measured Stage Hydrograph at G3334_H (calibration: 8/25/2004 to 9/4/2004)

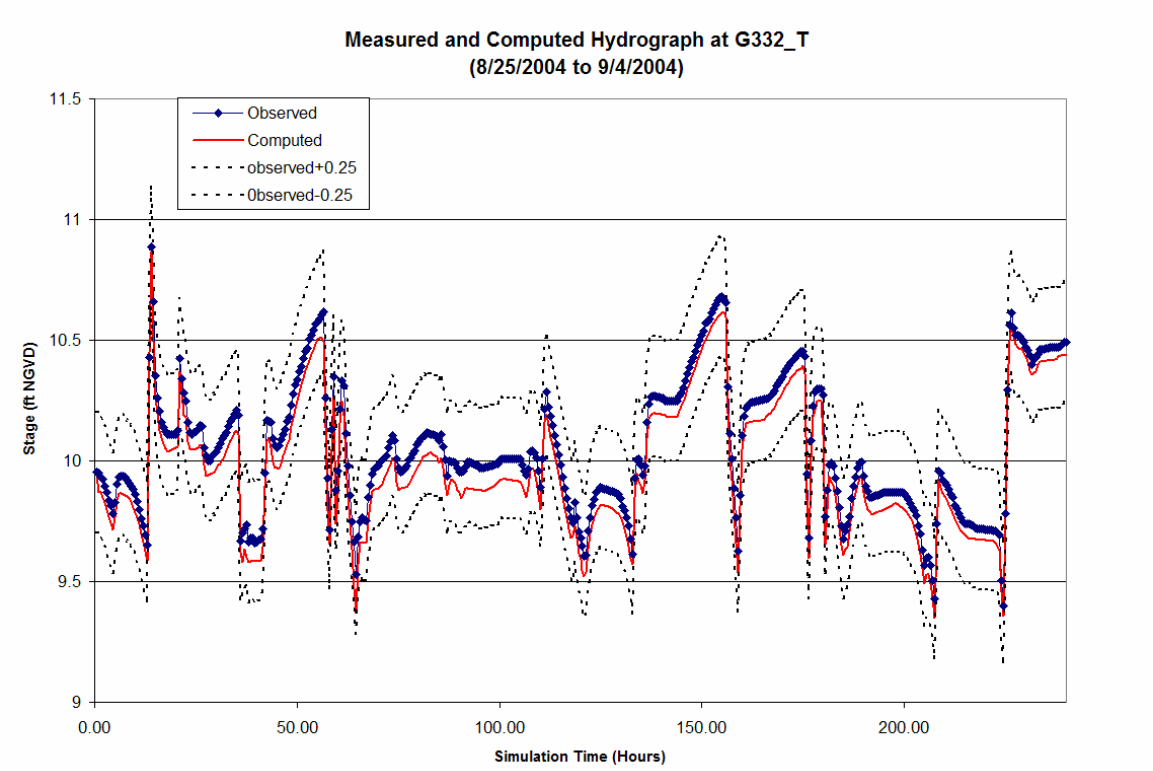

Figure 34 Computed and Measured Stage Hydrograph at G332_T (calibration: 8/25/2004 to 9/4/2004)

3.4 Model validation results

Independent observed stage and flow data that were not already used in model calibration were applied in model validation. The calibrated model parameters were kept unchanged during the model validation phase.

3.4.1 1st Model Validation

A time period of 120 hours (9/5/2004 to 9/10/2004, 5 days) was selected. The simulation was stopped right before a sudden total gate closing at G-334 (Figure 35; this can also be seen in G-332_H and G-334_H plots).

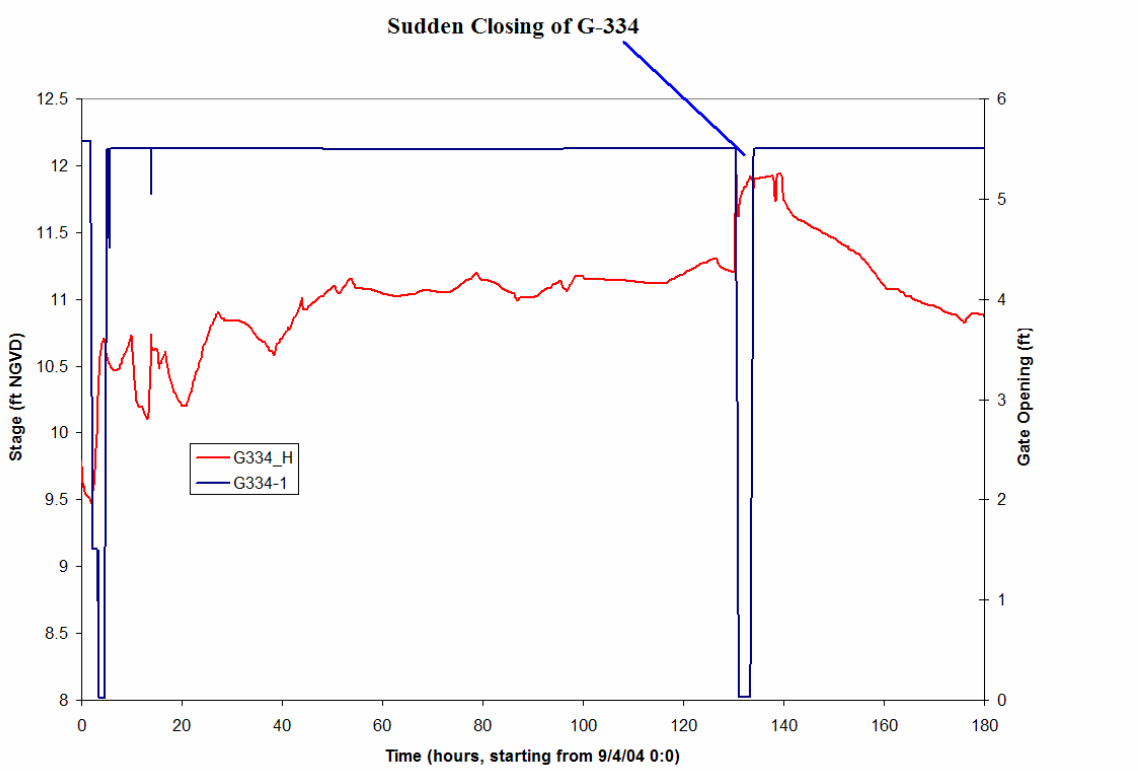

Figure 35 Sudden Closing of G-334 and Stage Spikes in G-334_H

The computed and observed stage data are compared in Figures 37-49. Similar to model calibration results, the small trends in Cell 3 stages (G-333_T, Figure 47) were not well captured by the model (R^2=0.17), although the absolute error is within 0.25 ft; Cell 1 stages are consistently well matched; the local variation in north end of Cell 2 stages (G-331B_T and G-331E_T) was not well reproduced in the model validation. These two stations are close to each other and gate opening were the same, but there is an approximate 0.3 ft difference in the observed water levels (Figure 36). The reason for this local hydraulic gradient is still unclear. The recorded sampling time intervals for G-331B_T are also large (e.g., 24 hours) for part of the time period.

In summary, there is only a time segment of about 40 hours where computed error in G-331B_T exceeds 0.25 ft. and G-331E_T is within ±0.25 ft target. For this reason, the overall model calibration is considered satisfactory.

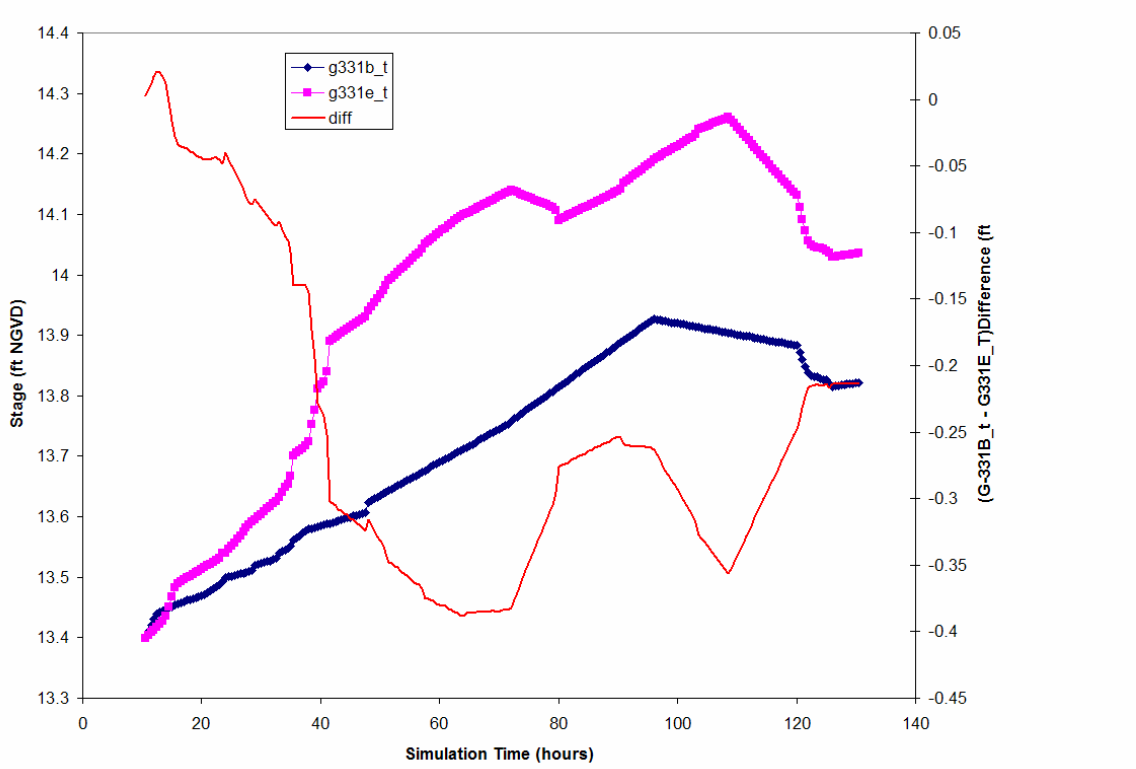

Figure 36: Observed Stages at North end of Cell 2 (G331B_T and G331E_T)

Table 4. Statistics on Model Validation

Stations	Maximum absolute error (ft)	Average absolute error (ft)	R-square
G328_T		As boundary	
G329_H	0.30	0.041	0.99
G329_T	0.07	0.038	0.99
G330A_H G330D_H	0.08 0.11	0.044 0.046	0.99 0.99
G331B_T G331E_T	0.48 0.25	0.23 0.12	0.92 0.88
G332_H		As boundary	
G333_T	0.24	0.15	0.17
G334_H		As boundary	
G332_T	0.32	0.075	0.99
G335_H		As boundary	
G331_H	0.32	0.092	0.99
G333_H	0.22	0.057	0.99

3.4.2 2nd Model Validation

Taking into consideration the results of the first model validation effort, another model validation run was performed. The second validation run was a 96-hour simulation period (9/11/2004 to 9/14/2004) with a cold start after the sudden closings of G-334 and G-332.

The computed water levels matched observed stages quite well except that there is over-prediction in G-331B_T and G-331E_T (Figures 50 to 60) over a short time segment. This may be a culvert flow computation problem. It can also be seen that the initial condition for Cell 1 was underestimated, but the history matching is very good for G-329_T, G-330A_H and G-330D_H after the initial condition impact.

These results further validate that the calibrated model can make water level predictions within the specified accuracy.

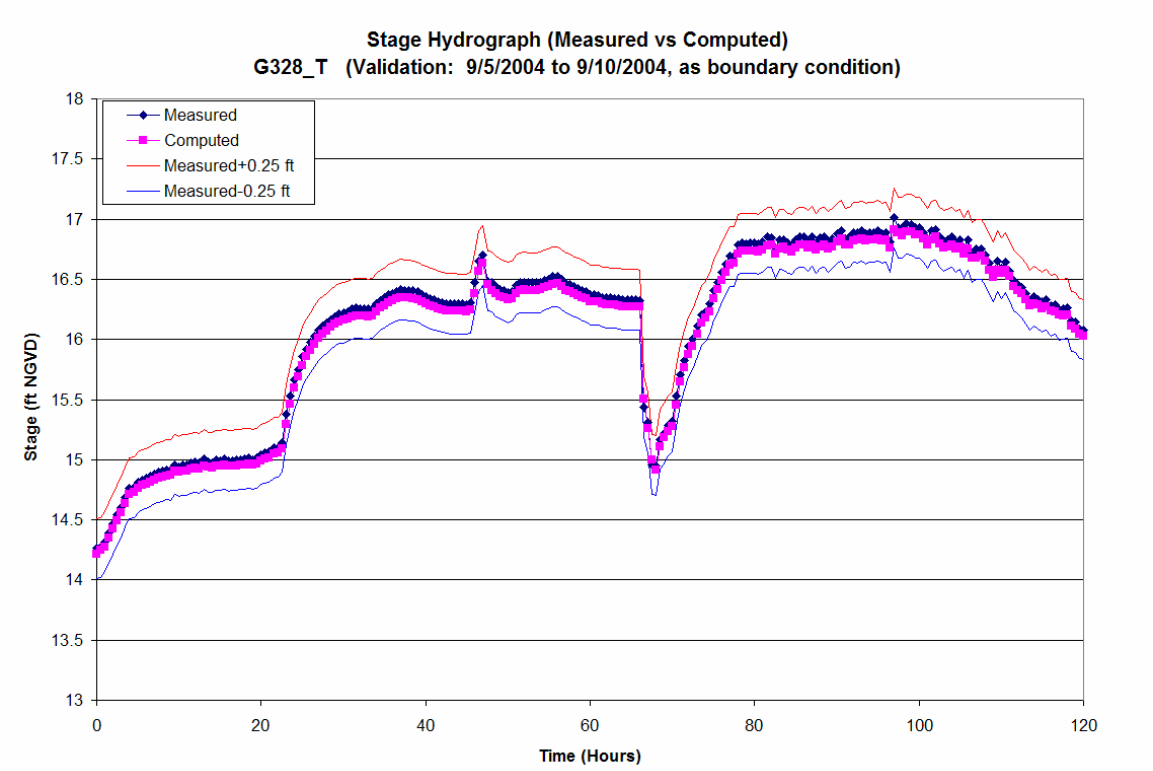

Figure 37: Computed and Measured Stage Hydrograph at G328_T (validation: 9/5/2004 to 9/10/2004, as boundary condition)

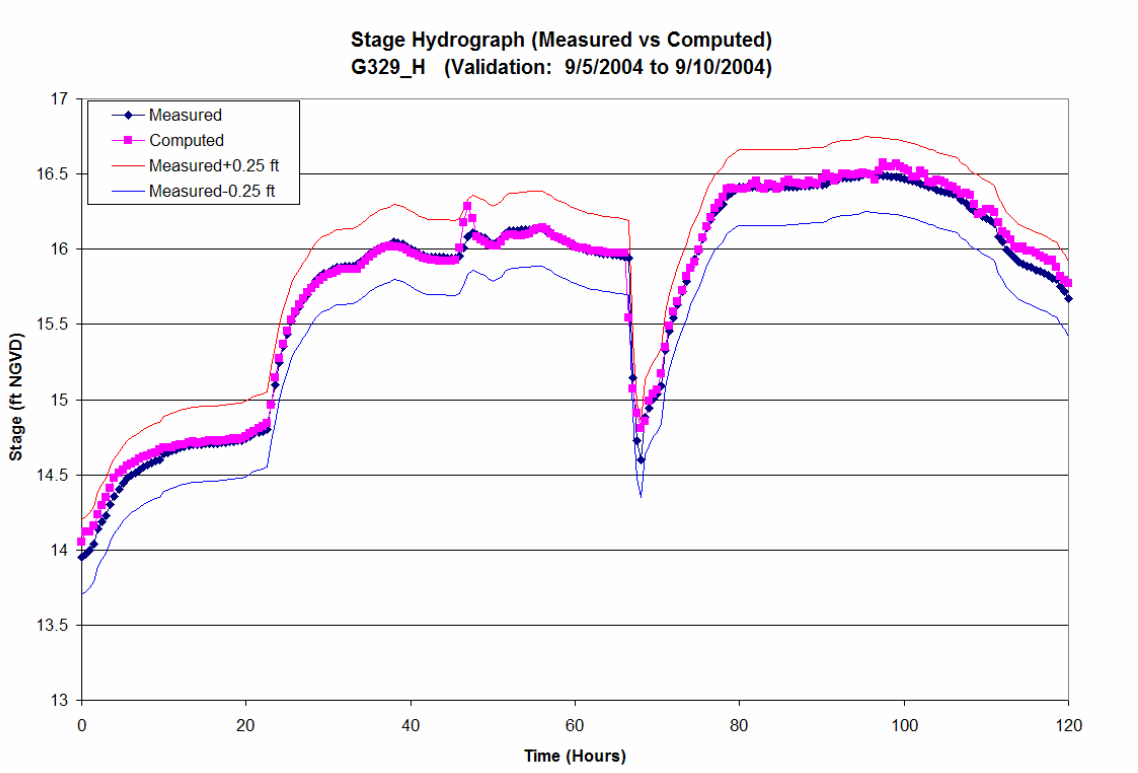

Figure 38: Computed and Measured Stage Hydrograph at G329_H (validation: 9/5/2004 to 9/10/2004)

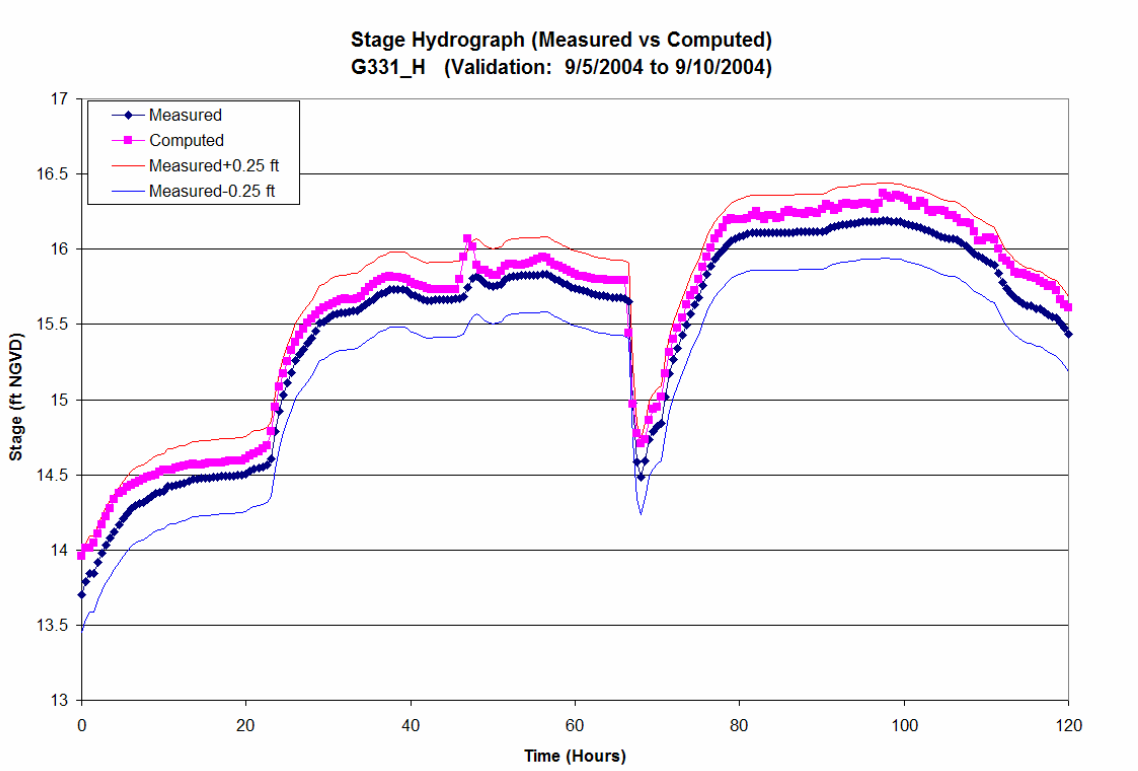

Figure 39: Computed and Measured Stage Hydrograph at G331_H (validation: 9/5/2004 to 9/10/2004)

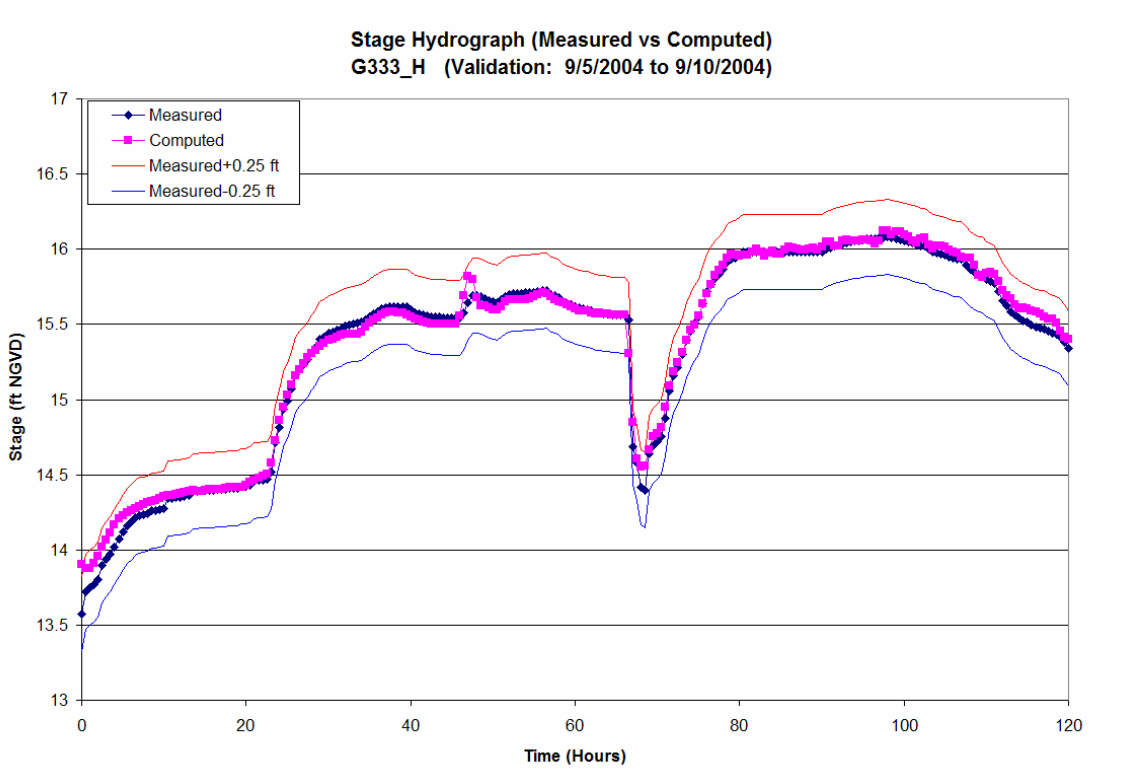

Figure 40: Computed and Measured Stage Hydrograph at G333_H (validation: 9/5/2004 to 9/10/2004)

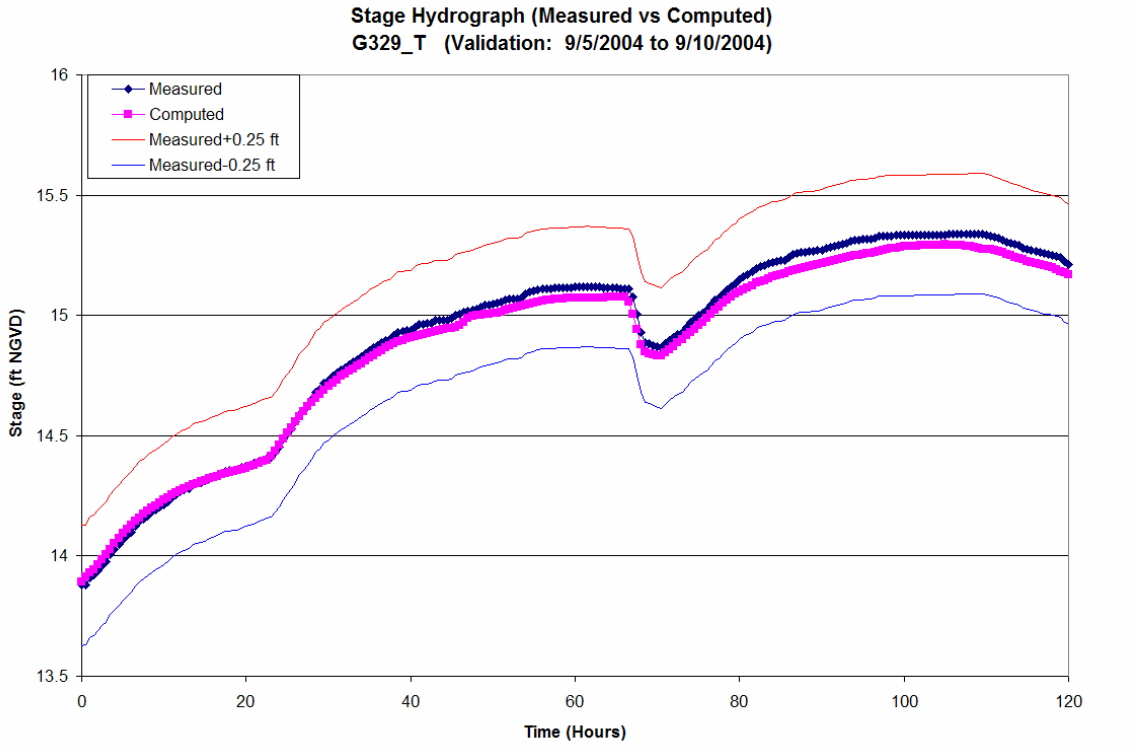

Figure 41: Computed and Measured Stage Hydrograph at G329_T (validation: 9/5/2004 to 9/10/2004)

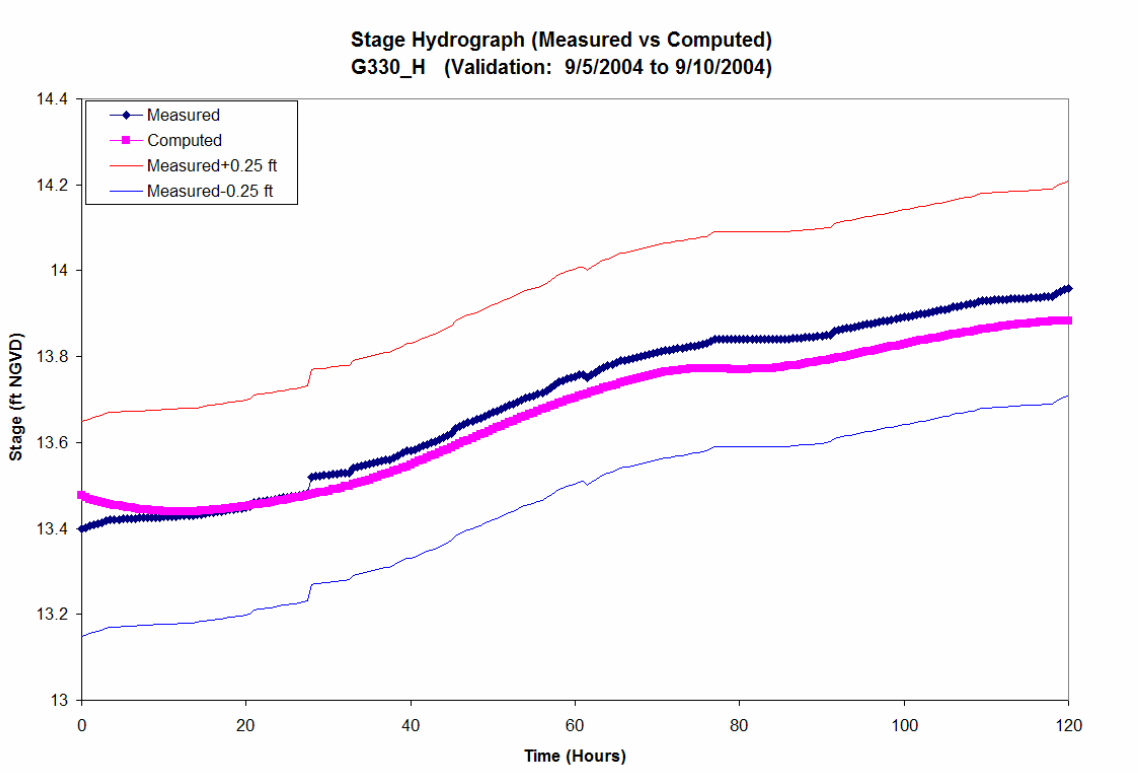

Figure 42: Computed and Measured Stage Hydrograph at G330A_H (validation: 9/5/2004 to 9/10/2004)

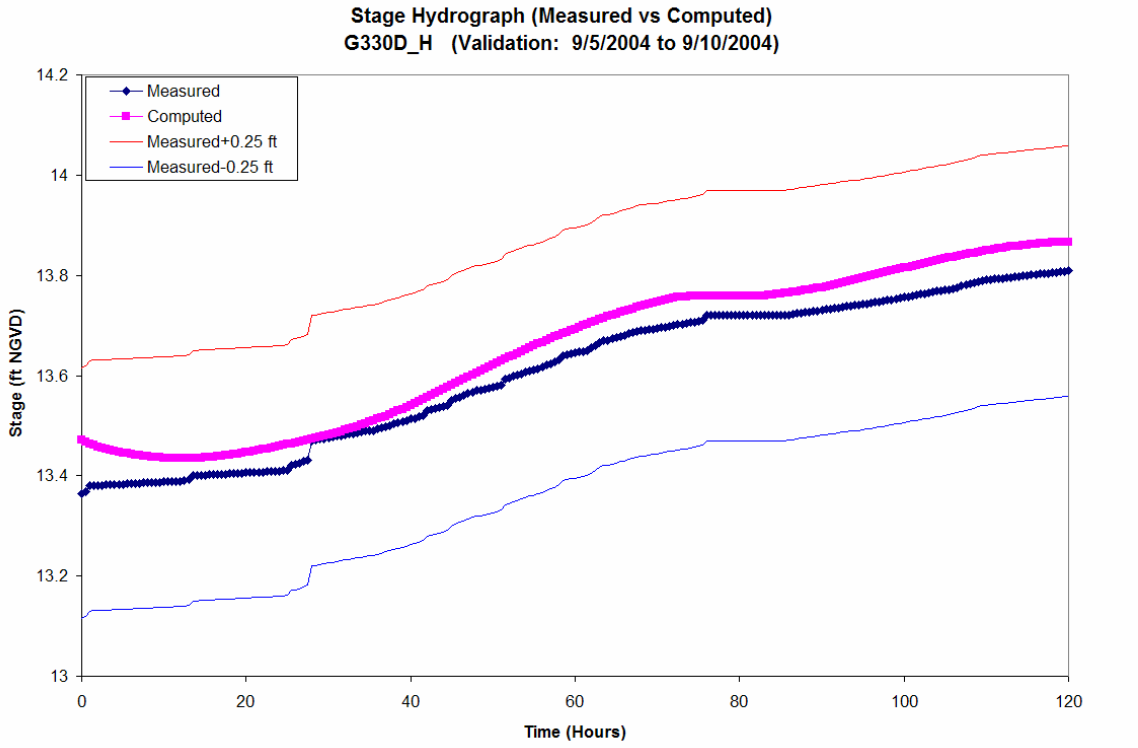

Figure 43: Computed and Measured Stage Hydrograph at G330D_H (validation: 9/5/2004 to 9/10/2004)

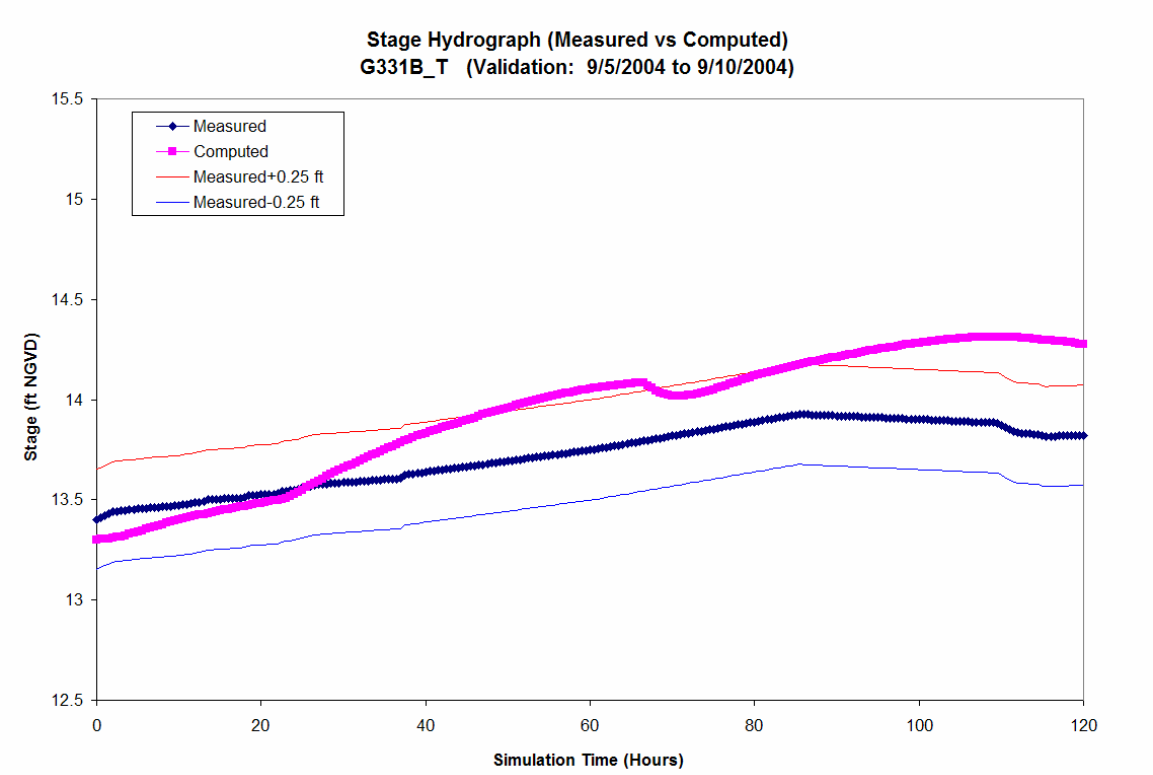

Figure 44: Computed and Measured Stage Hydrograph at G331B_T (validation: 9/5/2004 to 9/10/2004)

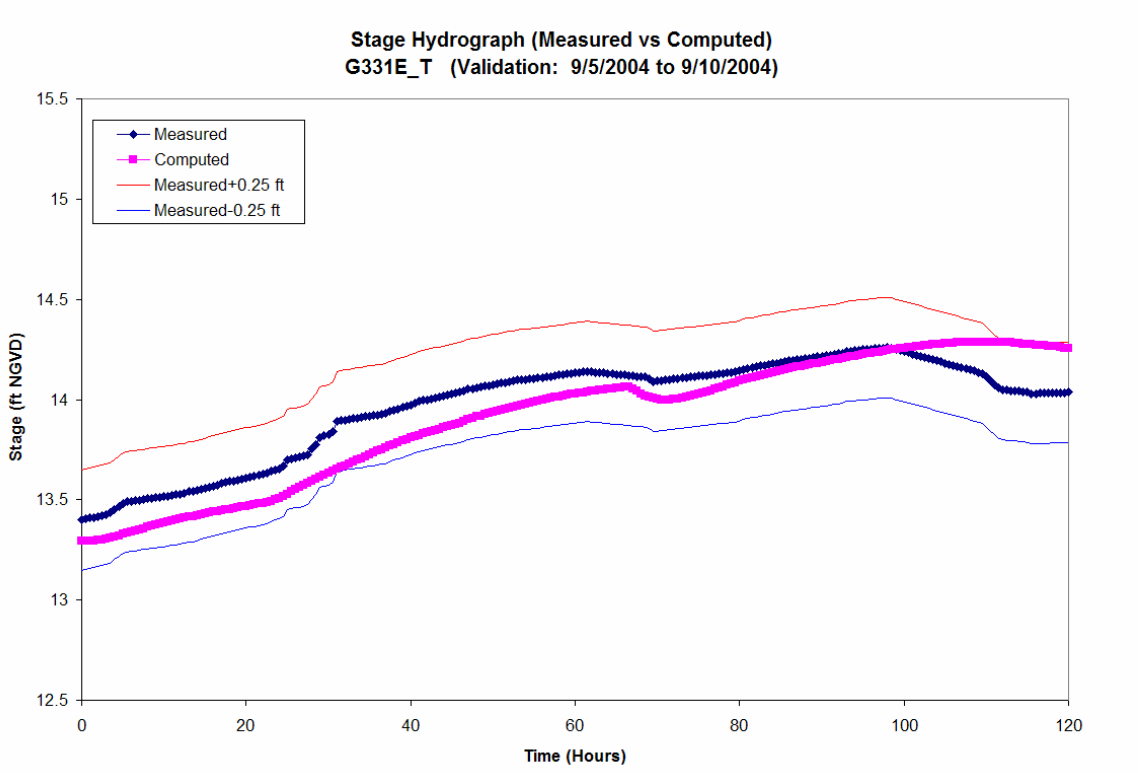

Figure 45: Computed and Measured Stage Hydrograph at G331E_T (validation: 9/5/2004 to 9/10/2004)

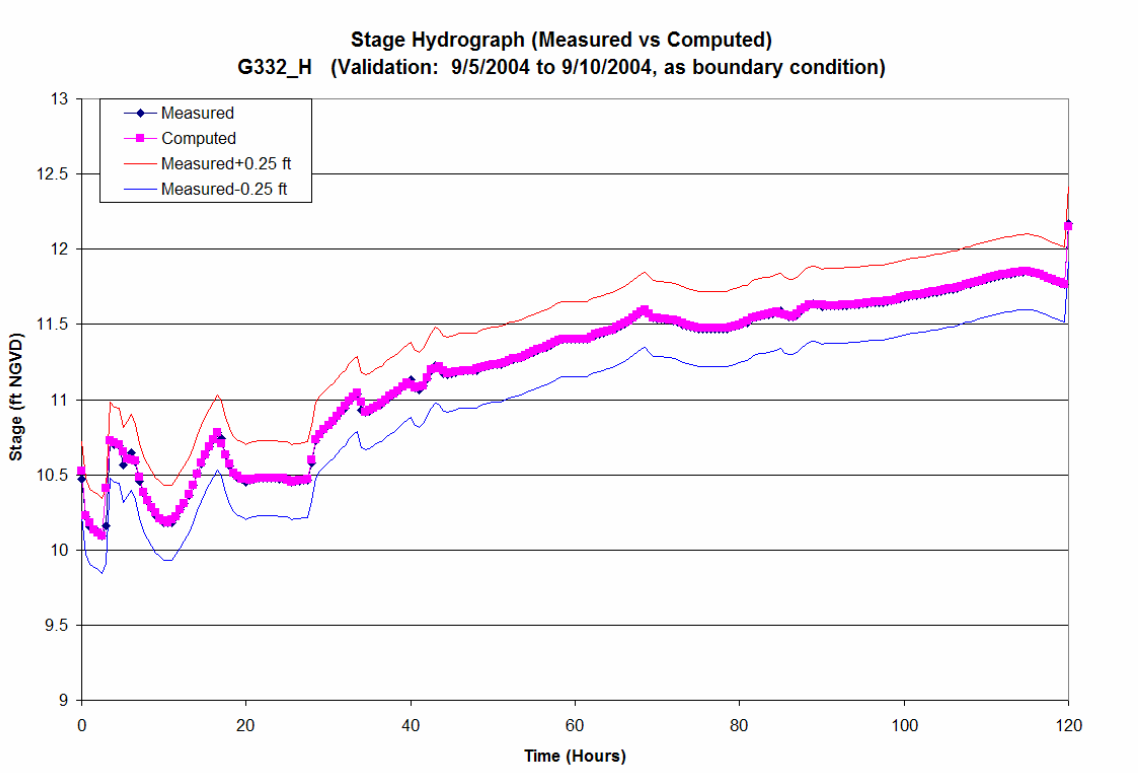

Figure 46: Computed and Measured Stage Hydrograph at G332_H (validation: 9/5/2004 to 9/10/2004, as boundary condition)

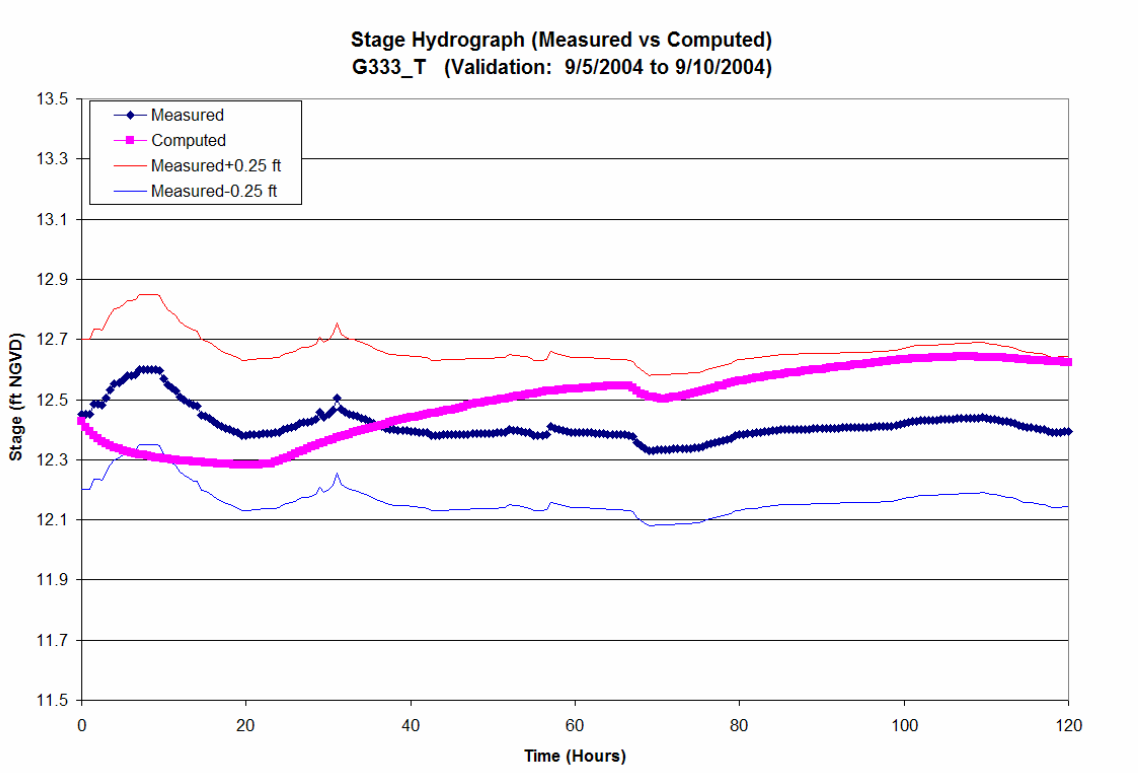

Figure 47: Computed and Measured Stage Hydrograph at G333_T (validation: 9/5/2004 to 9/10/2004)

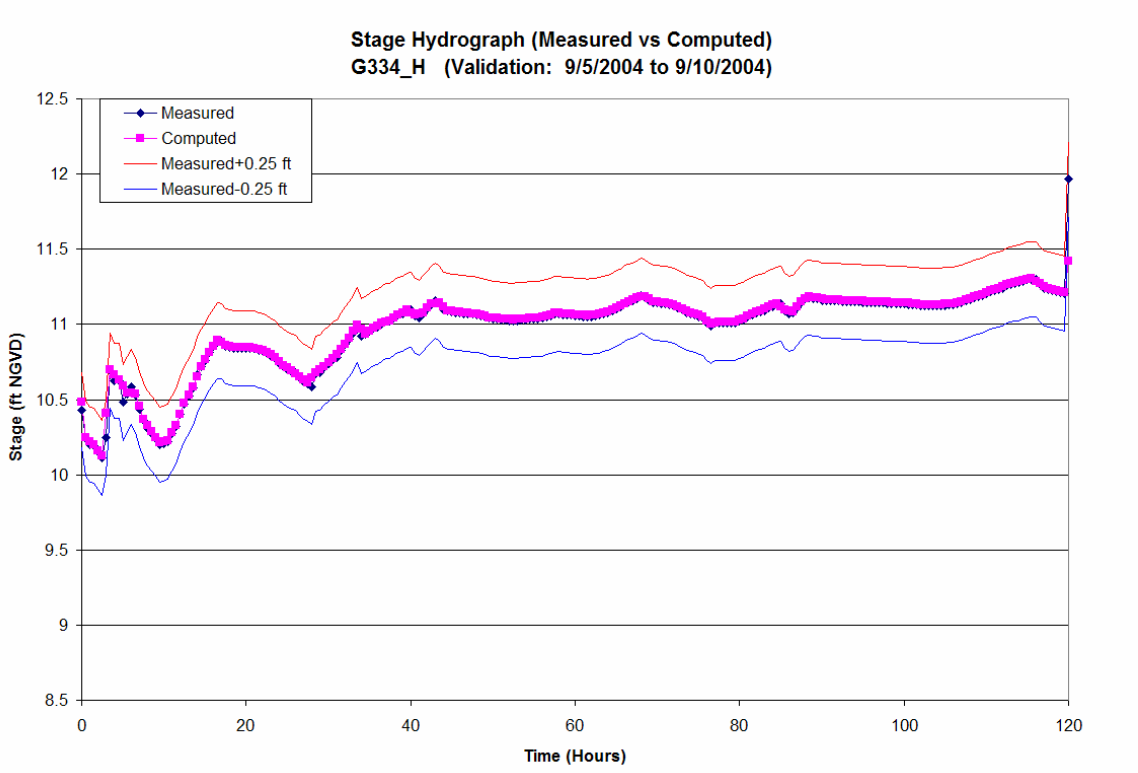

Figure 48: Computed and Measured Stage Hydrograph at G334_H (validation: 9/5/2004 to 9/10/2004, as boundary condition)

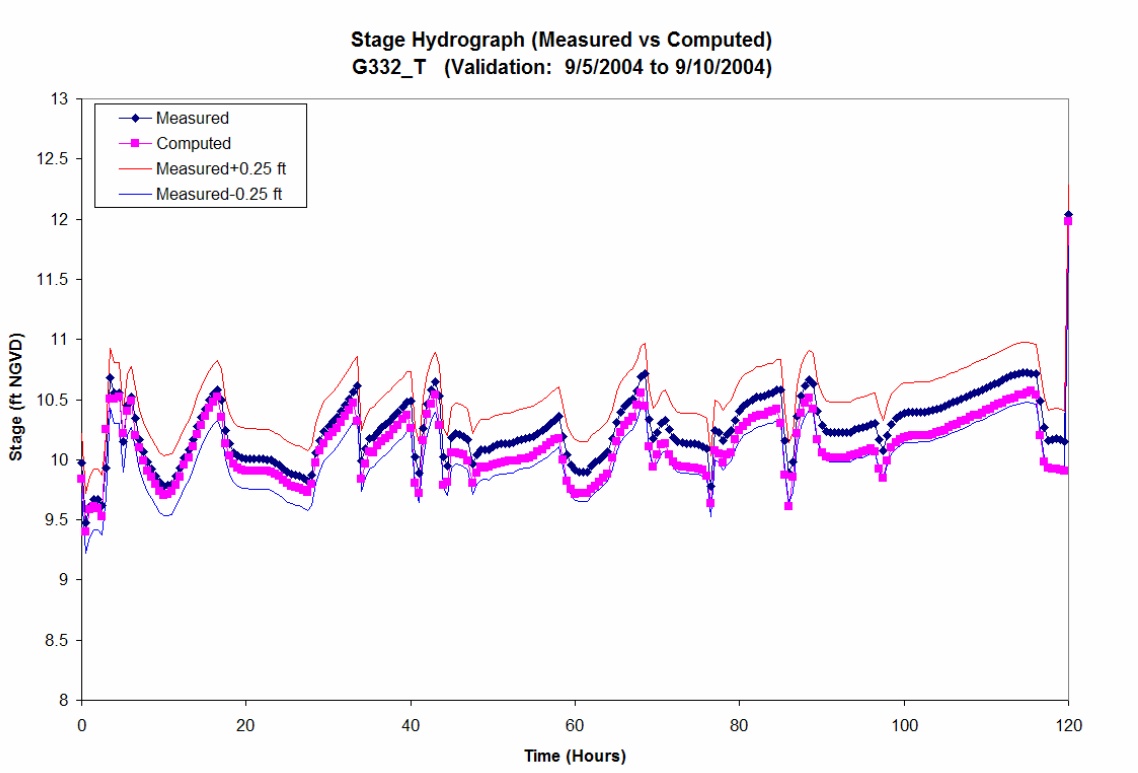

Figure 49: Computed and Measured Stage Hydrograph at G332_T (validation: 9/5/2004 to 9/10/2004)

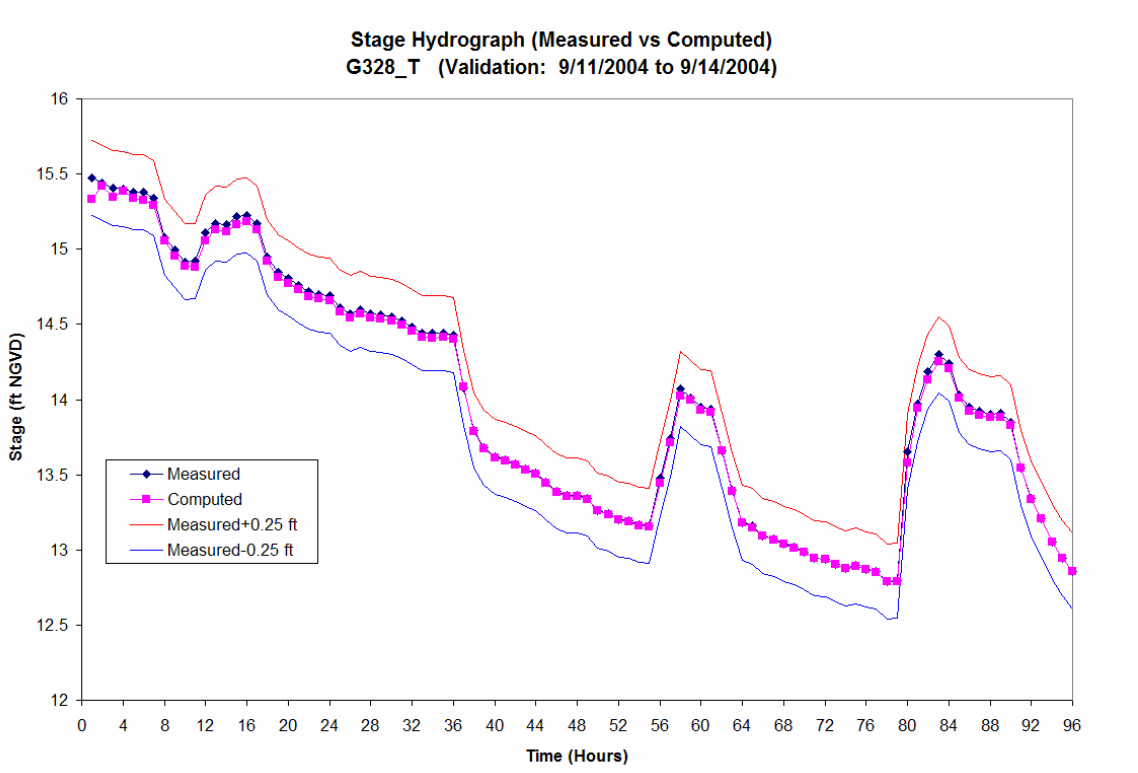

Figure 50: Computed and Measured Stage Hydrograph at G328_T (validation: 9/11/2004 to 9/14/2004, as boundary condition)

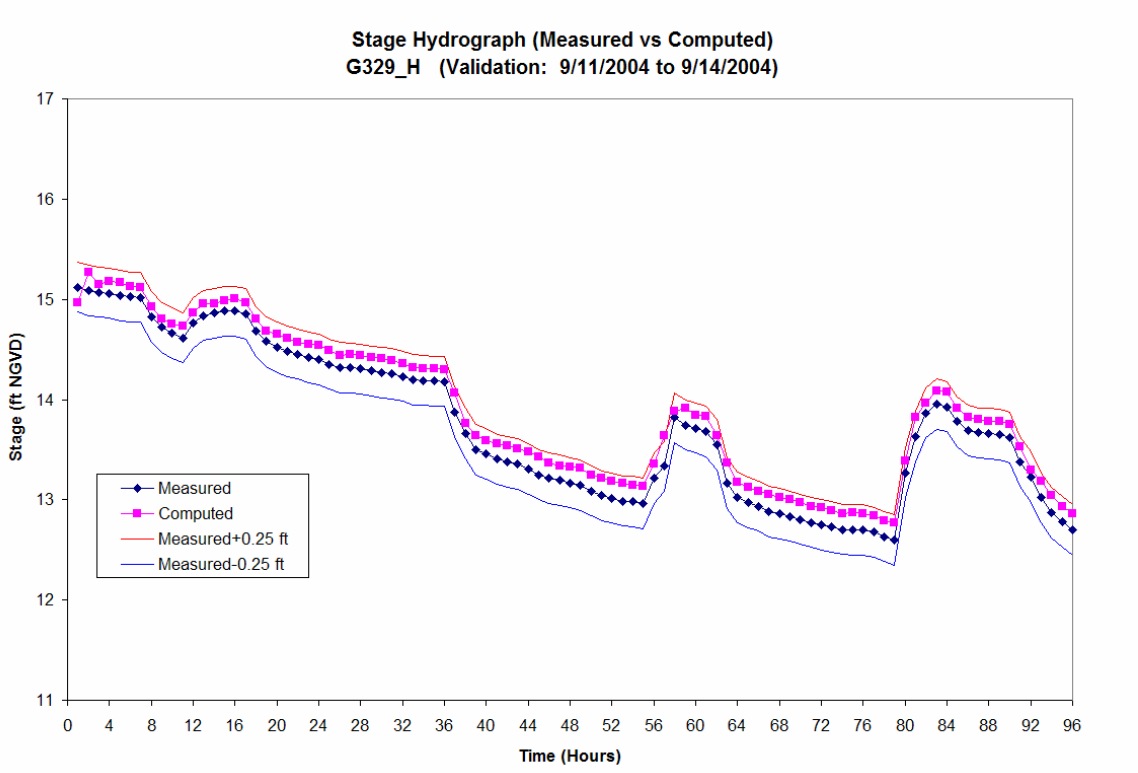

Figure 51: Computed and Measured Stage Hydrograph at G329_H (validation: 9/11/2004 to 9/14/2004)

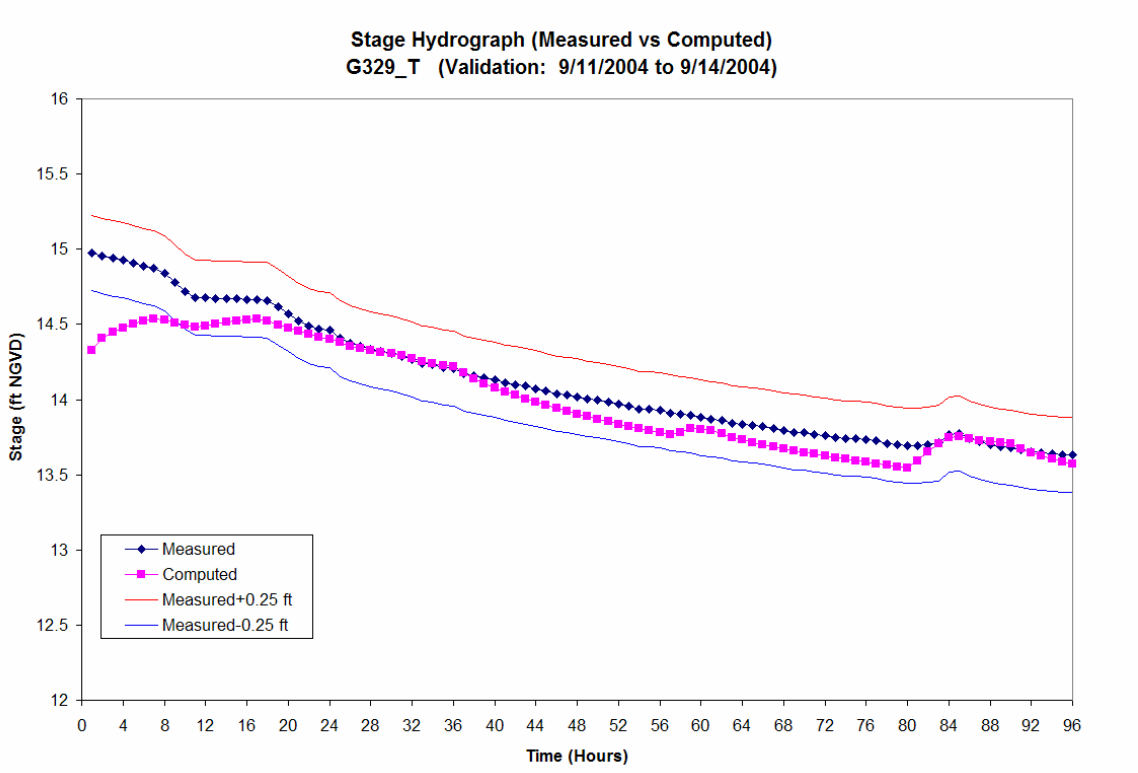

Figure 52: Computed and Measured Stage Hydrograph at G329_T (validation: 9/11/2004 to 9/14/2004)

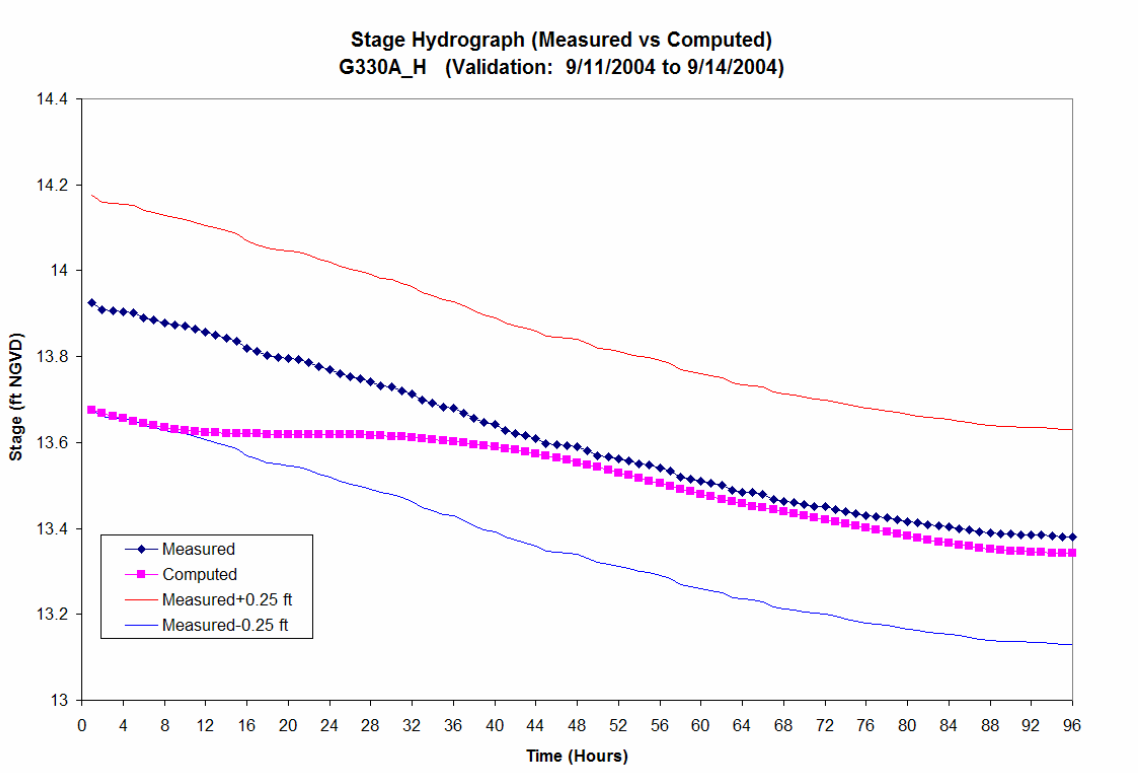

Figure 53: Computed and Measured Stage Hydrograph at G330A_H (validation: 9/11/2004 to 9/14/2004)

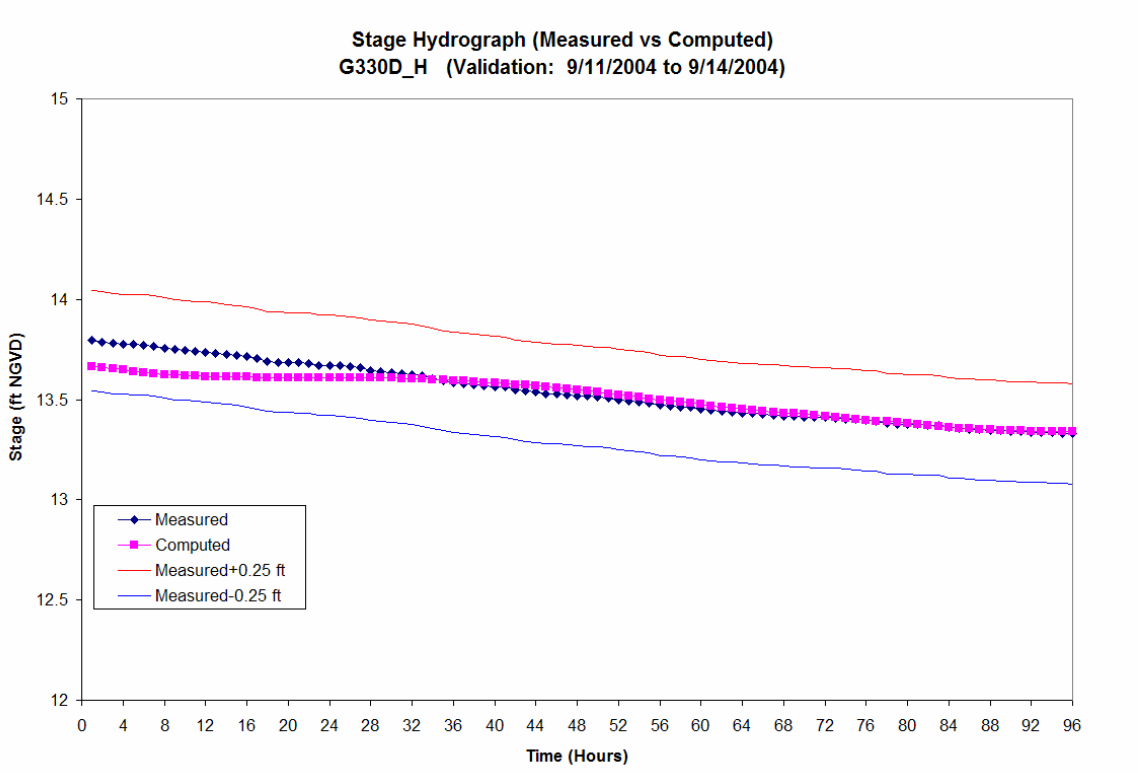

Figure 54: Computed and Measured Stage Hydrograph at G330D_H (validation: 9/11/2004 to 9/14/2004)

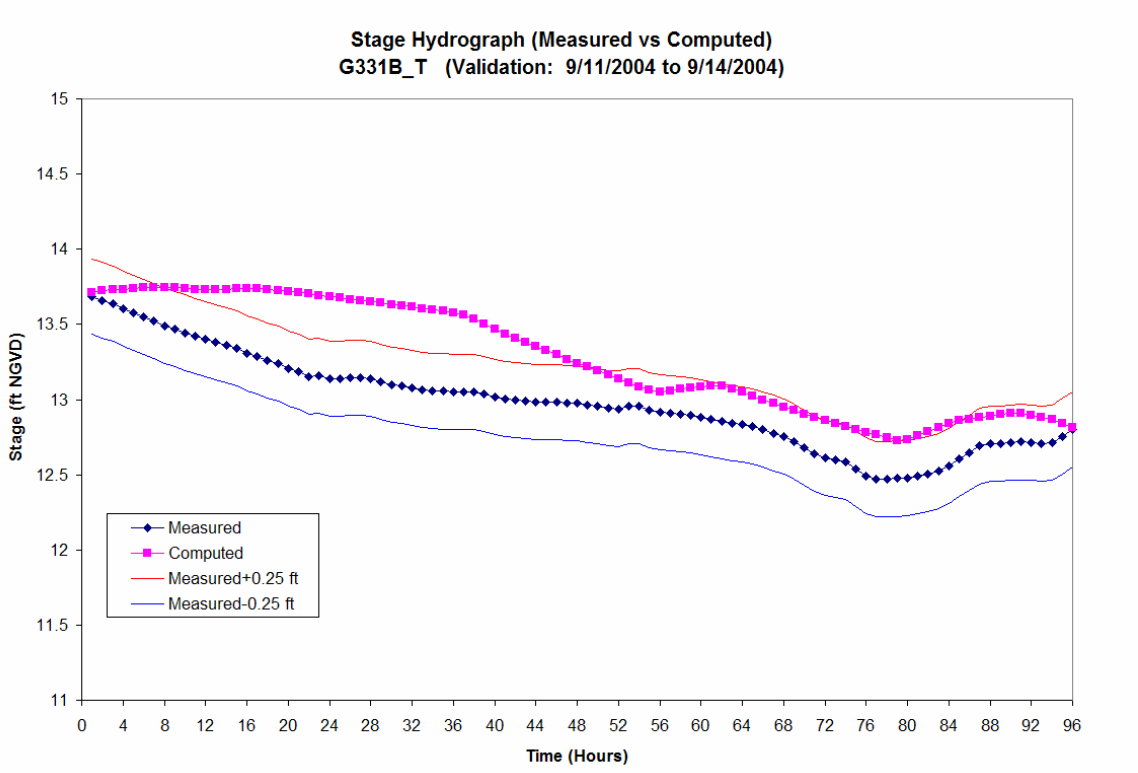

Figure 55: Computed and Measured Stage Hydrograph at G331B_T (validation: 9/11/2004 to 9/14/2004)

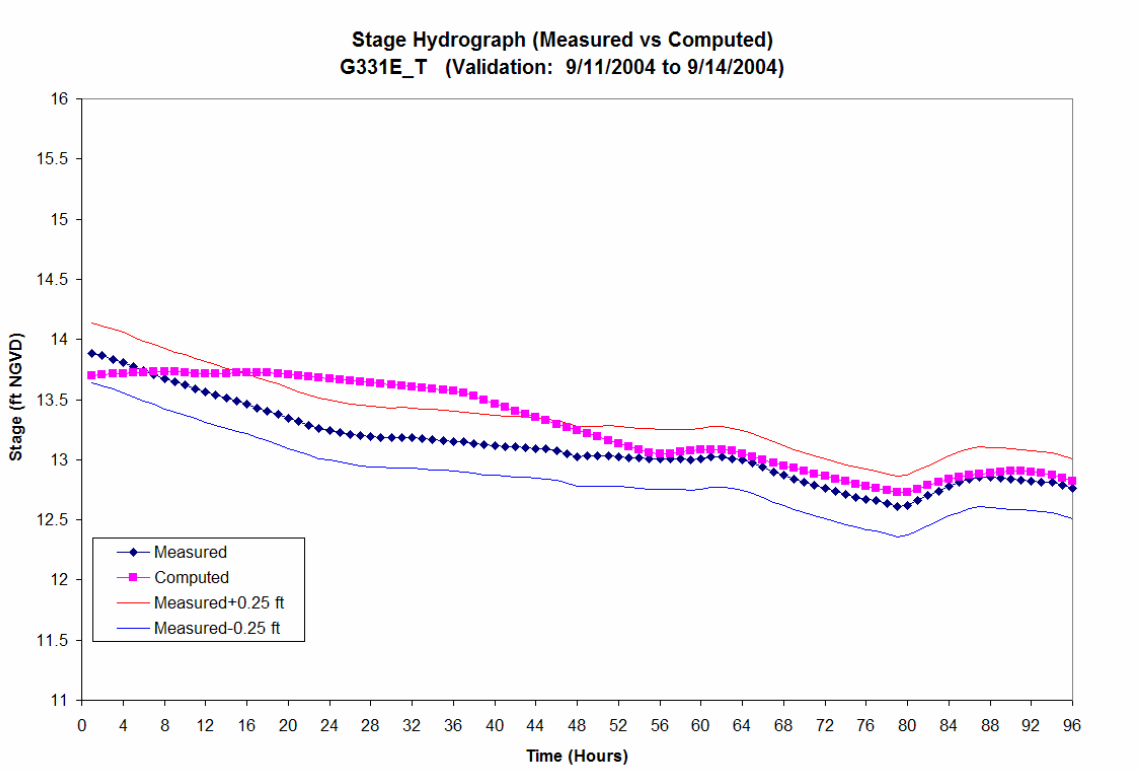

Figure 56: Computed and Measured Stage Hydrograph at G331E_T (validation: 9/11/2004 to 9/14/2004)

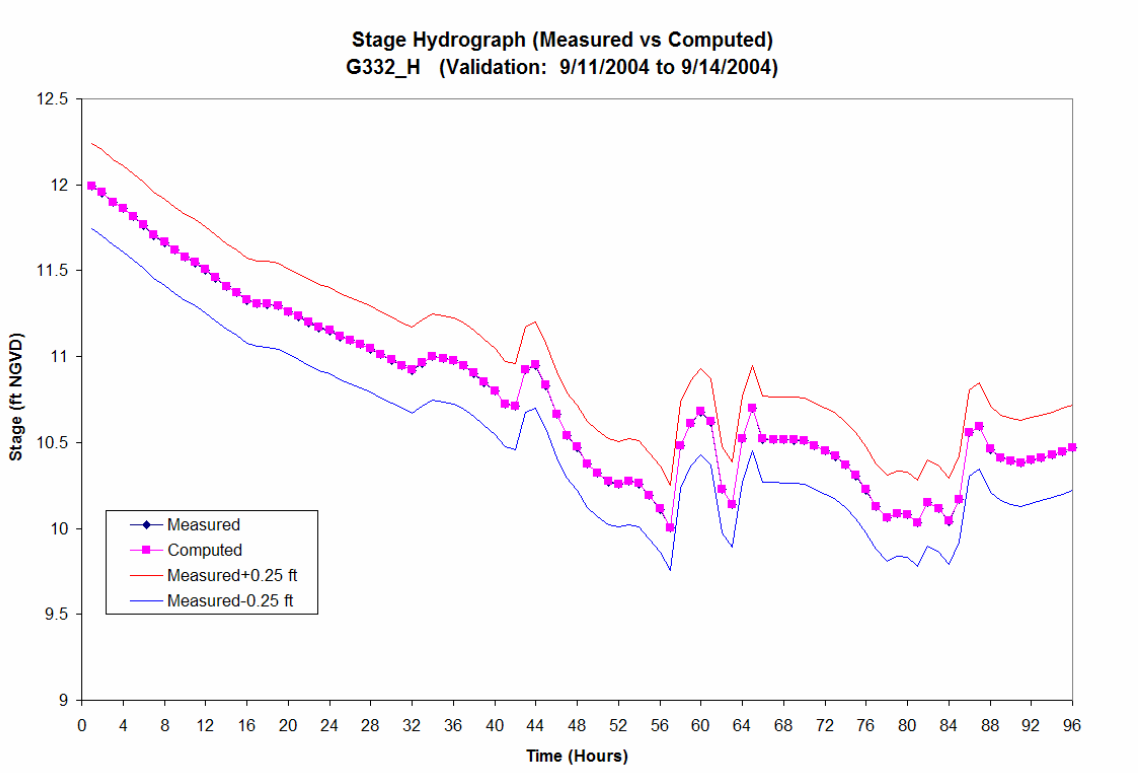

Figure 57: Computed and Measured Stage Hydrograph at G332_H (validation: 9/11/2004 to 9/14/2004, as boundary condition)

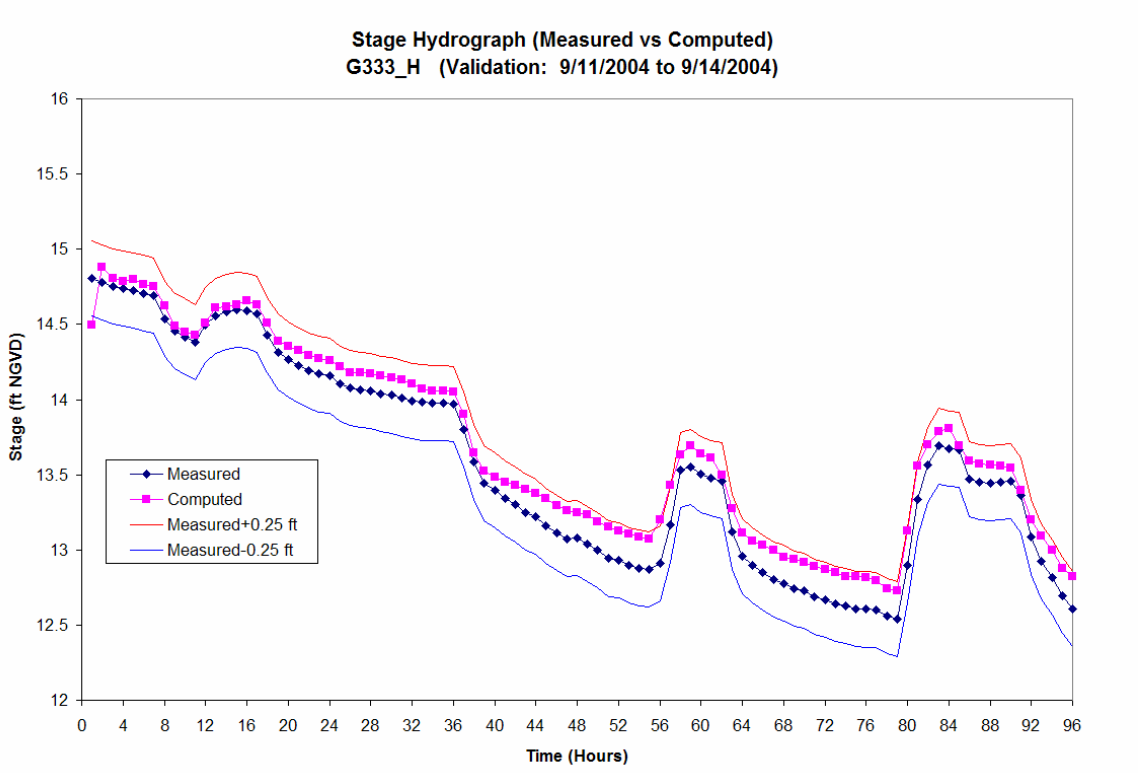

Figure 58: Computed and Measured Stage Hydrograph at G333_H (validation: 9/11/2004 to 9/14/2004)

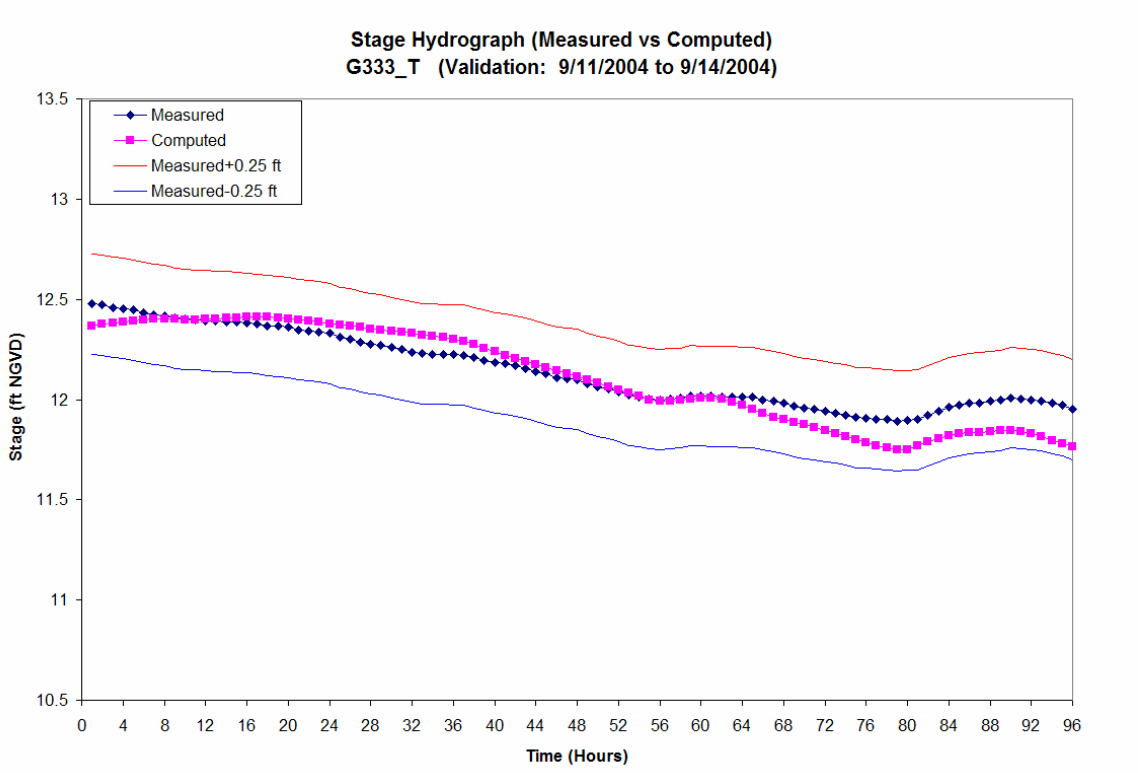

Figure 59: Computed and Measured Stage Hydrograph at G333_T (validation: 9/11/2004 to 9/14/2004)

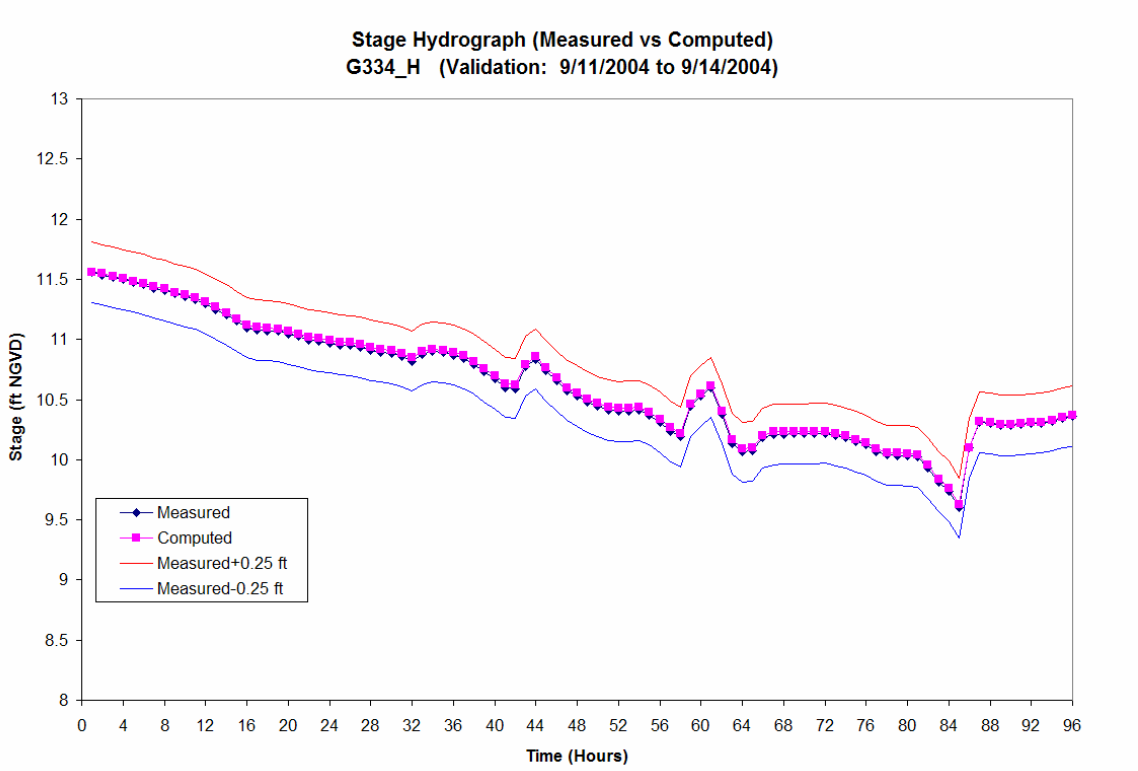

Figure 60: Computed and Measured Stage Hydrograph at G334_H (validation: 9/11/2004 to 9/14/2004, as boundary condition)

3.5 Calibrated Model Parameters

The final Manning's roughness coefficient values used in both model calibration and validation are listed in Table 5 and plotted in Figure 61. When compared to previous values for the STA-2 single cell models (Sutron Corp. 2004a), nearly identical depth-dependent Manning's n was used for SAV; for cattails, the base Manning's n value was increased from 0.5 to 0.8 to better match observed stages at various structure locations. Manning's n values for different types of canals were also been increased by 0.02 to 0.03. As discussed before, previous single cell model calibration was based on measured daily water depth data from water quality data collection and should be considered less reliable and less accurate than the results of the current modeling effort.

The piecewise linear depth dependent relationship for Manning's roughness coefficient has been coded into FLO2DH. The most relevant reference of the impact of vegetation on flow resistance is (Wu et al. 1999). The referenced experiment study showed that Manning's n value of unsubmerged vegetation (such as cattails) is dependent only on water depth; however for submerged vegetation (such as SAV), Manning's n value is positively correlated to height of vegetation and negatively related to depth of flow.

The flow depth threshold for submergence is 0.5 ft for SAV to approximate its submergence region. For cattails, the general relationship of decreasing Manning's n values with increasing flow depth is reflected.

Table 5. Manning's n Values for Different Materials

Depth (ft)	For cattails	For SAV	Canals
>3.0	0.8	0.3	0.05 to 0.06
3.0	0.8	0.3	
3.0 to 1.0	Varies linearly	Varies linearly	
1.0	1.1		
<=0.5	1.1	0.8	

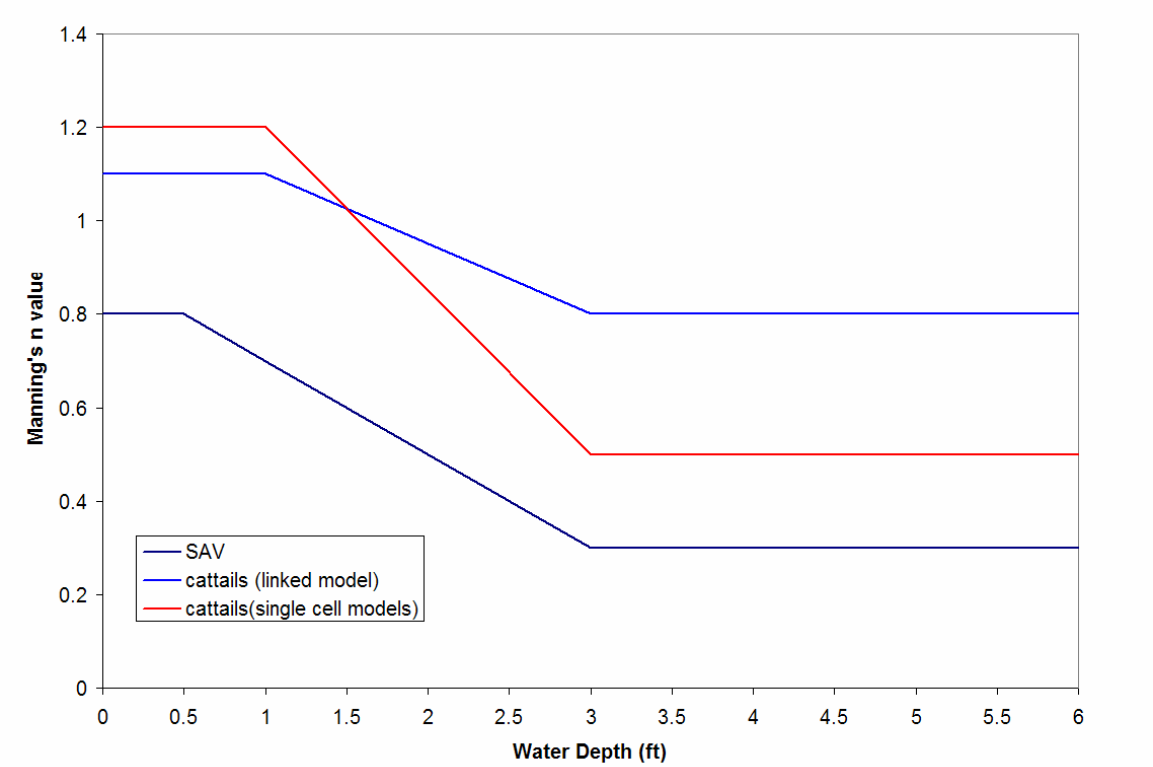

Figure 61: Water Depth-dependent Manning's n Values

4. Model Limitations and Uncertainty

Major limitations of FLO2DH in simulating STA hydraulics include:

- Hydraulics structures are not well represented. Some STA inflow/outflow structures cannot be explicitly simulated. Gate operations also cannot be simulated.
- The model simulates surface water flow only. The surface water/groundwater interaction cannot be represented.
- Rainfall and evaportranspiration cannot be conveniently represented.
- The computation is intensive and model calibration and validation cannot make use of long-term historic time series data (several years for most STAs).
- The computer code cannot handle extensive and frequent wetting and drying well. Numerical instabilities are encountered for low flow condition.

The major uncertainties that may affect model calibration and validation results are discussed as follows.

Flow distribution among the three treatment cells is computed by FLO2DH's culvert option. The headwater and tailwater levels at inflow culverts G-329 A-D, G-331 A-G, G-333 A-E are largely determined by flow through the culverts.

The limitation of FLO2DH in flow structure representation and treatment of seepage losses, rainfall and evapotranspiration are the major uncertainty in model calibration.

- **Gate opening approximation**

The issue of partial gate openings has been previously discussed in this report. The best approach may be to calibrate parameters in the FLO2DH culvert flow equation to match measured flow data (stream gauging data). This is beyond the current scope of work. If the source code of FLO2DH is made available, then the District's culvert flow routines can be implemented into FLO2DH in a future work effort.

- **S-6 and G-328, G-337 pumping rate as upstream boundary condition**

In theory, the use of a specified flow rate or specified stage as an upstream boundary condition should yield almost identical model calibration and validation results. In reality, the uncertainty in structure representation and flow rating equations will have an impact on the simulation results. The model calibration and validation simulations were performed with a combined flow rate (S-6+G-328+G337 pumping) and the history-matching result is close to those with specified stage as boundary conditions. As an example, the computed and observed stages at G-329_T (Cell 1 north end) are compared for model validation (9/5/2004 to 9/10/2004) in the following Figure 62.

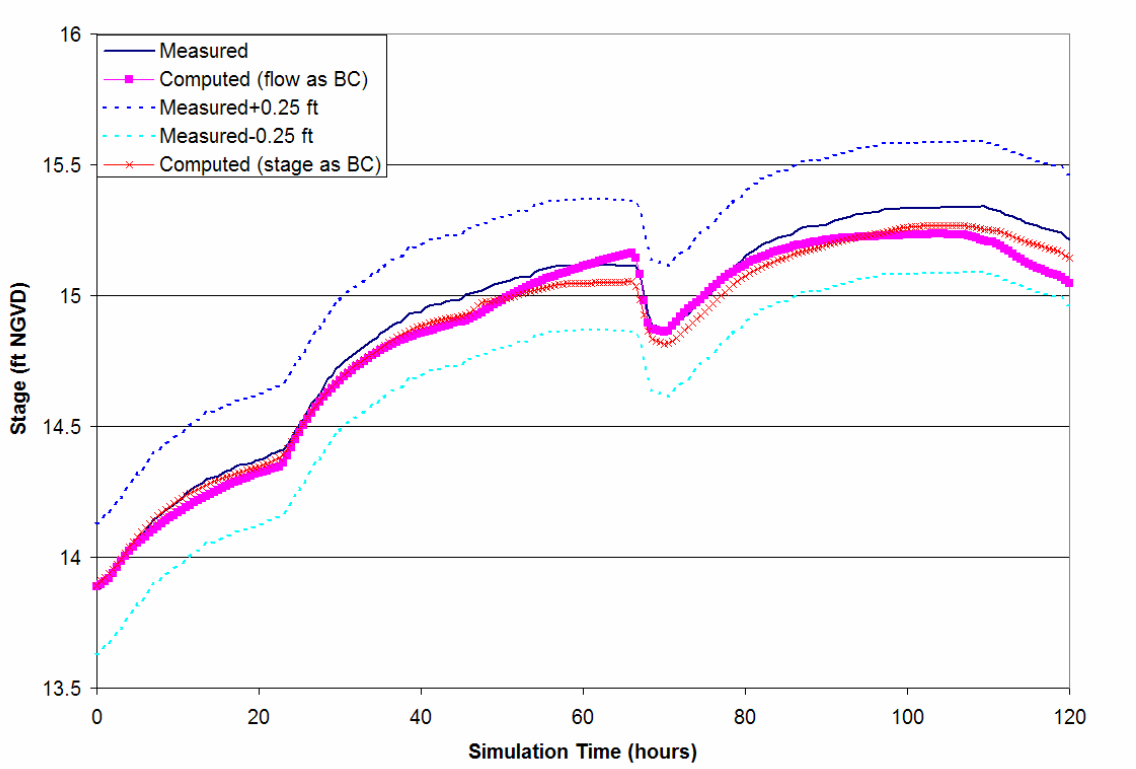

Figure 62: G-329_T Stages (validation: 9/5/2004 to 9/10/2004) Under Different Boundary Conditions

- **G-332 and G-334 weir coefficients**

Gated spillways G-332 and G-334 theoretical flow equations have an estimated relative error of 20% to 30% in flow computation when compared to flow measurements from stream gauging (SFWMD 2004a). During model calibration and validation, it was found that when the standard weir coefficient in FLO2DH, C_w =0.544 (C_d=3.1 in District's definition in FLOW Program) was used, G-332 and G-334 headwater levels were over-predicted. C_w was therefore increased to 0.944 to match G-332_H observed data (Figure 63).

As a result, observed G-332_H and G-334_H stage data were applied as specified stage boundary conditions for Cell 2 and Cell 3, respectively, to avoid this complication for model calibration and validation.

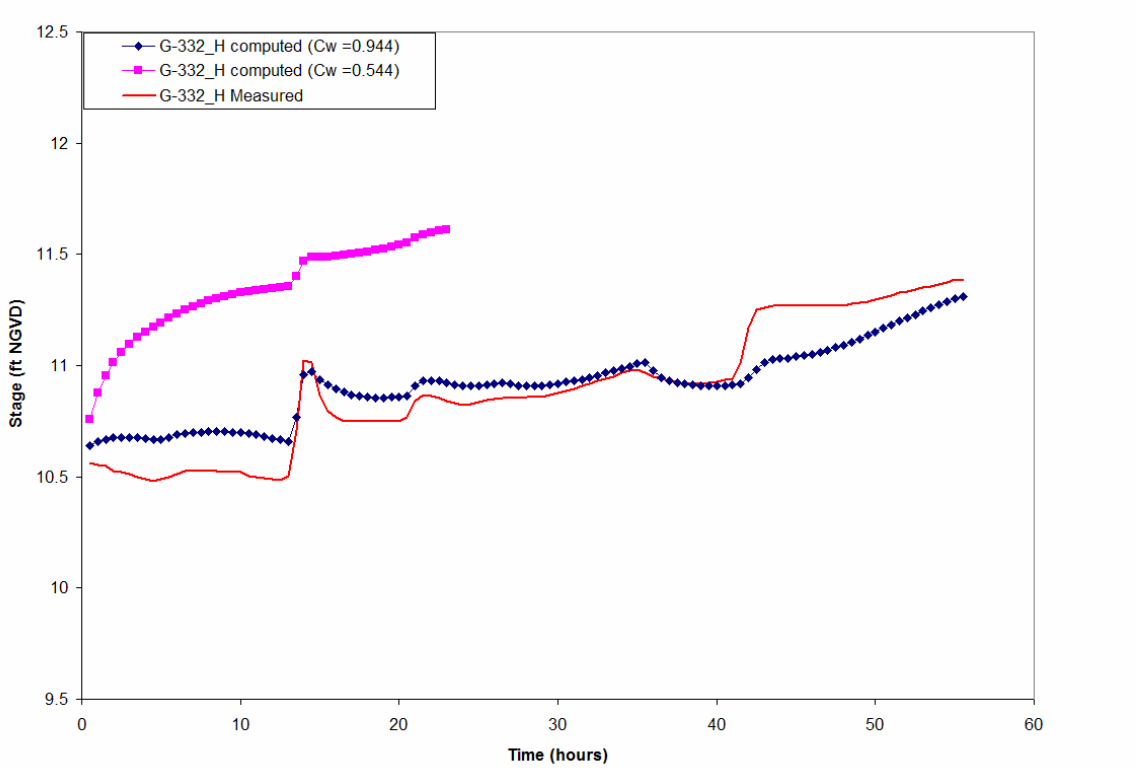

Figure 63: Effect of Weir Coefficient values (Cw) on G-332_H Stages (Calibration: 8/25/2004 to 9/4/2004, partial plot)

- **Rainfall, evapotranspiration and seepage losses**

Based on an analysis of rainfall data at S-6 and evapotranspiration (ET) data at STA-1W, it was confirmed that the net input from rainfall and ET is insignificant compared to structure inflows during model calibration and validation. From 8/25/2004 to 9/10/2004, the average total structure inflow is 7.14 inches/day, while the average rainfall rate is 0.14 inch/day and the evapotranspiration rate is 0.16 inch/day. As for seepage losses, the anticipated seepage rate is less than the design capacity of G-337 (240 cfs) and the seepage return flow was captured by actual pumping rate at G-337. A sensitivity run was also made for this in Section 6.

5. STA-2 Cells 1-3 Linked Existing Model

After the 2-D hydraulic models have been validated with field data, they can be applied for hydraulic analysis to gain insight and understanding of water flows in the STA-2 cells.

The new Cells 1-3 linked model was used to simulate steady flows under Low, Normal and High Flow conditions for the STA-2 existing configuration.

The Design, Low and High Flow and the desired outflow structure G-335 headwater levels are from the STA-2 Operation Plan (SFWMD 2001b). The Design Flow condition is the Design Peak Flow condition in the STA-2 Operation Plan. The High Flow condition is the Standard Project Storm Flow in the same reference. The Low Flow condition is assumed as a 600 cfs flow condition.

The design rainfall for the High Flow condition is the Standard Project Storm (23.6 inches in 24 hours) described in the Operation Plan. Table 6 lists the flow values used for Low, Design and High Flow conditions.

Table 6. Flow Rate for Different Steady Flow Conditions (cfs)

	Cell 1	Cell 2	Cell 3	STA-2 total
Effective area (acres)	1800	2270	2270	6340
Low Flow				600
Design Flow				3370
High Flow (rainfall only)	1784.75	2250.77	2250.77	6286.29
Structure inflow for High Flow condition				2570

Unlike the pre-assumed flow rates into each treatment cell in previous single cell models, flow distribution among Cells 1-3 was internally computed by the model.

In evaluating STA hydraulic performance, the following design criteria are considered:

- Minimum flow depth……..….. 0.5 feet
- Maximum flow depth ……. 90% of area equal to or less than 4.5 ft deep
- Maximum velocity in marsh areas..... 0.1 feet per second

5.1 Normal Flow (Design Peak Flow) Simulation Result

Under Normal Flow condition, 3,370 cfs of structure inflow (S-6+G-328) enters the STA-2 Supply/Inflow Canal, and then it is distributed into treatment Cells 1, 2 and 3 by the fully opened interior culverts G-329A-D, G-331A-G and G-333A-E.

Model simulations show that flows through Cells 1, 2 and 3 are approximately 776 cfs, 1416 cfs and 1178 cfs, respectively. This is quite close to the rough estimation of flow distribution by effective areas: 788, 1483 and 1099 cfs for Cells 1, 2 and 3.

Water levels in the Supply/Inflow Canal ranges from 17.5 ft NGVD at G-328 to 16.6 ft NGVD at G-333A-E (Figure 64).

In Cell 1, the water level is 15.6 ft NGVD at the north end and 14.0 ft NGVD at the south end. Stage in Cell 2 is about 14.4 ft NGVD at G-331A-G tailwater and 13.50 ft NGVD at outflow structure G-332. Water levels in Cell 3 are 13.30 ft NGVD at G-333A-E tailwater and 12.50 ft NGVD at G-334 headwater. These stage values are a little higher than those results in the single cell models (Sutron Corp. 2004a). This is partially attributed to the higher downstream stage in Cells 1-3. In the current linked cells model simulation, downstream stages in Cells 1-3 are part of the solution while they were specified stage values in the single cell models.

Water depth distribution (Figure 65) shows that water depth ranges from 1.54 ft to 6.0 ft in the marsh area. Only a small portion of the marsh area has a water depth over 4.5 ft.

Velocity magnitude and unit flow distributions are closely related to local topographic features and variation in land surface elevation (Figures 66 and 67). Velocity magnitude in the marsh area is less than 0.1 ft/s, and unit flow is less than $0.5 ft^2/s$.

The mean hydraulic residence time (MHRT) for STA-2 was estimated from steady flow condition under Design Peak Flow.

The total volume of water in all of the tree treatment cells was calculated and divided by the flow rate (3,370 cfs). The estimated MHRT is 4.2 days. This is to be interpreted as the minimum limit of the MHRT for STA-2, since historic total inflow rate is always less than 3,370 cfs. This value compares favorably with measured MHRT values in other STAs. For example, the measured MHRT values for STA-5 treatment cells range from 3.0 days in the wet season, to 32.0 days in the dry season (Parrish and Huebner, 2004).

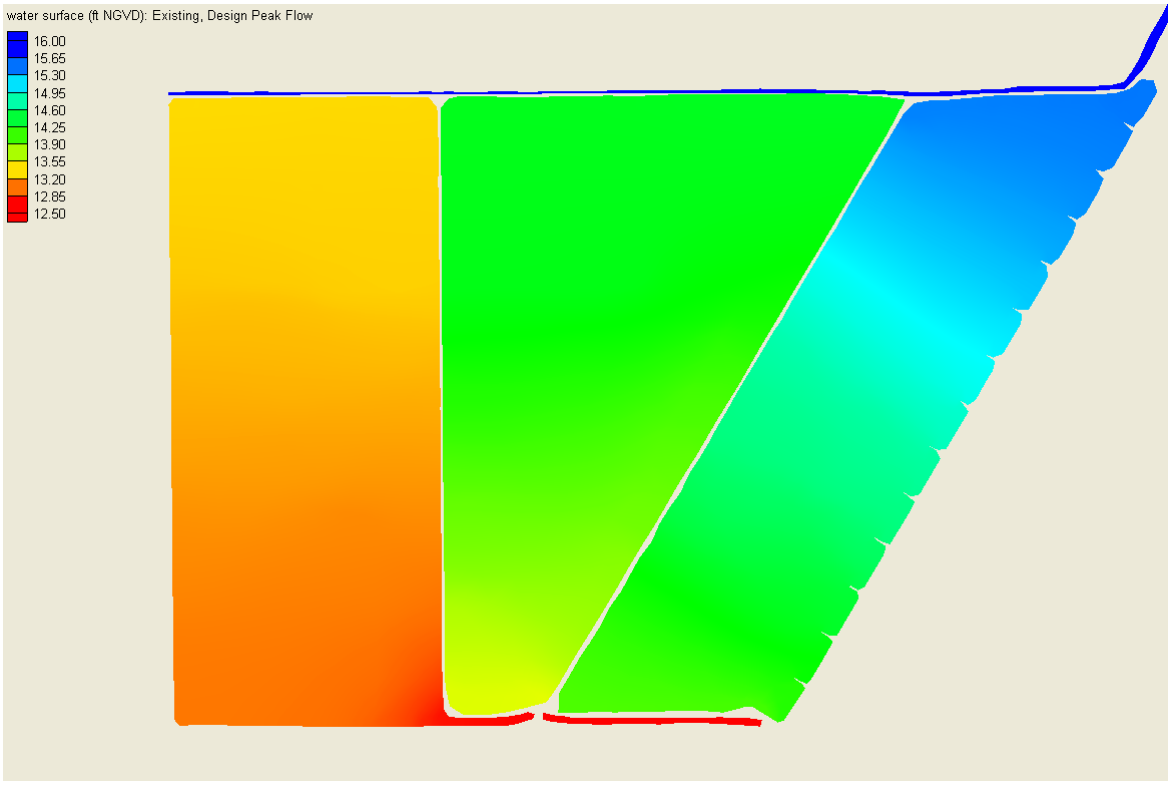

Figure 64: Water Surface Elevation (ft NGVD) (Existing Condition, Normal Flow)

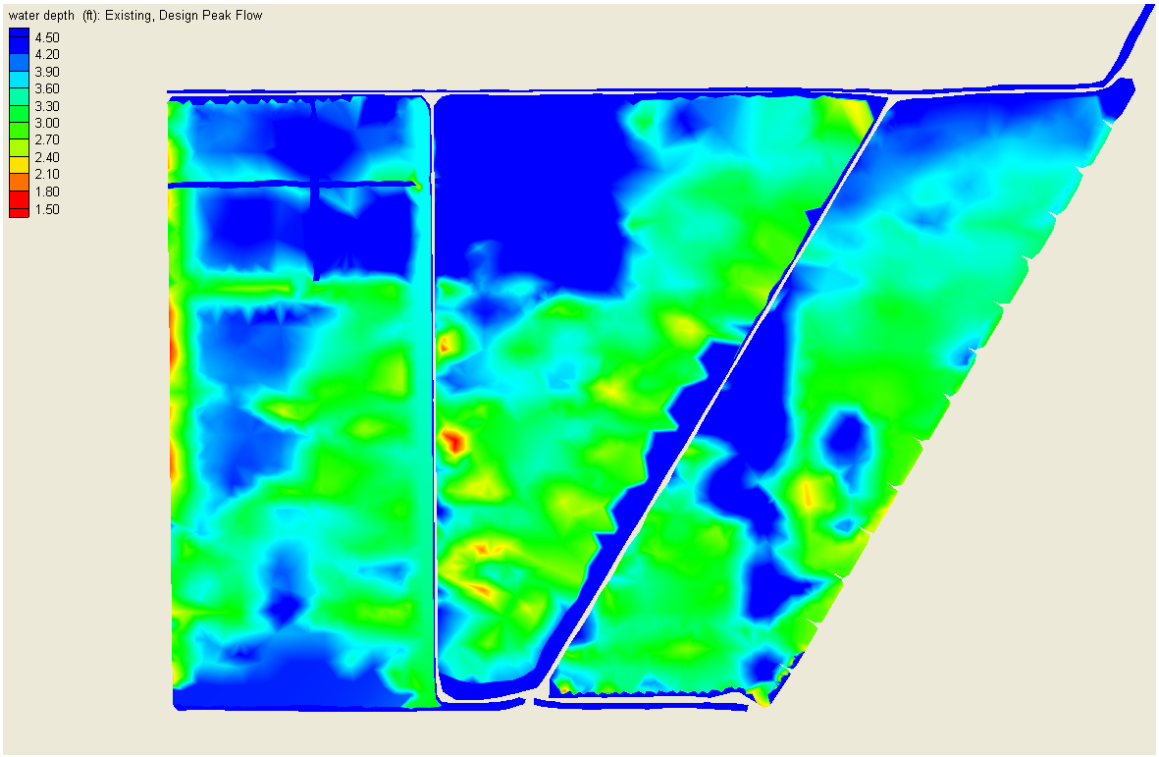

Figure 65: Water Depth Distribution (ft) (Existing Condition, Normal Flow)

Figure 66: Velocity Magnitude Distribution (ft/s) (Existing Condition, Normal Flow)

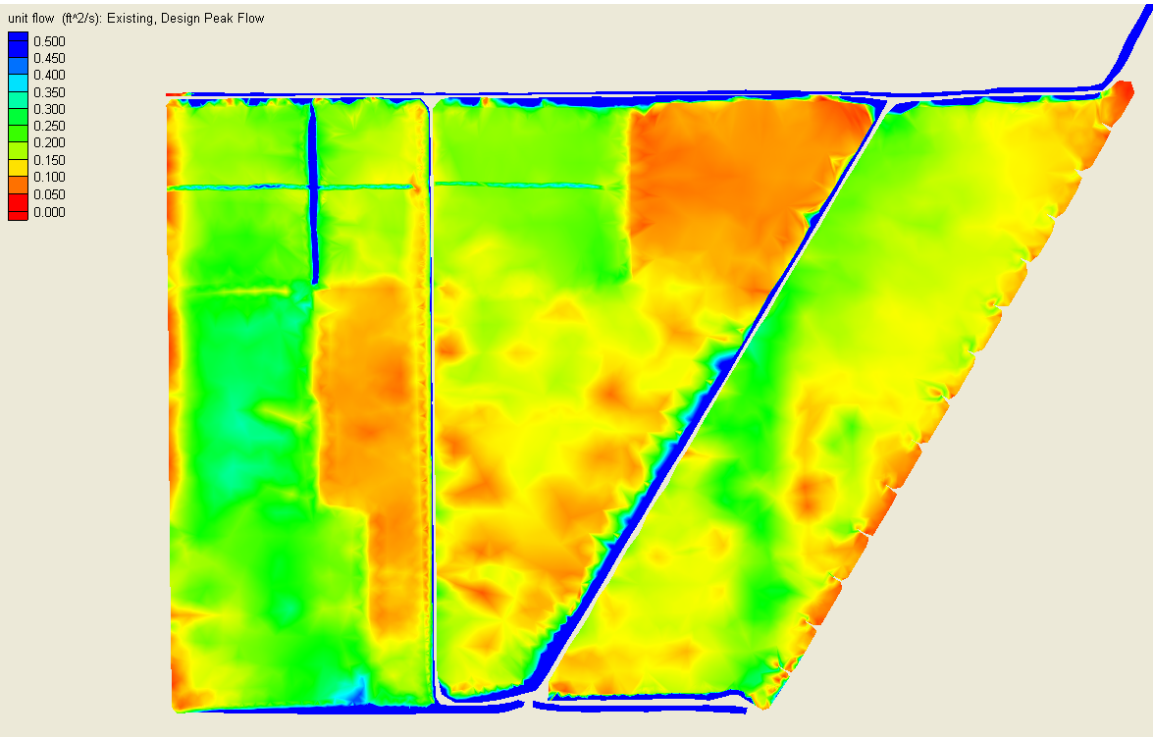

Figure 67: Unit Flow Distribution (ft^2/s) (Existing Condition, Normal Flow)

5.2 Low Flow Simulation Result

Under Low Flow condition, the total structure inflow is 600 cfs, which is less than 20% of the Normal Flow rate (3,370 cfs), and all flow structures are assumed fully opened.

Some local dry-out areas appeared at the highest land surface elevations in the treatment cells (Figure 68). Water surface elevation in Cell 1 is almost level since the crest elevation of weir boxes G-330A-D is about 13.0 ft NGVD. Water surface elevations range from about 10.5 ft NGVD to 12.6 ft NGVD in Cells 2 and 3. Water depth in the marsh area is between 0.0 ft and 3.0 ft (Figure 69). Velocity magnitude and unit flow plots (Figures 70 and 71) demonstrated much lower velocities under the Low Flow condition.

The total volume of water in all of the tree treatment cells was calculated and divided by the flow rate (600 cfs). The estimated MHRT is 11.6 days.

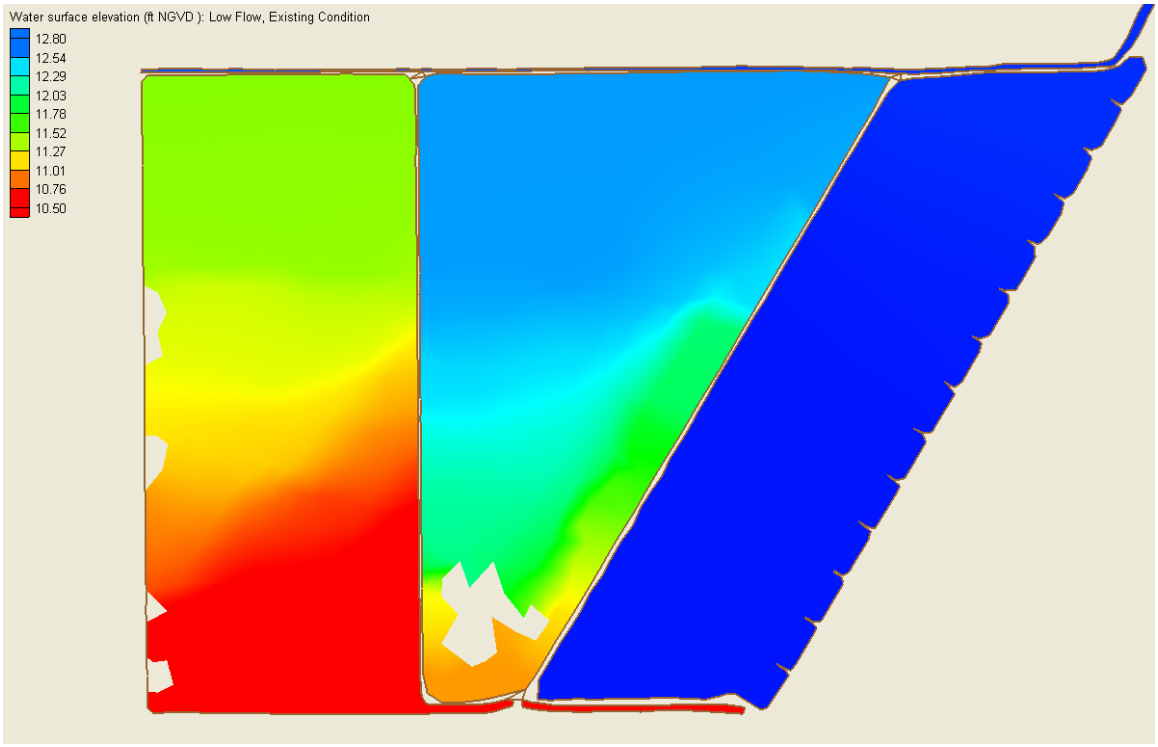

Figure 68: Water Surface Elevation (ft NGVD) (Existing Condition, Low Flow)

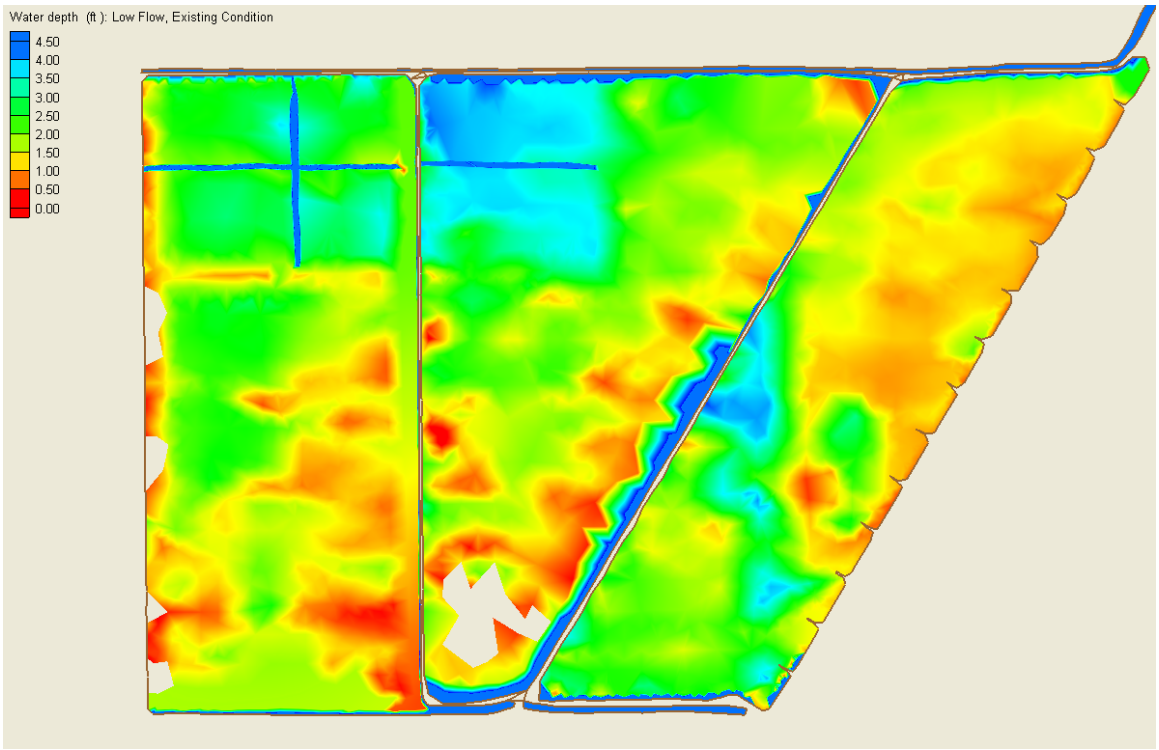

Figure 69: Water Depth Distribution (ft) (Existing Condition, Low Flow)

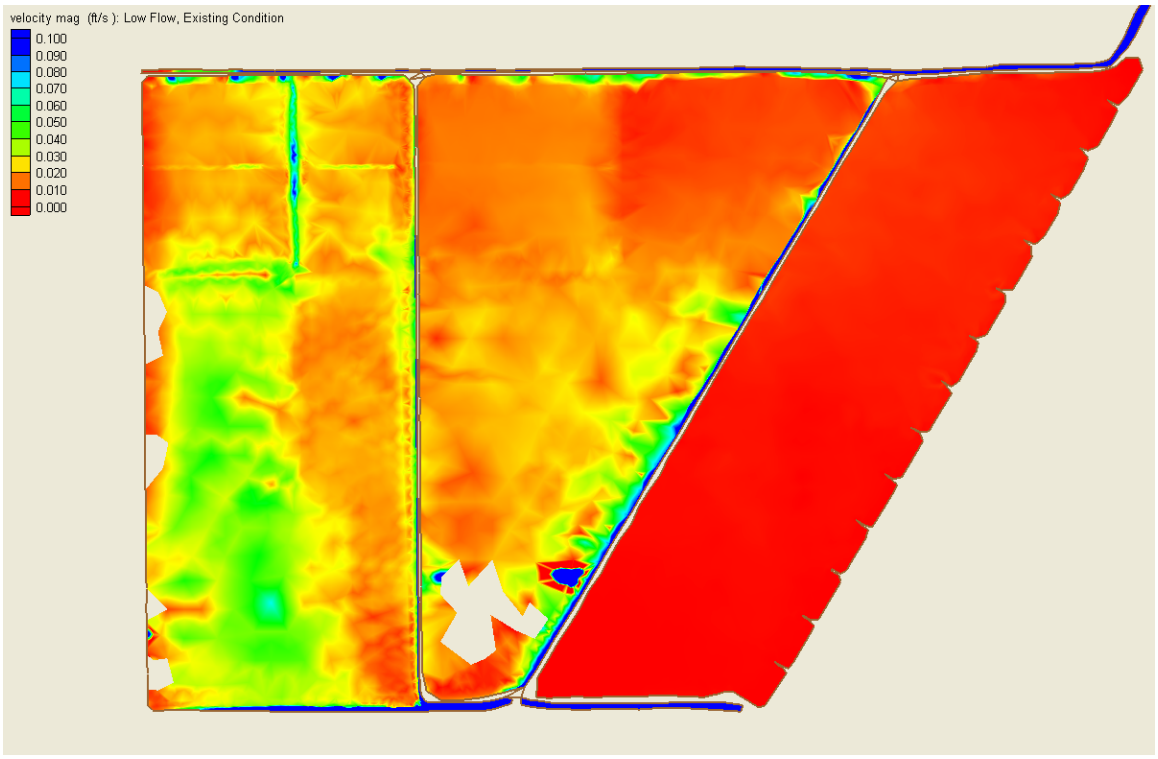

Figure 70: Velocity Magnitude (ft/s) (Existing Condition, Low Flow)

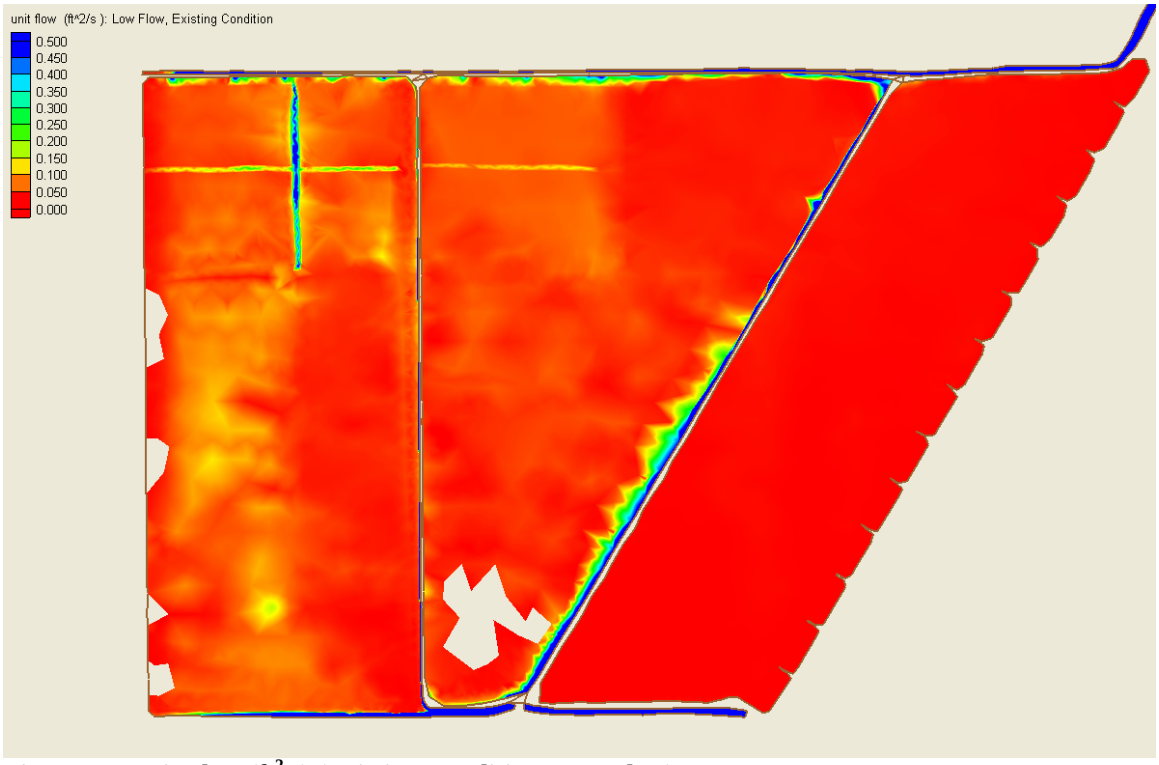

Figure 71: Unit Flow (ft^2/s) (Existing Condition, Low Flow)

5.3 High Flow (Standard Project Storm Flow) Simulation Result

The Standard Project Storm event (SPS) for STA-2 was estimated as 23.6 inches of rainfall over a 24-hour period (SFWMD 2001b). Structure inflow into the treatment cells is reduced from 3,370 cfs to 2,570 cfs by diverting 800 cfs of inflow through G-339. With this assumption, a net inflow of 2,570 cfs was applied. Furthermore, it was assumed that the flow condition before an SPS storm was the steady flow under Design Peak Flow condition. All inflow and outflow structures are fully opened during the High Flow simulation.

A specified stage of 14.20 ft NGVD was applied at the G-335 headwater. Under this high water level condition, the gated spillways G-332 and G-334 are fully opened, but the gates were submerged. This condition is the controlled-submerged flow regime. Due to the limitation of FLO2DH, no gates could be applied and the flow over G-332 and G-334 was uncontrolled submerged weir flow. It should be noted that this has an impact on the simulation results.

The transient model run demonstrated the dynamic response of STA-2 to the design 24-hour storm event (Figures 72 and 73).

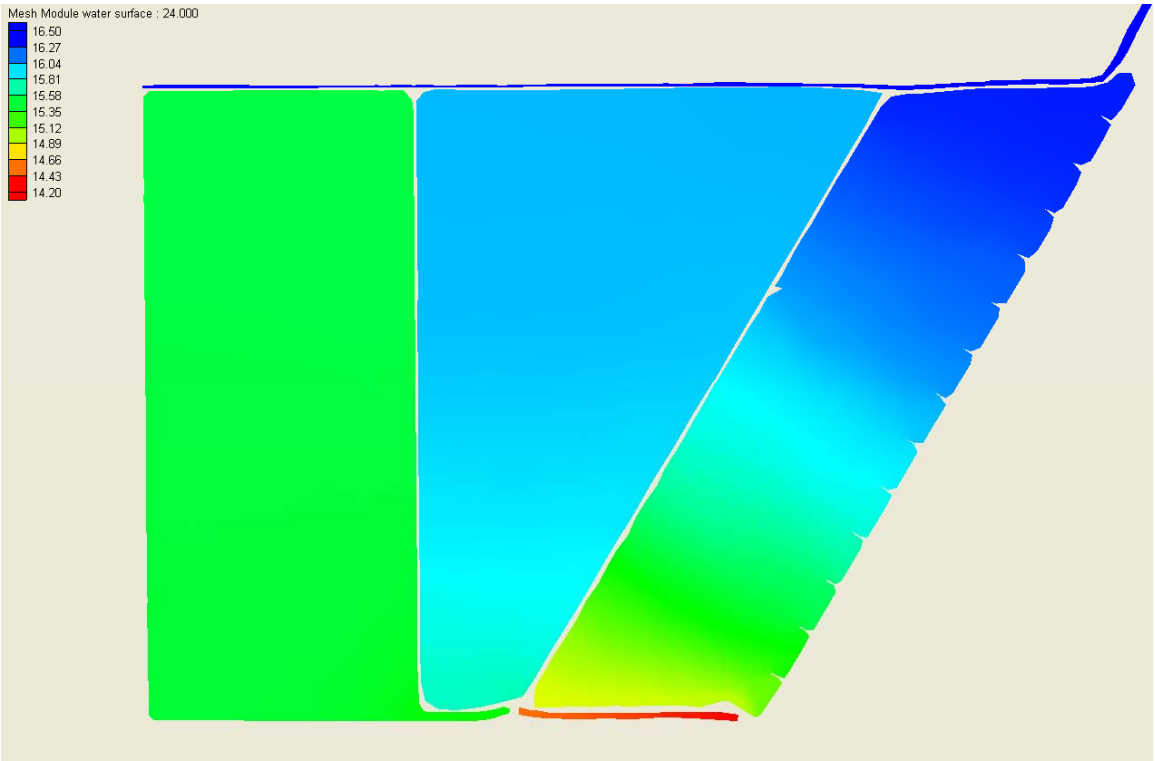

Figure 72: Peak Water Surface Elevation (ft NGVD) (Existing Condition, High Flow)

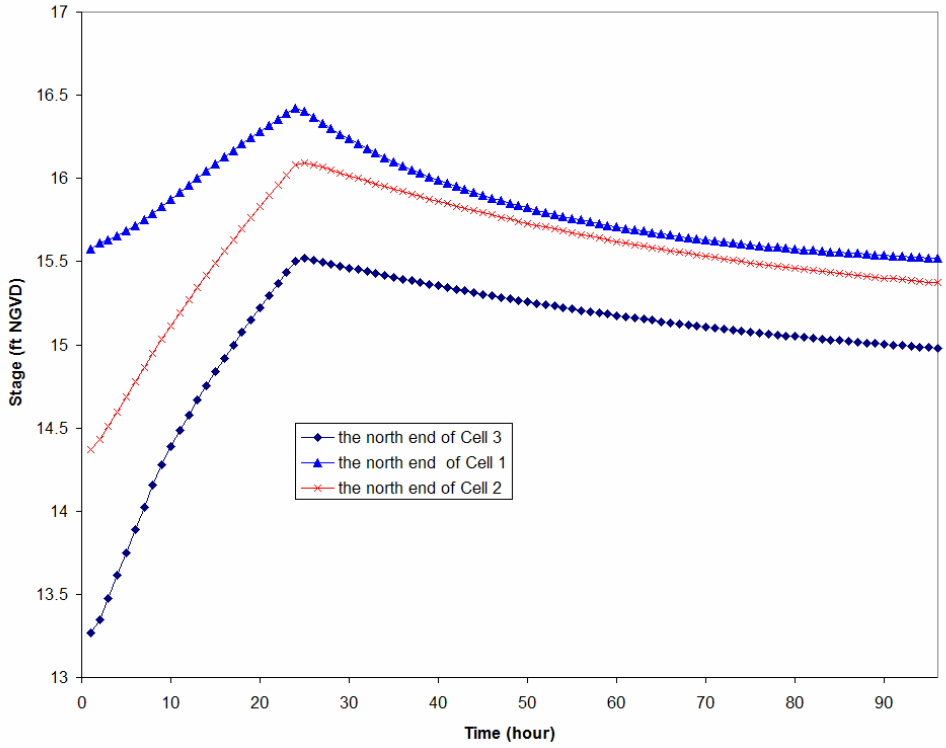

Figure 73: Stage Hydrograph during (High Flow, Existing Condition) Simulation

6. Sensitivity Analyses

Sensitivity analyses were conducted on some of the predictive scenario model runs. The base case is the steady flow result of Normal Flow (Design Peak Flow, 3370 cfs) under Existing Condition.

The first sensitivity model run was made by reducing Manning's n values for cattails from 0.8 to 0.5 (for depth of flow greater than 3.0 ft), with all other factors unchanged.

The impact on water levels is significant. Since Cell 1 is cattails dominant, the decrease in G-329A-D tailwater level is 0.5 ft. maximum changes in water levels for Cell 2 and Cell 3 are -0.25 ft and -0.15 ft, respectively (Figure 74). Smaller Manning's roughness coefficient values tend to lower hydraulic gradient across the treatment cells.

The changes in velocity magnitude are only significant along borrow canals and farm canals (Cell 2 eastern borrow canal). This is due to more flow will be through marsh areas when Manning's n values for marsh area are reduced.

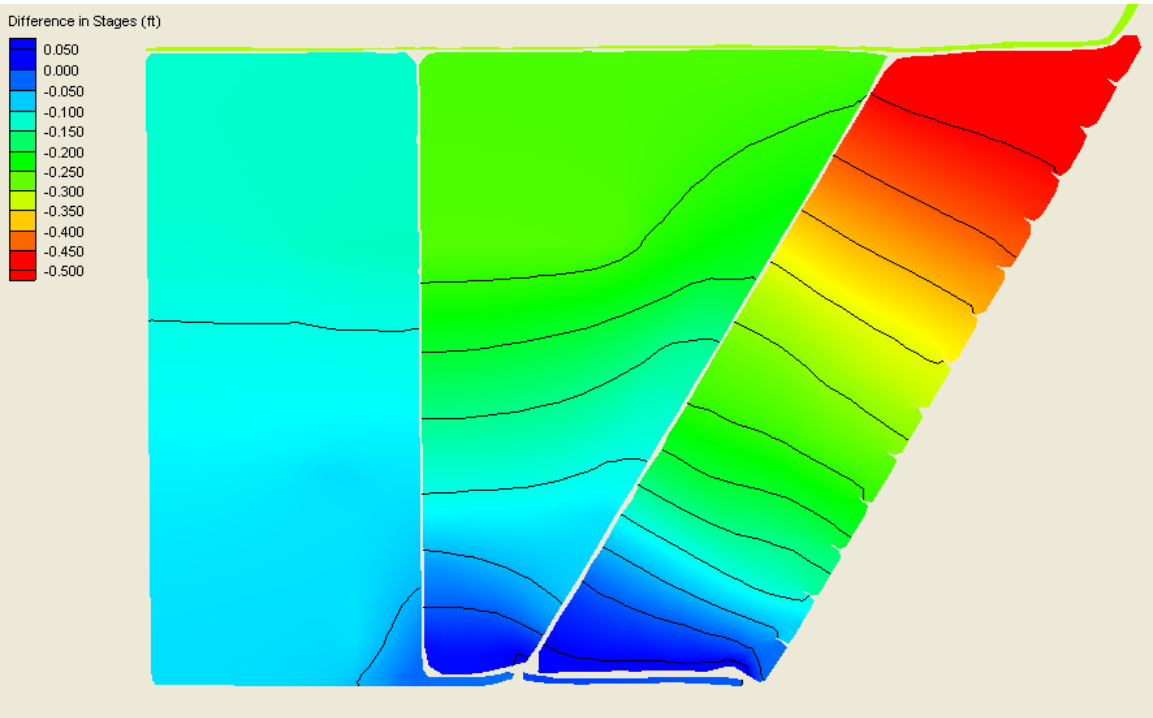

Figure 74 Changes in Water Levels due to different Manning' n values for Cattails

The second sensitivity model run is for SAV. The base Manning's n value for SAV was decreased from 0.3 to 0.1 (for depth of flow greater than 3.0 ft), with all other factors unchanged.

Since Cell 3 is SAV dominant, water levels in Cell 3 changed accordingly (Figure 75). The changes in Cell 3 stages are from -0.2 ft to 0.15 ft. In contrast, water level changes in Cell 1 and Cell 2 are very small. The changes in velocity magnitude are only significant along borrow canals and farm canals (Cell 3 eastern borrow canal). This is due to more flow will be through marsh areas when Manning's n values for marsh area are reduced.

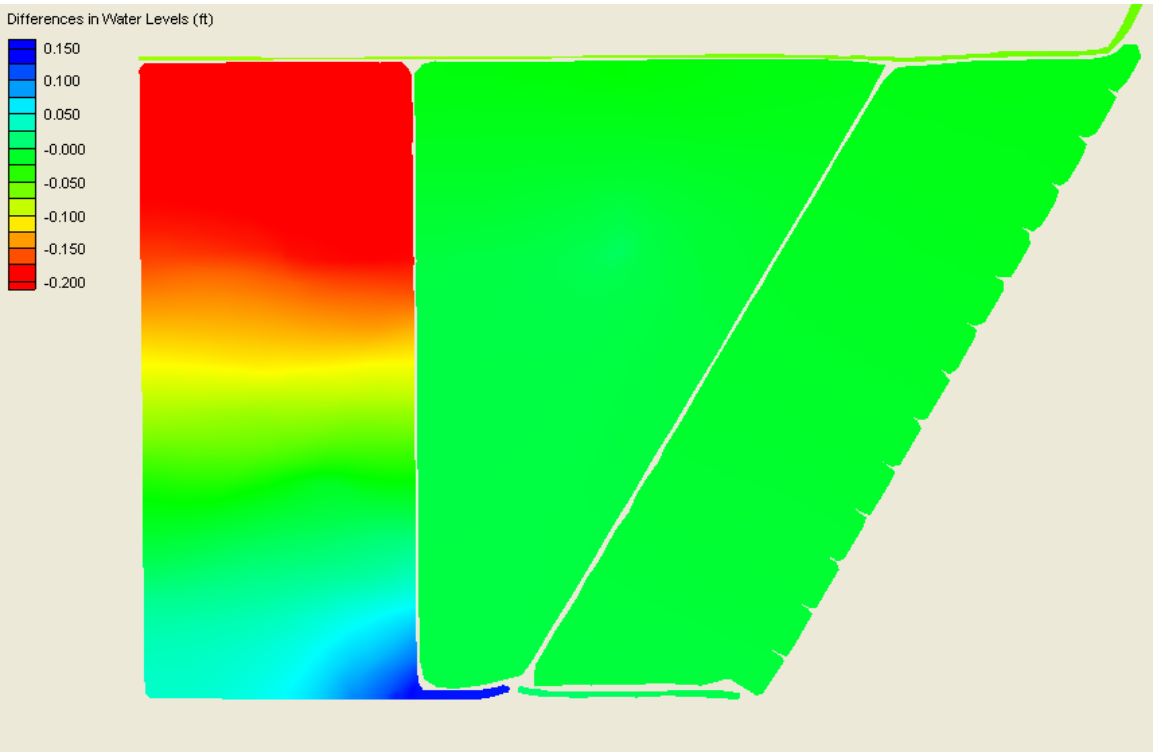

Figure 75 Changes in Water Levels due to different Manning' n values for SAV

The third sensitivity run is for impact of rainfall and evapotranspiration (ET) on simulation results. Based on previous water budget analyses of STAs, on average, ET value exceeds rainfall and the difference is about -2 to -5% of the total STA inflow during wet season. Since FLO2DH has no distributed elemental source/sink option, nodal point sinks in equivalent to -210 cfs was applied to mimic the rainfall/ET effect. 70 cfs of net water losses was applied to each treatment cell. This can be interpreted as a net loss of 210 cfs (about 6% of 3,370 cfs) from the surface area of STA-2 through ET or the vertical seepage losses.

The decrease in water levels is less than -0.13 ft (Figure 76). The changes in water levels in the northern part of treatment cells are insignificant.

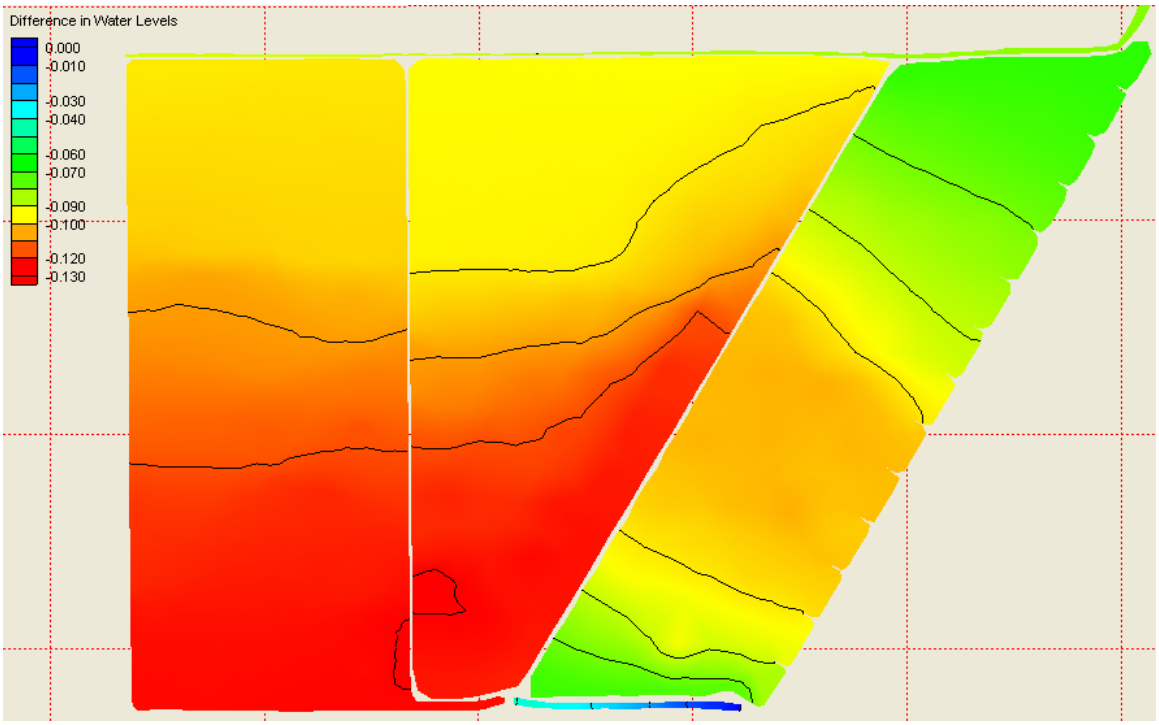

Figure 76 Changes in Water Levels due to ET or Vertical Seepage Losses

The last sensitivity run is about seepage losses through levees. In a STA-2 seepage study, the seepage loss per foot of head, per mile of levee is estimated to be 3 to 4 cfs /ft/mile (Dames & Moore, 2000). The following equation can be applied to estimate seepage rate (Parrish and huebner, 2004):

$$G=K_{sp}*L*\Delta H$$

G = seepage (cfs); Ksp = seepage coefficient (cfs/mile/ft); L = length along the seepage boundary (ft); ΔH = hydraulic head difference between the cell stage and the water level along the cell boundary (ft).

The seepage collection canal has a total length of 13.9 miles. The normal water level in the seepage collection canal is 9.0 ft NGVD and the seepage coefficient is 3.7. If the average stage in treatment cells along the boundary is 13.0 ft NGVD, then the estimated seepage rate is:

G=3.7 x 13.9 x (13-9) = 205.72 cfs.

The design pumping capacity of seepage return pump station G-337 is 240 cfs.

We applied a constant seepage rate (160 cfs, based on historic data) along the southwestern boundary of Cell 3. This seepage loss rate is equal to about 5% of total Design Peak Flow. The model results show that there is a marked water level decrease (up to 0.40 ft) at the vicinity of G-334 due to diverted seepage flow (Figure 77).

Insignificant changes in water levels and velocity magnitudes were found in other remaining areas. This shows that tailwater levels of inflow structures are less sensitive to consideration of seepage losses and these water levels were the major model calibration target.

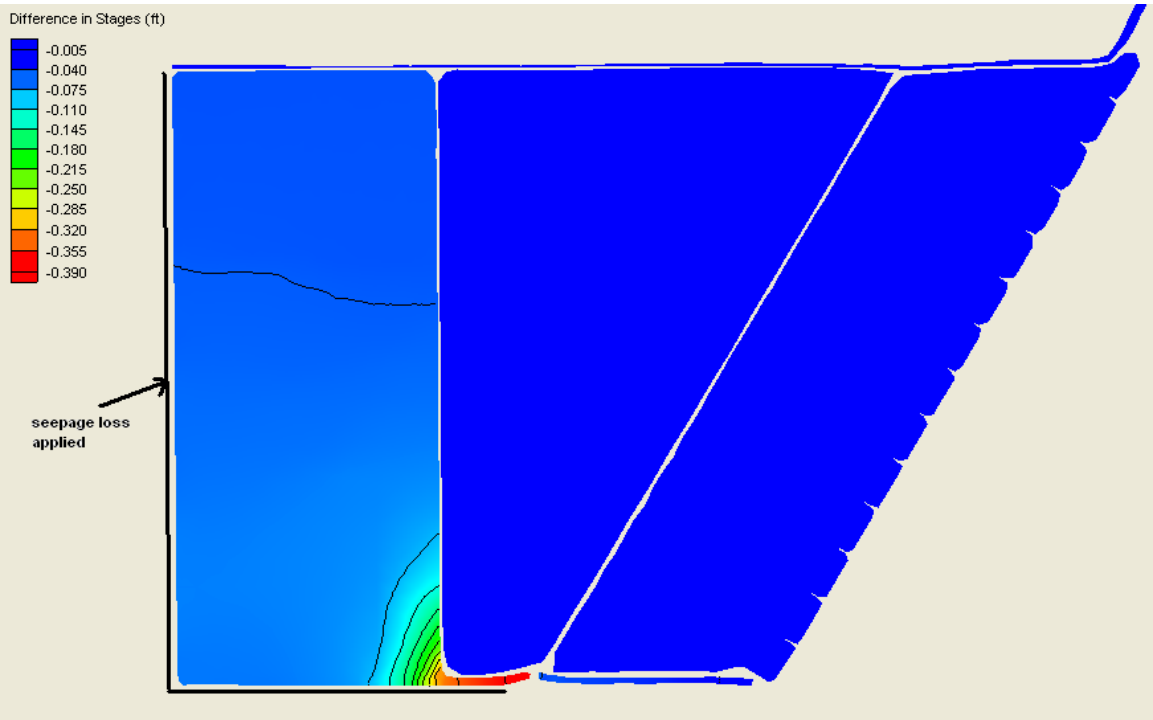

Figure 77 Changes in Water Levels With/without Seepage losses

7. STA-2 Cells 1-3 Linked Enhanced Model

The recommended enhancements for STA-2 in the Long-Term Plan for Achieving Everglades Water Quality Goals (Long-Term Plan) and its revised version (Burns and McDonnell 2003; SFWMD 2004b) are:

- Subdivide Cell 1 into Cells 1A and 1B, Cell 2 into 2A and 2B, and Cell 3 into 3A and 3B by constructing an interior levee in each of the cells;
- Add control structures through the new interior levees between cells in series (8' x 10 'gated reinforced concrete box culverts);
- Convert vegetation in the new downstream Cells 1B and 2B into SAV.

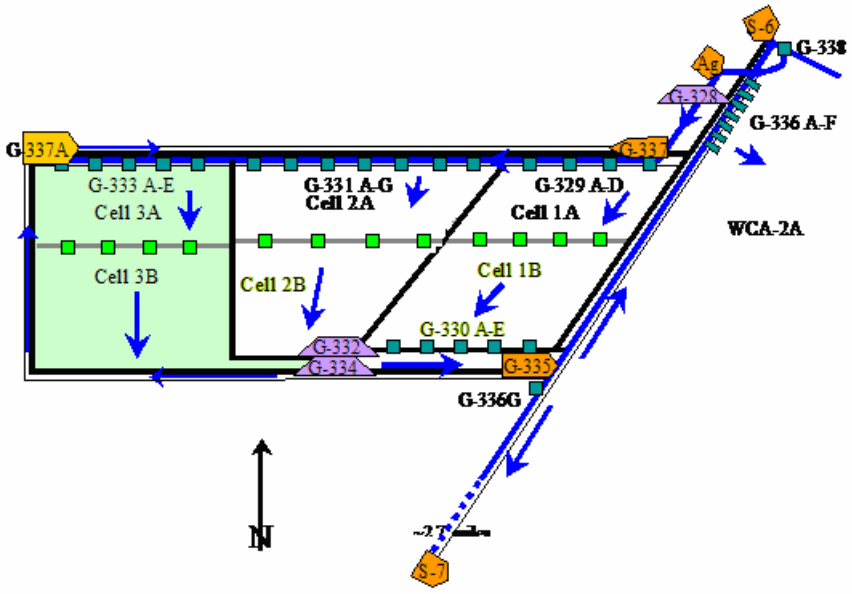

Figure 78: Schematic of STA-2 Enhanced Conditions as Simulated

At the request of the District, the conversion of existing emergent vegetation is for Cell 3 only. The STA-2 Cell 1 and Cell 2 existing vegetation is performing quite well and the conversion to SAV recommended in the Long-Term Plan will be postponed. Therefore, the same vegetation types used for the Existing Conditions models were used for the Cells 1 and 2 Enhanced Conditions models (Figure 78).

- **Design Peak Flow**

Under Enhanced Conditions, the interior levees divide each existing treatment into two separate new cells in series. Model simulation results show some storage effect in the new upstream cells (Figure 79).

In Cell 1A, water surface elevations range from 15.56 ft to 15.26 ft; in Cell 1B, water surface elevations range from 15.05 ft to 14.0 ft. This is very close to those under Existing Conditions.

In Cell 2A, water surface elevations range from 14.66 ft to 14.63 ft; in Cell 2B, water surface elevations range from 14.0 ft to 13.25 ft. Water levels in Cell 2A are about 0.2 ft higher than those in the same area under Existing Conditions. Water levels are lower downstream of the new interior levee (i.e., Cell 2B).

In Cell 3A, water surface elevations range from 13.46 ft to 13.43 ft; in Cell 3B, water surface elevations range from 13.0 ft to 12.5 ft. Water levels in Cell 3A are about 0.15 ft higher than those in the same area under Existing Conditions. Water levels are lower downstream of the new interior levee (i.e., Cell 3B).

The water depth distribution (Figure 80), velocity magnitude and unit flow plots (Figures 81 and 82) are similar to those under Existing Conditions. The major difference is the existing short-circuit paths, i.e., the borrow canals in Cells 2 and 3, are totally cut off by the new interior levees. However, the canals are still a faster flow way in the new cells.

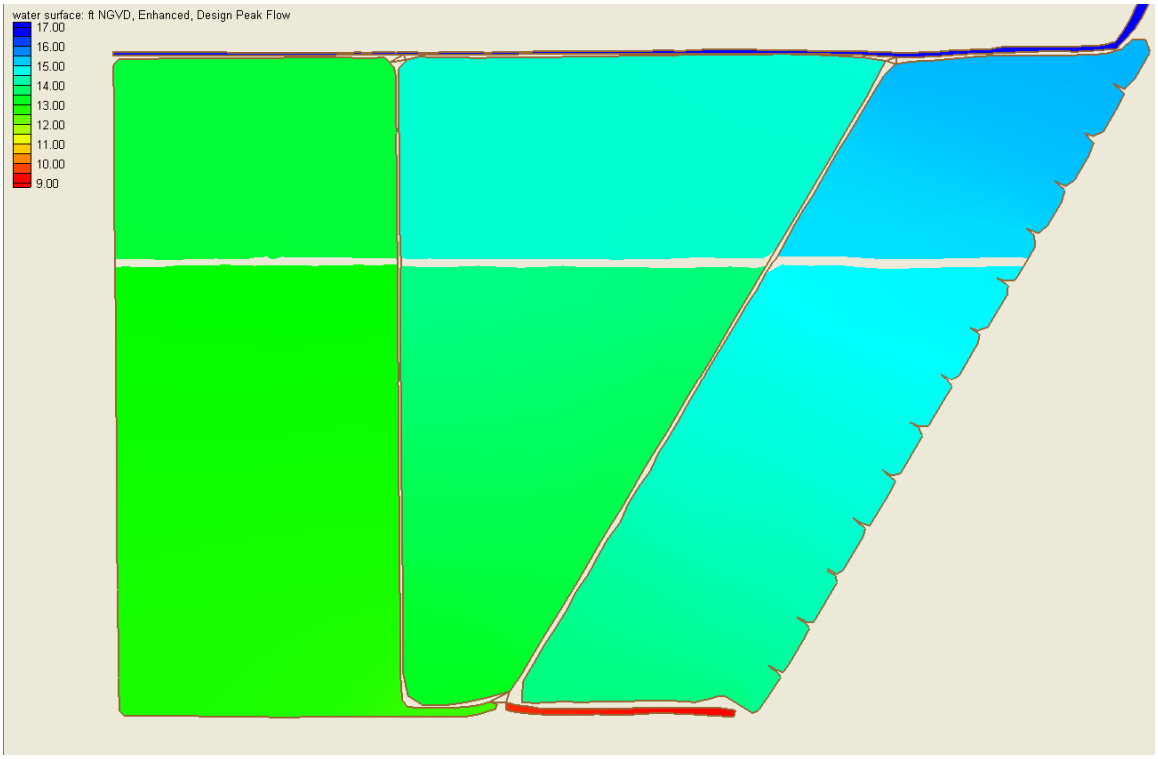

Figure 79: Water Surface Elevation (ft NGVD) (Enhanced Condition, Normal Flow)

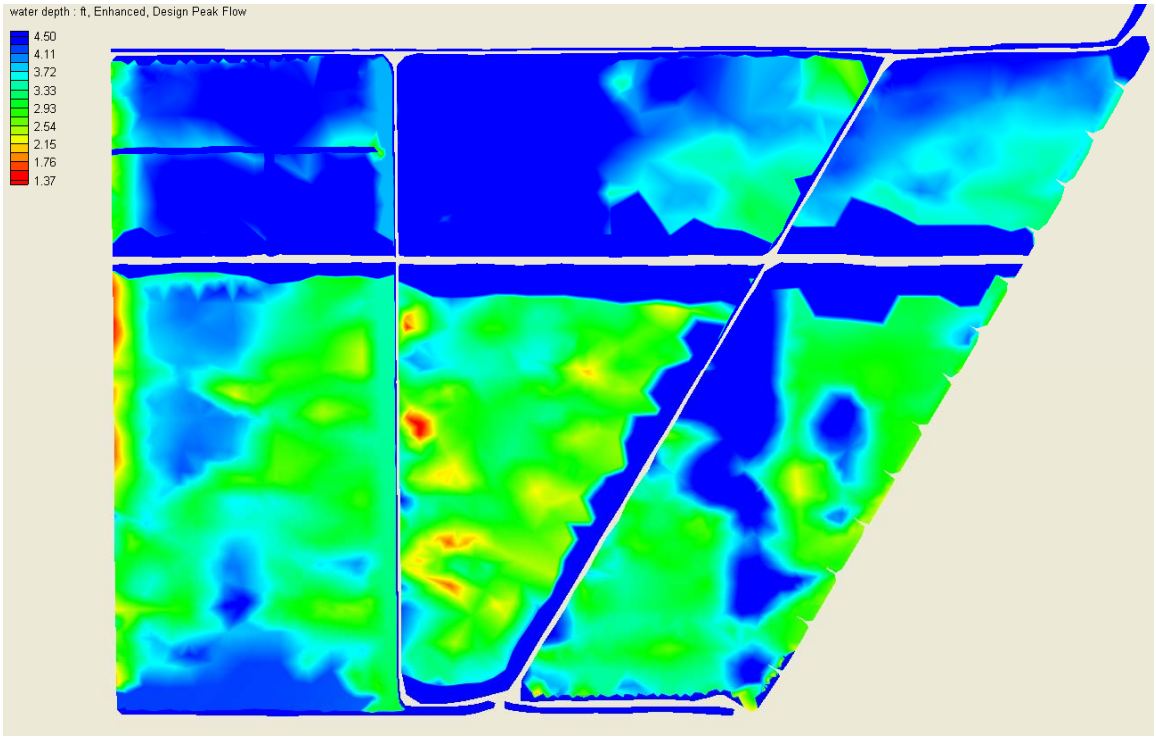

Figure 80: Water Depth Distribution (ft) (Enhanced Condition, Normal Flow)

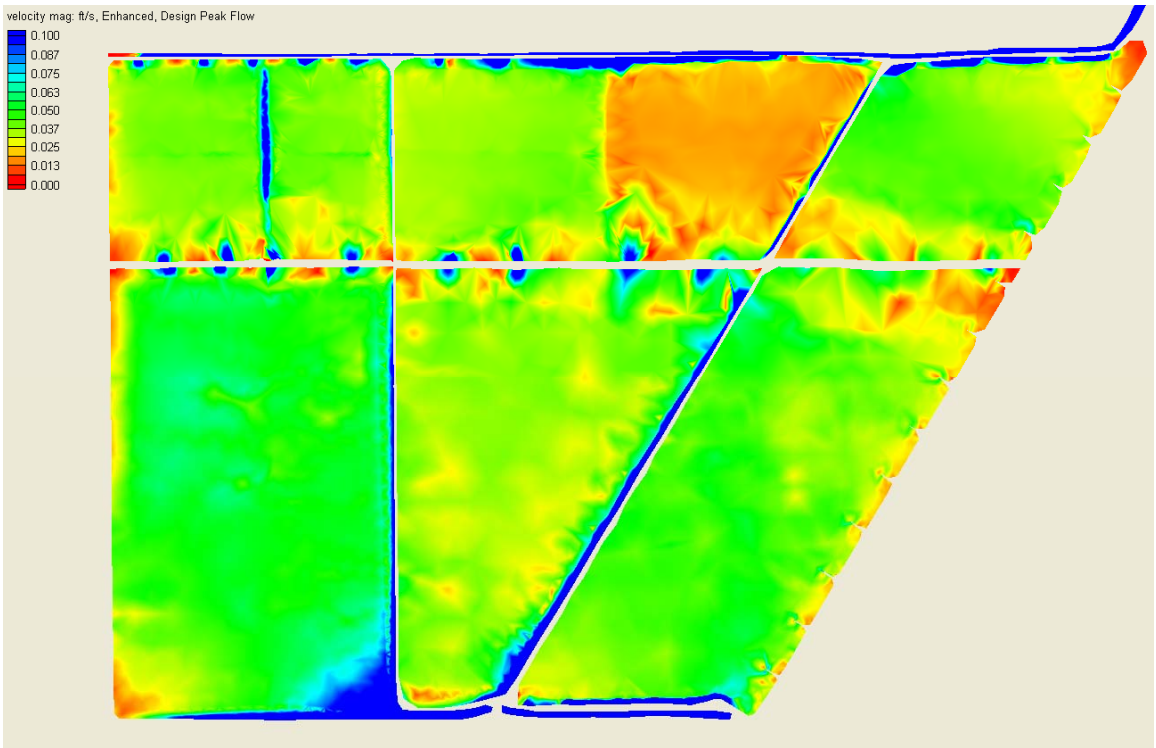

Figure 81: Velocity Magnitude Plot (ft/s) (Enhanced Condition, Normal Flow)

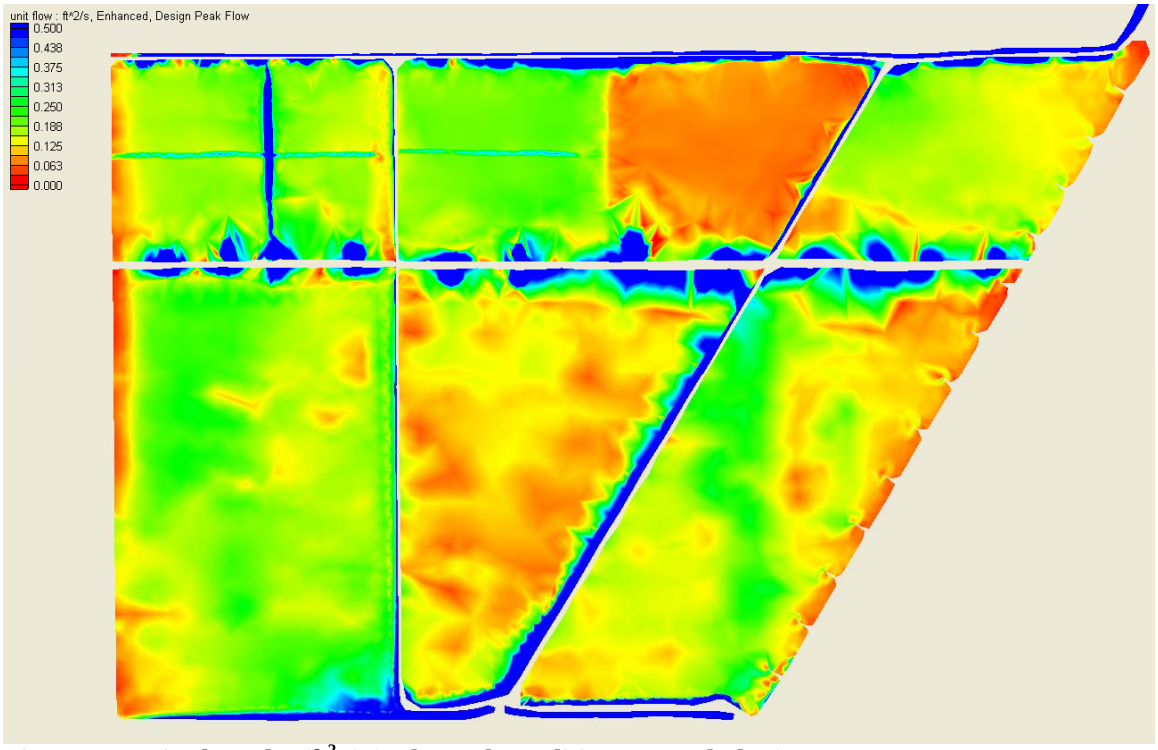

Figure 82: Unit Flow Plot (ft^2/s) (Enhanced Condition, Normal Flow)

- **Low Flow and High Flows**

Model simulation results for Low Flow (Figures 83-86) and High Flow (Figures 87-89) are very close to the results obtained under Existing Conditions.

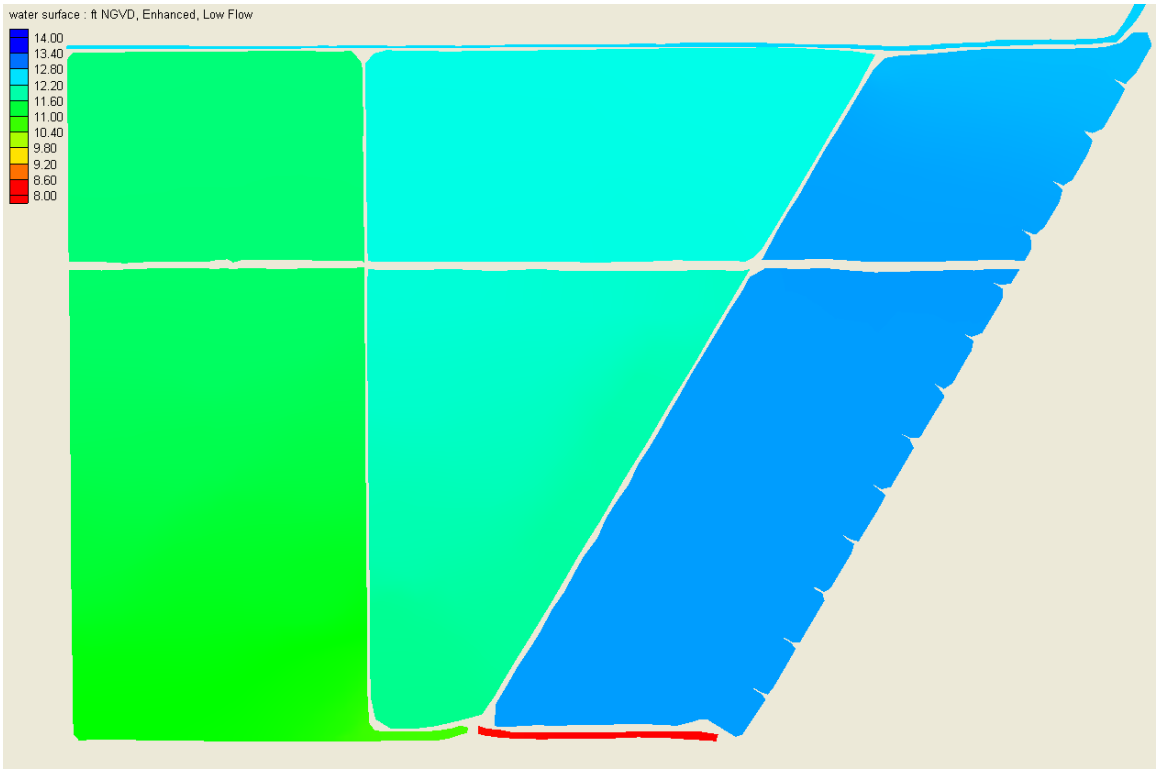

Figure 83: Water Surface Elevations (ft NGVD) (Enhanced, Low Flow)

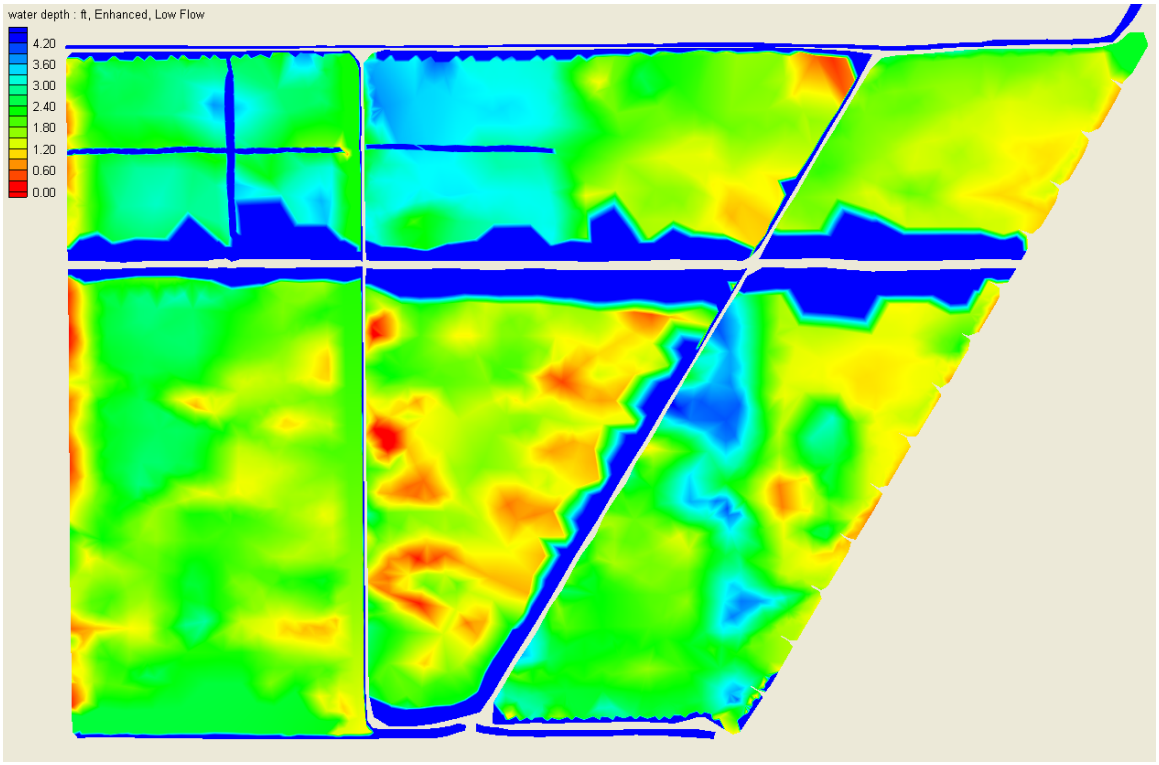

Figure 84: Water Depth (ft) Distribution (Enhanced, Low Flow)

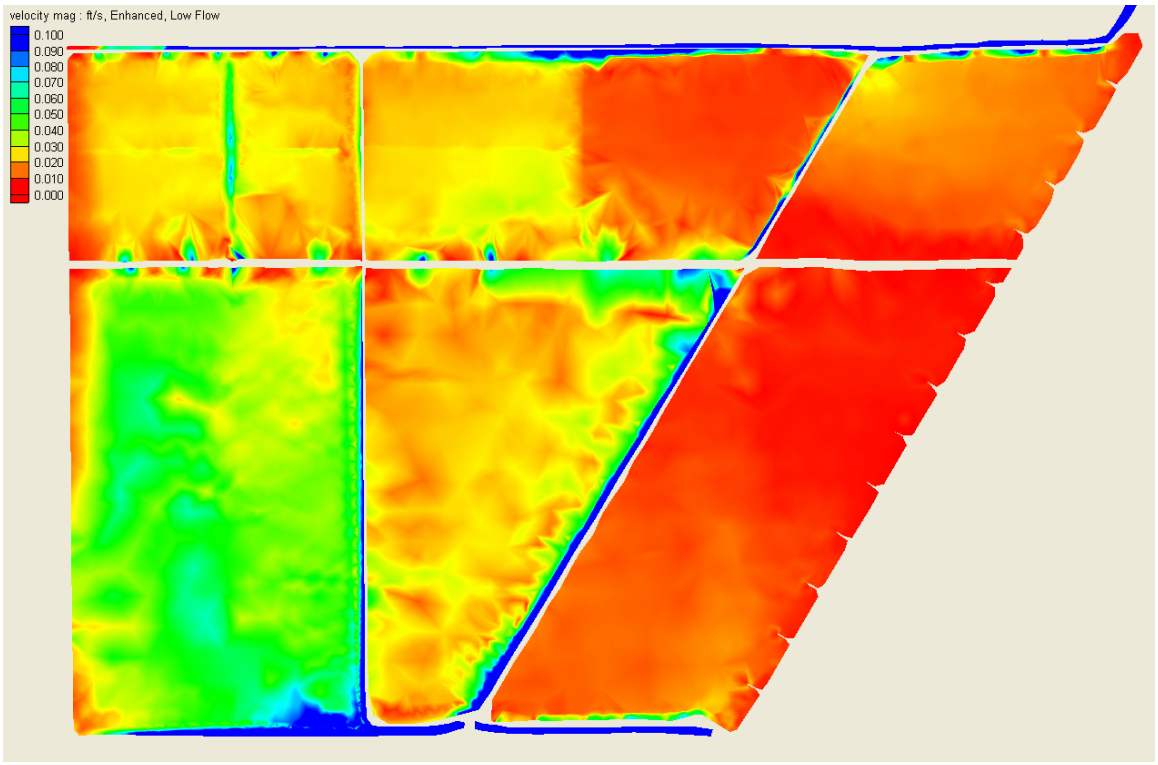

Figure 85: Velocity Magnitude Plot (Enhanced Condition, Low Flow)

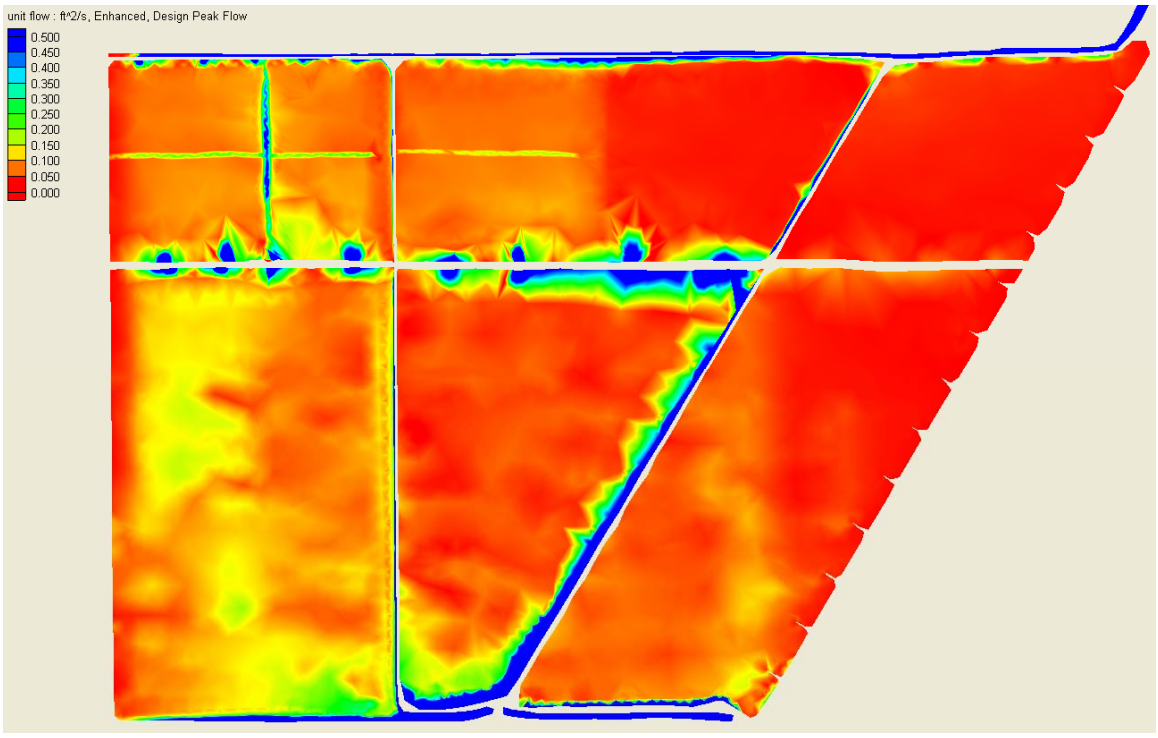

Figure 86: Unit Flow Distribution (Enhanced Condition, Low Flow)

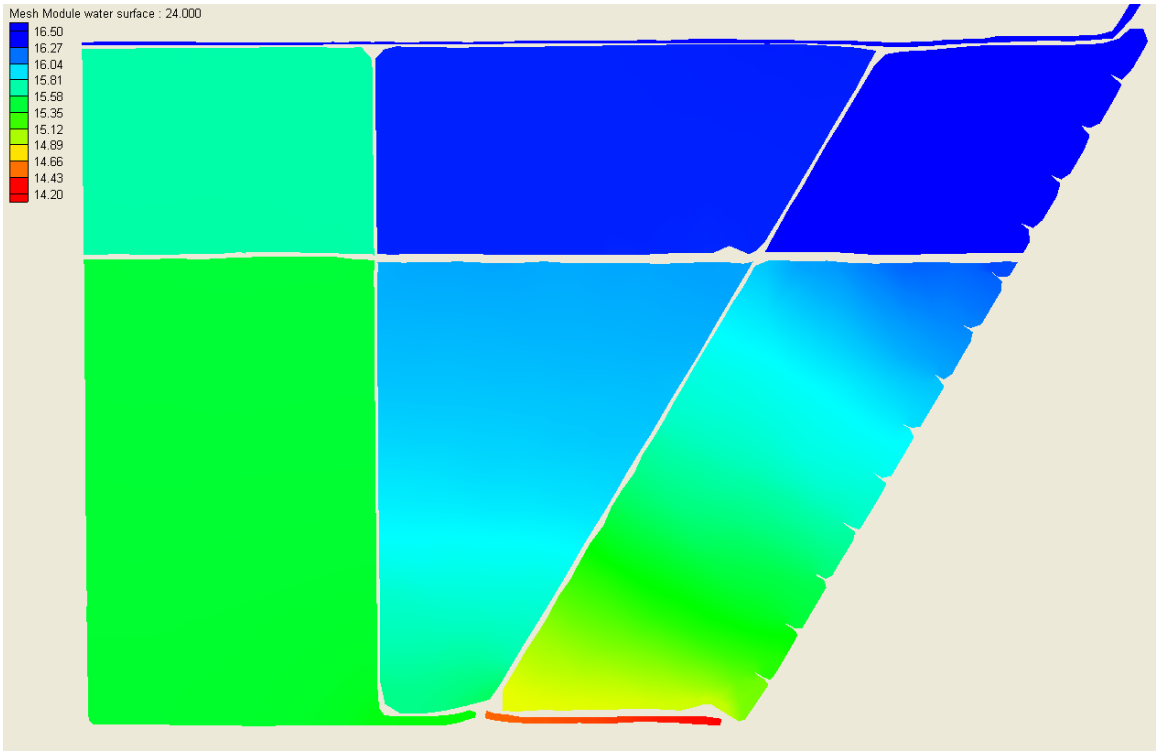

Figure 87: Peak Water Level (Enhanced Condition, High Flow)

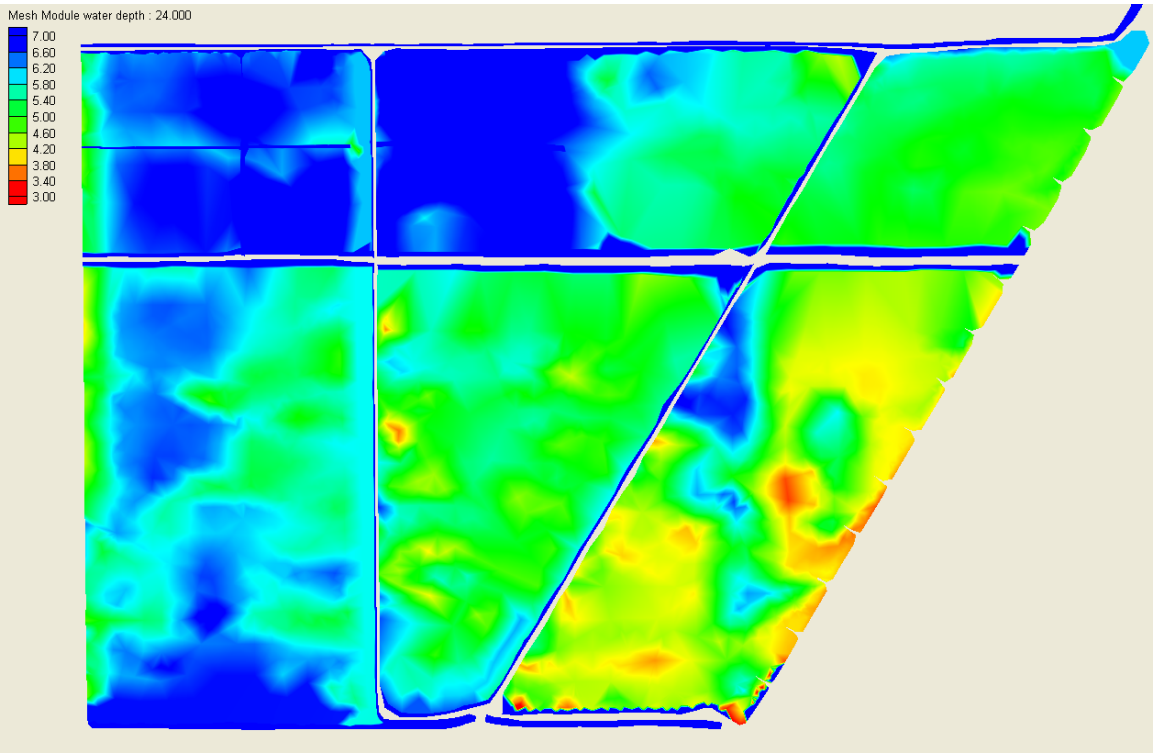

Figure 88: Water Depth Distribution (Enhanced Condition, High Flow)

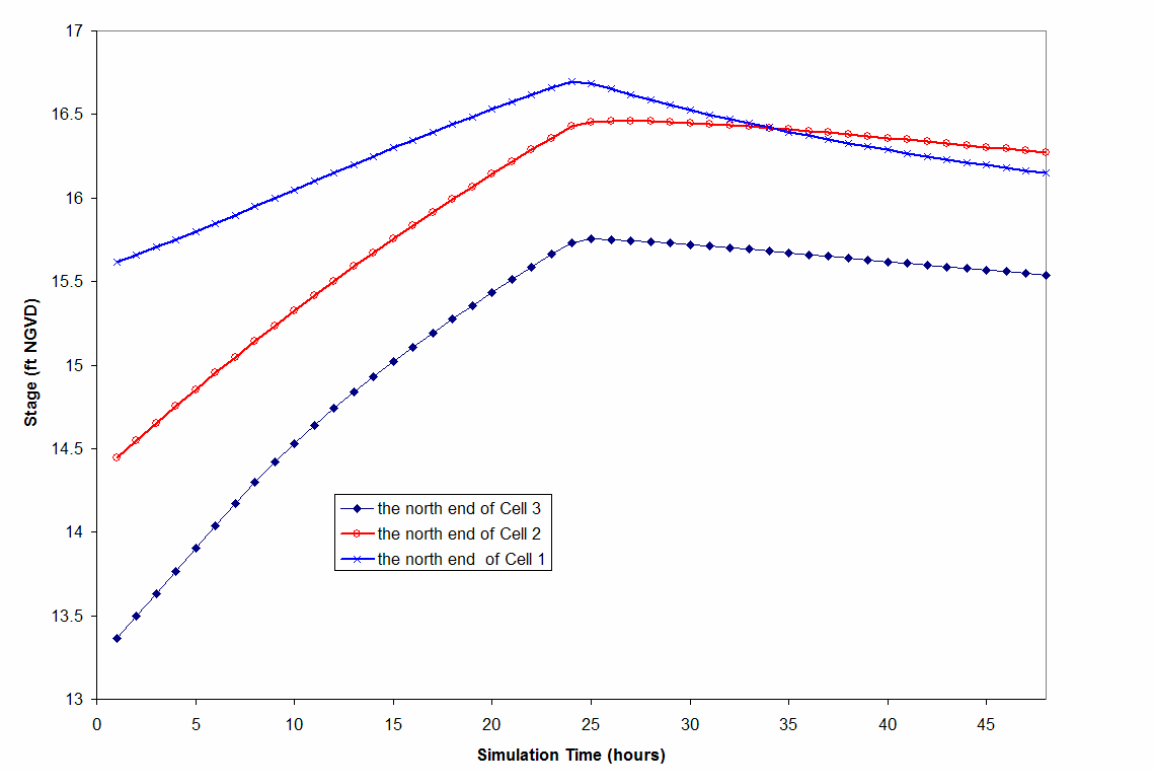

Figure 89: Stage Hydrograph (Enhanced Condition, High Flow)

8. Conclusions and Recommendations

A new STA-2 Cells 1-3 linked 2D hydraulic model was developed. This is an improvement over previous STA-2 single cell 2D hydraulic models. Model calibration and validation were completed by using historic stage and flow data at interior control structures. The limitation of FLO2DH in handling gated culverts and gated spillways made it very challenging to get good model calibration and validation results. Although some approximations had to be made on this aspect, the model calibration and validation results were satisfactory in history-matching of observed stage values. The newly developed 2D models were also used for hydraulic analyses of existing and enhanced configurations of STA-2.

The following recommendations are made for this modeling work:

- Variable gate opening should be incorporated into STA 2-D hydrodynamic models; otherwise, it is very difficult to get good result on model calibration and verification.
- Continuous stage monitoring should be set up at the center of the marsh areas similar to those stations at STA-1W.
- Flow rating equations should be updated and checked with more stream-gauging measurement data.

References

Burns & McDonnell, 2000. 2D Hydrodynamic Modeling Stormwater Treatment Area 3/4 and East WCA-3A Hydropattern Restoration.

Burns & McDonnell, 2003. Long Term Plan for Achieving Water Quality Goals. October 27, 2003.

Dames & Moore, 2000. Factual report submittal offsite seepage study for Stormwater Treatment Area 2. Prepared for South Florida Water Management District. Boca Raton, Florida 33487.

Froehlich D C. 2002. User's Manual for FESWMS Flo2DH- Two-dimensional Depth-averaged Flow and Sediment Transport Model, Release 3, Publication No. FHWA-RD-03-053, Federal Highway Administration, September 2002.

Harvey J.W. and Krupa S.L. et al. 2002. Interaction between surface water and groundwater and effects on mercury transport in the North-central Everglades, USGS Water Resources Investigations Report WRIR 02-4050.

Parrish M. and Huebner R. S., 2004. Water Budget Analysis for Stormwater Treatment Area 5. Technical Publication EMA # 418. June 2004. South Florida Water Management District, West Palm Beach, Florida 33406.

Refsgaard, J.C. and Henriksen J., 2004. Modeling guidelines – terminology and guiding principles, Advances in Water Resources, Vol. 27, Issue 1, January 2004, Pages 71-82.

South Florida Water Management District (SFWMD). 2001a. Two dimensional Hydraulic Analysis for Cell 3 of STA-2, a SAV-dominated Treatment Cell. March 21, 2001. West Palm Beach, Florida.

South Florida Water Management District (SFWMD). 2001b. STA-2 Operation Plan (revised March 2001). SFWMD, West Palm Beach, Florida.

South Florida Water Management District (SFWMD). 2004a. State of flow monitoring in stormwater treatment areas. May 2004, SFWMD, West Palm Beach, Florida.

South Florida Water Management District (SFWMD). 2004b. Revised Long Term Plan for Achieving Water Quality Goals: Part 2 Revisions to Pre-2006 Strategies, ECP Basins. November, 2004, West Palm Beach, Florida.

Sutron Corporation, prepared for South Florida Water Management District. 2004a. STA-2 Hydraulic Modeling Task 1.4 Final Report, May 28, 2004

Sutron Corporation, prepared for South Florida Water Management District. 2004b. STA-6 Hydraulic Modeling Task 2.3 Draft Report, August 19, 2004

Sutron Corporation, prepared for South Florida Water Management District. 2005. STA-1W Hydraulic Modeling Task 5.4 Final Report. February 14, 2005.

Wantman Group, Inc., 8/25/2003. Stormwater Treatment Area No. 2 Topographic Survey.

Wu F.C., Shen H.W. and Chou Y.J., 1999. Variation of roughness coefficients for unsubmerged and submerged vegetation. Journal of Hydraulic Engineering, ASCE, Vol. 125, No.9.